Site Suitability Analysis of ground-based solar energy in the Netherlands

Poomisub Manonukul

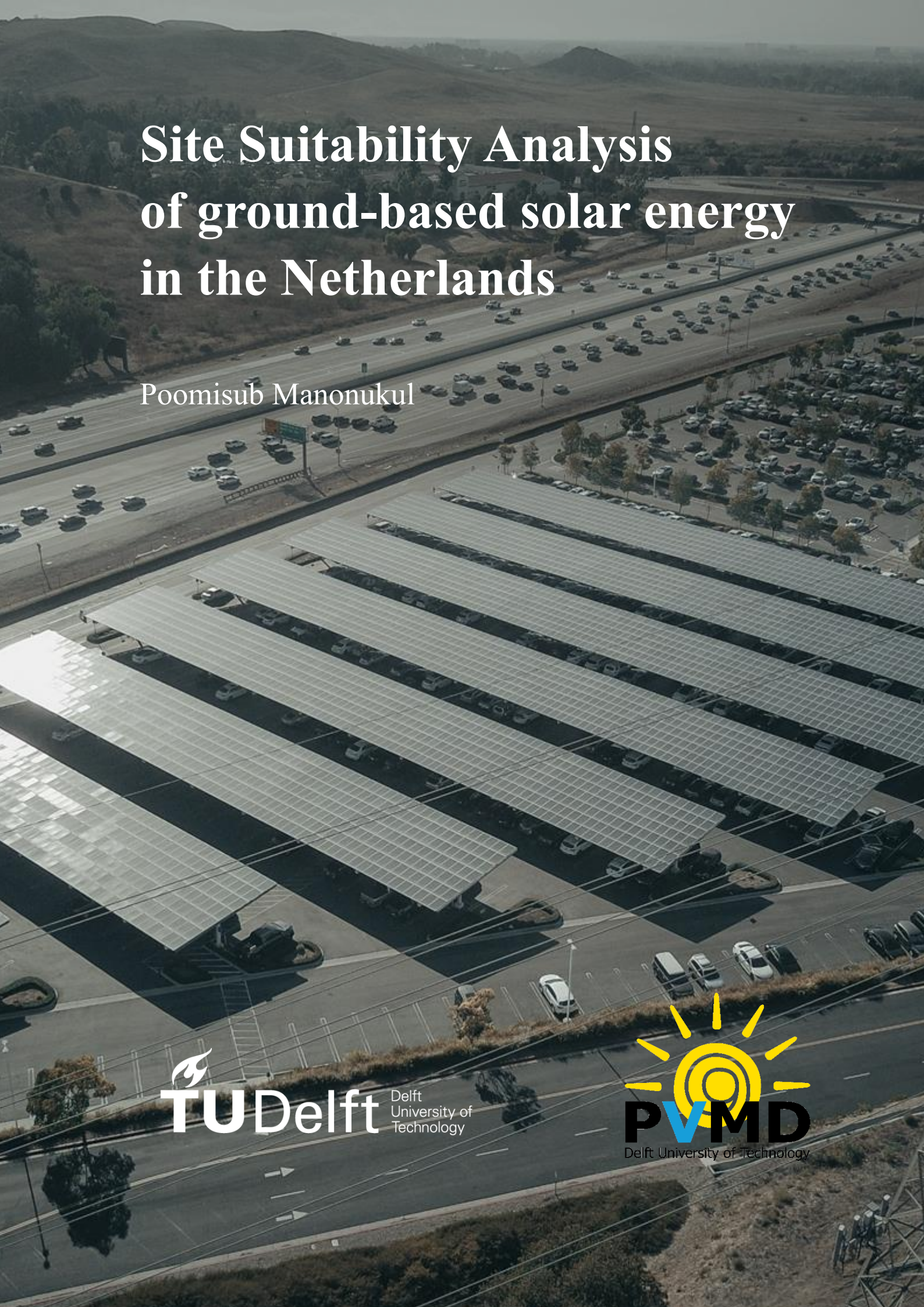

TU Delft Delft University of Technology

PVMD Delft University of Technology

Site Suitability Analysis of ground-based solar energy in the Netherlands

by

Poomisub Manonukul

to obtain the degree of Master Science
at the Delft University of Technology,
to be defended publicly on Tuesday August 29th, 2023 at 15:00 P.M.

Student number	5282829	
Project duration	November, 2022 – August, 2023	
Thesis Committee	Prof.dr.ir. Olindo Isabella	TU Delft, Head of the PVMD group
	Dr. Hesan Ziar	TU Delft, Assistant Professor, Thesis supervisor
	Dr.ir. Özge Okur	TU Delft, Assistant Professor, External committee member
	ir. Victor Arturo Martinez Lopez	TU Delft, Ph.D.candidate, Daily supervisor

TU Delft

Preface

This report is a product of the thesis project course (SET3901) in the Sustainable Energy Technology (SET) master programme at Delft University of Technology. I am delighted to present this thesis research to all the readers. Prior to enrolling in this SET program, I worked as an engineer in an oil and gas business company in Thailand. With the realization of the significance of sustainable energy and its transition, I foresee the necessity to broaden my knowledge in this area with the expectation that it would brighten a great opportunity in my future career path. I hope that this report would be beneficial and motivating to all readers, especially the one who is interested in solar energy development.

At the end of this project, I have greatly strengthened my skill to utilize a specific spatial-related software, ArcGIS, to evaluate a massive amount of data and perform the analysis. One key takeaway is that the model's capability to generate an accurate result is highly dependent on the input data quality of land identification. Although there is still room for development in the model for more realistic results, I am optimistic that the approach and methods described in this report to conduct the suitability model will be applicable and helpful for further application.

I would like to acknowledge the contributions of all personnel to this work. Starting with Victor Arturo Martinez Lopez, my daily thesis supervisor and the person who initiated this project, not only did he regularly offer me constructive feedback during the weekly progress meetings, but he also encouraged me that this project is worthy of being my thesis. I hope that this work is also helpful to his Ph.D. research. Next, I would like to thank my official thesis supervisor, Dr. Hesan Ziar, for sharing his thoughts on the subject and pointing out a few overlooked details during the midterm and Greenlight sessions. In addition, I am grateful to have Prof.dr.ir. Olindo Isabella and Dr.ir. Özge Okur as my thesis committee member. Apart from the PVMD group, I couldn't have started my academic life without the strong encouragement from Pimchanipa Pensiri at the beginning of my journey. I cherish the memorable time with the Thai association in Delft which was always filled with wonderful food and lots of laughs. I would like to also thank Siwarak Unsiwilai, on whom I can always rely whenever I need administrative assistance, and Chanakan Roongthitithum, who has provided constant support throughout the thesis period from afar. Lastly, I would want to thank all of my friends, including, Ilkin, Saurabh, Santiago, Limberis, and others, for accompanying me throughout this academic experience.

Poomisub Manonukul
Delft, August 2023

Abstract

With the rapid increase in renewable energy demand, various kinds of renewable technologies have been realized. Of particular interest is that they require a certain amount of space, and they may conflict with other land utilization purposes such as food production, protected nature areas, and life-sustaining services, thus the land use pressure is multiplying. For this reason, spatial management is required to analyze the optimal locations for such implementation.

A site suitability analysis is one of the applications that could be used to address this issue. Typically, it was done by mainly examining two constraints: technical and economical criteria, and excluding natural locations from the analysis. The challenge is that without the consideration of an environmental aspect, rich nature areas that are not included in the protection zones, cannot be identified. Therefore, this research aims to conduct the site suitability analysis for ground-based solar energy technology in the Netherlands and advance a suitability model by incorporating the environmental criterion in the assessment.

The study was designed into four phases. Beginning with *Phase 1*, a compatibility index was developed based on the concept of area degradation. This technique evaluates the compatibility level of an area in terms of an environmental constraint by quantifying the existing land degradation. Subsequently, it was combined with other factors from technical and economical criteria, constructing the suitability index in *Phase 2*. The Analytic Hierarchy Process (AHP) is a method that was adopted in this combination process. At the end of this phase, five suitability maps were generated from the shift in focus among technical, economical, and environmental criteria. Later in *Phase 3*, an additional suitability map was developed by analyzing the locations of existing solar projects in the Netherlands. Finally, an example of applying the suitability results was demonstrated in *Phase 4* through a case study that set an energy target of 35 TWh as a minimum requirement for solar energy development.

As a result, the preferable locations were specified by the suitability model for this energy realization. They are mostly distributed in the western part of the country (Zeeland, Zuid-Holland, and Noord-Holland provinces) around the major urban and industrial sectors. The proportion of land features in these areas is comprised of 0.4% for border of infrastructure, 17.9% for natural areas, 19.3% for urban areas, and 62.4% for agricultural areas.

Nomenclature

Abbreviation	Description
RET	Renewable Energy Technology
IEA	International Energy Agency
SDE	Stimuleringsregeling Duurzame Energieproductie en Klimaattransitie
MCDA	Multi-Criteria Decision Analysis
CEEC	the Carnegie Energy and Environmental Compatibility Model
CBS	Centraal Bureau voor de Statistiek
GIS	Graphical information system
BGT	Basisregistratie Grootschalige Topografie
BRT	Basisregistratie Topografie
BRK	Basisregistratie Kadaster
BAG	Basisregistratie Adressen en Gebouwen
BRO	Basisregistratie Ondergrond
WOZ	Waarde Onroerende Zaken
BRP	Basisregistratie Percelen
OSM	OpenStreetMap
NNN	Netherlands Nature Network
NEN	the National Ecological Network
PV	Photovoltaic
RES	Regional Energy Strategies

CONTENTS

List of Figures

List of Tables

1

INTRODUCTION

Renewable energy technology (RET) is now realized globally as a potential strategy to address the future climate issue of global warming. Several targets were agreed upon and set as benchmarks for needed actions, for example, the Net Zero Emissions by 2050 Scenario [1] introduced by International Energy Agency (IEA). The term 'net zero' refers to a carbon neutral which is a balance between CO_2 that can be reduced or mitigated and those that will still be emitted. These targets could be regarded as an important driver for the advancement of renewable technologies. A record from the IEA demonstrates that the proportion of renewables in global electricity production in 2021 has grown by about 10 percent since 2010 [2]. This trend also proves that more countries are now paying attention to this topic.

The Netherlands is one of the nations that aims to reduce greenhouse gas emissions through its government policies. With the cooperation of various sectors (residents, business communities, electrical network operators, social organizations, etc.), multiple measures have been legally proposed to encourage citizens to invest more in green energy, for instance, a new subsidy scheme for renewable energy generation (SDE++) in 2020 [3]. In addition, there is a target of 35 TWh of sustainable generation on land by 2030 [4], which is one of the Climate Agreement's measures and one of the most frequently mentioned targets. It entails a significant amount of renewable energy development. A report by Cornax, et al. [5] also made an indication of this amount of energy that 10 TWh of solar energy, if fully realized on agricultural land, would therefore cover approximately 0.7 percent of all agricultural land in the Netherlands (equivalent to 166.5 km^2).

With this rapid increase in renewable technology demand, the land use pressure is multiplying. Since land is a limited resource, there is always a controversial debate on which kind of development would be ideal for a particular location. In one aspect, it may conflict with other land utilization purposes such as food production, protected natural areas, and life-sustaining services. For this reason, spatial management is one of the challenging tasks that need to be strategically carried out to mitigate this issue.

The problem gets more complicated when RET technically requires a large area. This is because its energy conversion efficiency is usually low, so it needs more space for additional installation to compensate for the energy losses. Another reason could be economies of scale which describes why the cost advantages can be achieved by increasing production. From an investment standpoint, this explains that a larger scale of development is preferable to the smaller one [6].

Attempts to emphasize these spatial problems in the Netherlands can be seen through recent government strategies and policies. Focusing on solar energy, one interesting campaign is the so-called *Solar Ladder* [7]. It was introduced based on the realization that the country has less free space for solar fields. In principle, it promotes multifunctional use of space on the premise that solar electricity generation can be coupled with other existing applications. As a result, the order of preference for installing solar panels has been listed, and municipalities can use it to prioritize, for example, projects on rooftops or buildings in built-up areas over agricultural land in the countryside. Moreover, there is an initiative project named *Eco Certified Solar Fields* [8], which examines how the negative impacts of solar panels on biodiversity and soil quality can be identified and mitigated. It recommends a quality-based design for solar fields that incorporates other ecological functions, such as livestock, pollination, etc., in the same area. This project is scheduled to be applied in 2025. A last example of remarkable initiatives is *Regional Energy Strategies (RES)* [9]. It is a national program under the Climate Agreement that investigates the suitability of an area for renewable technology development. All areas in the Netherlands are divided into 30 regions where local authorities in each region are responsible for determining how they can best generate sustainable energy concerning the specific characteristics of the region. Figure 1-1 depicts one of this program's case studies, *Solarpark De Kwekerij*, which is the most biodiverse solar park in the Netherlands in 2021 [10].

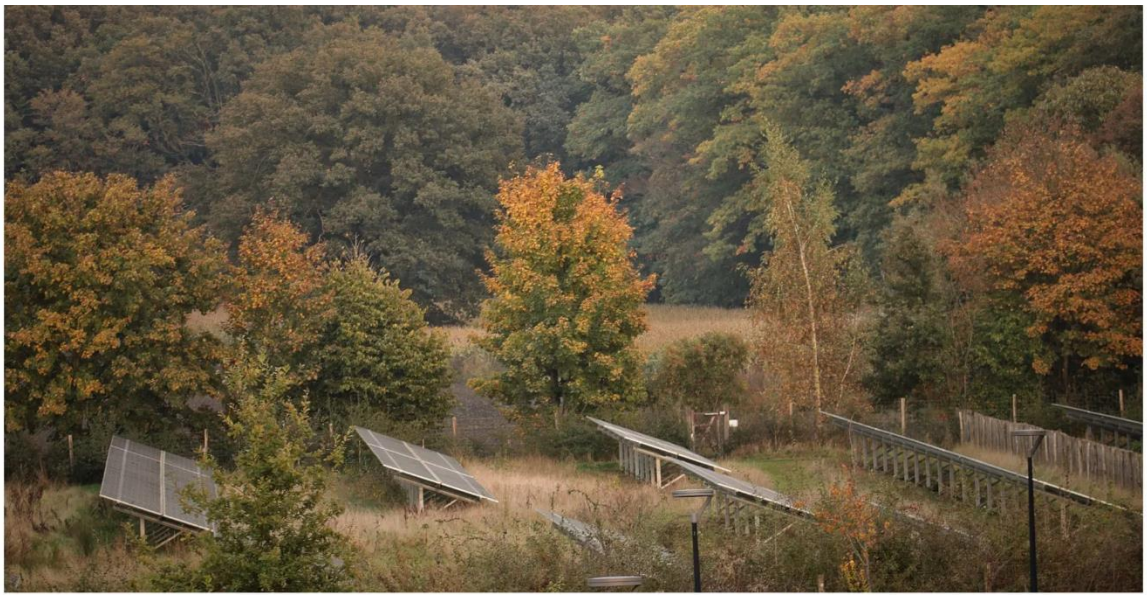

Figure 1-1: *Solarpark De Kwekerij* in Hengelo (Gelderland), where the configuration of the solar field was designed to support the surrounding ecological system [10].

Given the above, strategic spatial planning is necessary to balance the contrast between the need for renewable energy and the limited land space. This conflict is the beginning point of this report's study. In the following sections, it will be explored in greater detail what measures are typically employed and how they might be improved in the context of the spatial problem of utility-scale solar development.

1.1 State of the art

Where are the proper locations in the Netherlands to install solar fields? This is a guiding question for the workflow of this work. To begin with, it is necessary to acknowledge that there is a number of factors that are known to either support or oppose the transformation of an area to solar energy development. Examples of them are economic benefits, property values, project size and details, construction process, etc. Some factors, such as local environment impacts and public opinions, also play a vital role in the selection process, but they are likely to vary depending on regional characteristics. With different forms of data and information, the problems become more complex, and difficult to make a decision on the suitable locations [11].

The most widely used approach to tackle this issue is called a Multi-Criteria Decision Making Analysis (MCDA). It is an operational method that addresses a particular problem that involves the consideration of multiple perspectives or criteria in order to assess the decision alternatives [12]. Wang, et al. [13] reviewed this corresponding approach through four main stages, consisting of selecting a set of related criteria, assigning relative importance to each criterion, evaluating the result, and aggregating all alternatives resulting from different sets of criteria weights. In this section, the literature review will investigate which parameters are commonly adopted for the MCDA of sustainable energy, which technique is used to determine the criteria weight, and how the authors draw conclusions from their findings.

Regarding the criteria selection, several concepts have been proposed [11, 14, 15], but the one that was followed by this research is *the sustainable energy landscapes* introduced by Stremke [16]. This concept was created by underlining the impact of renewable energy development on local landscapes. In principle, it begins with a slight distinction between the definitions of “renewable” and “sustainable” stating that sustainable energy needs to be obtained from a renewable energy source, yet renewable energy is not always sustainable. This brings up the controversy of “Green on Green” to consideration [17], where the first Green refers to clean energy from renewable technologies and the second Green represents the environment. It has been suggested that sustainable energy landscapes require not only renewable technology but also an understanding of how it might be deployed in a sustainable manner taking into account the landscape properties, the existing inhabitants, and other landscape users.

As an end result of Stremke [16], a comprehensive conceptual framework for the sustainable energy landscapes was developed with four dimensions: Sustainable technical, Economical, Environmental, and Socio-cultural as illustrated in Figure 1-2. It was explained that the decision-making result would be affected by factors that fall under these four categories. Depending on which variables are assigned and how stringent they are, the framework can be utilized for a variety of objectives. A few examples of them are shown in the same figure.

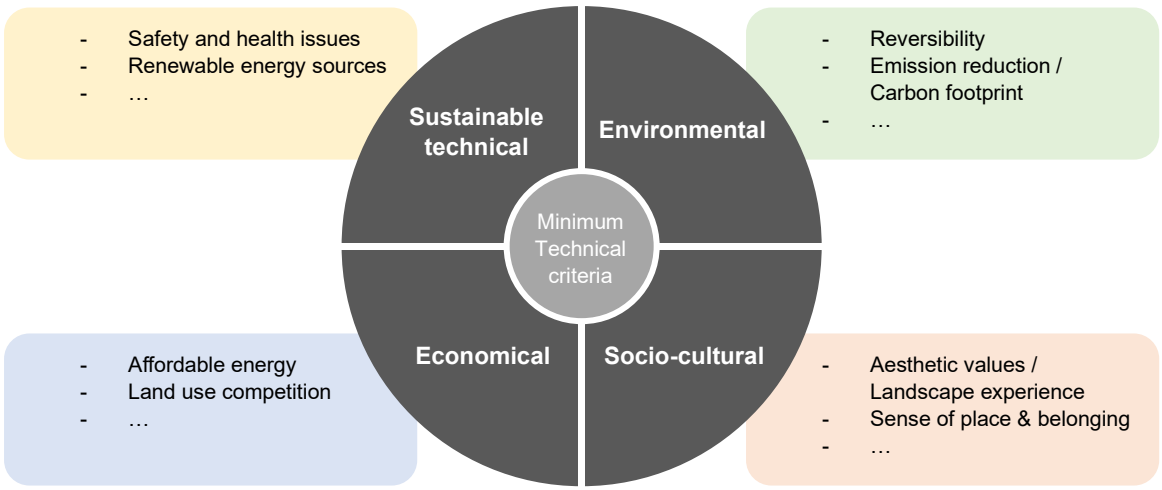

Figure 1-2: The conceptual framework of sustainable energy landscapes [16], which consisted of four sustainability dimensions: Sustainable technical, Economical, Environmental, and Socio-cultural, with examples of factors in each criterion.

Focusing on the site suitability analysis of utility-scale solar development, Table 1-1 provides examples of factors and exclusion areas that had been selected from other literature. They are reclassified into four aspects of sustainability dimensions based on the view of the energy landscapes framework mentioned in the previous paragraph. The table reflects the most common criteria used in each study. This proves that the framework is a helpful tool for this kind of analysis.

It can be concluded from the table that factors in technical and economical criteria are typically selected for the four sustainability dimensions, while those in the other two criteria, environmental and socio-cultural, are mostly classified as an exclusion area. This interpretation is also consistent with the discussions from Sward, et al. [18]. They examined existing solar siting studies and compiled a list of the criteria that were frequently used in those references. According to their observation, the top three factors of decision criteria are solar insolation, distance to power stations, and land slope, whereas the top three exclusion areas are protected land, farmlands, and open water & wetlands. Besides, they provided a recommendation to integrate more components that better represent environmental and social aspects in the analysis.

However, a method to collect both environmental and socio-cultural aspects in the analysis is challenging. One reason is that there are considerable factors that could influence the making decision on renewable energy projects. An example of this is a study carried out by Enserink, et al. [11] in which almost sixty factors from both aspects had been diagnosed. Another reason is the fact that those factors, such as biodiversity, ecological impact, aesthetic, place attachment, etc., are frequently subjective and difficult to be quantified. Thus far, most literature ended up presenting these two aspects in a descriptive way, leaving only a few of them to deal with these difficulties.

Table 1-1: Examples of factors used in the MCDA of solar energy development (sorted according to the sustainable energy landscapes framework).

	Author Year	Four sustainability dimensions				Excluded areas
		Sustainable Technical criterion	Economical criterion	Environmental criterion	Socio-cultural criterion	
1	Arán Carrión, et al. 2008 [19]	- Global irradiance - Diffuse radiation - Equivalent sun hours - Temperature - Slope - Aspect	Proximity to - Roads - Substations - Urban areas	- Land use	- Visual impact	- Protected nature reserves - Sites of community interest - Livestock trails - Road networks - Rivers - Coastal zones
2	Charabi and Gastli 2011 [20]	- Solar radiation	Proximity to - Roads	-	-	- Dams - Flood areas - Land use - Village boundary - Historical and touristic monuments - Rivers - Sand dunes - Roads - Slope > 5°
3	Effat 2013 [21]	- Solar radiation - Aspect	Proximity to - Roads - Cities - Power lines	-	-	- Water bodies - Cultivated lands - Natural vegetation areas - Urban areas - Wetlands - Road buffers

Table 1-1: Examples of factors used in the MCDA of solar energy development (sorted according to the sustainable energy landscapes framework). *(Continued)*

	Author Year	Four sustainability dimensions				Excluded areas
		Sustainable Technical criterion	Economical criterion	Environmental criterion	Socio-cultural criterion	
4	Brewer, et al. 2015 [22]	- Solar irradiance - Slope	Proximity to - Roads - Power lines - Water sources	-	-	Buffer distances - Nesting sites - Historic landmarks - Recreation areas - Agricultural areas - Residential areas
5	Alami Merrouni, et al. 2018 [23]	- Global Horizontal Irradiation - Slope	Proximity to - Residentials - Roads - Railways - Electricity grids - Waterways - Dams - Groundwater	-	-	Buffer distances - Roads ≤ 100 m - Railways ≤ 100 m - Vegetation covers ≤ 500 m - Hydrological features ≤ 500 m - Residential areas ≤ 5 km - Small cities ≤ 2 km
6	Giamalaki and Tsoutsos 2019 [24]	- Solar potential - Slope - Aspect - Elevation	Proximity to - Roads - Coastlines - Power lines - Water bodies	- Land cover	- Visibility from most-visited sites	- World heritage areas, archaeological monuments and historical places of high importance - Areas of absolute protection of nature - Centre of national forests, nature monuments, aesthetic forests - Other areas that fall under a special land-use regime - Sites of Community of the NATURA 2000 network - Aesthetically and scientifically highly values geotopes - Rocky islets - Settlements and traditional settlements

Table 1-1: Examples of factors used in the MCDA of solar energy development (sorted according to the sustainable energy landscapes framework). *(Continued)*

	Author Year	Four sustainability dimensions				Excluded areas
		Sustainable Technical criterion	Economical criterion	Environmental criterion	Socio-cultural criterion	
7	Messaoudi, et al. 2019 [25]	- Potential of hydrogen production - Hydrogen demand - Digital elevation model - Slope	Proximity to - Roads - Railways - Power lines	-	-	- Slope > 5.71° - Elevation > 2000 m Buffer distances - Roads < 500 m - Railways < 500 m - Power lines < 250 m - Waterbodies < 1000 m - Waterways < 500m - Land use < 500 m
8	Finn and McKenzie 2020 [26]	- PV potential - Slope - Aspect	Proximity to - Roads - Residentials - Hydrological features - Restricted areas	-	-	- Urban/developed land - Water - Woodland (deciduous and coniferous) - Slope ≥ 5° - Aspect (Southwest to Southeast orientation only) Buffer distances - Hydrological features ≤ 10 m - Transport features ≤ 100 m - Address points ≤ 100 m - Restrictive areas ≤ 500 m
9	Wang, et al. 2022 [27]	- Solar radiation - Slope - Landslide risk areas	- Energy substations - Energy use centers - Public lands - Transportation facilities - Transportation ways	- Environmental protected land - Other important natural areas - Other natural areas - Agriculture lands - Aquaculture lands	-	-

In terms of sociocultural constraints, the method for measuring societal acceptance is highly diverse [28-30] because it requires an opinion from individuals that is vulnerable to being biased by variables such as age, location, education, political ideology, etc. In order to connect the social term to the site suitability analysis, the core principle is to determine quantifiable parameters that could represent social criterion. This is exemplified in a survey study by Carlisle, et al. [31] that examined the public's attitudes toward large-scale solar energy development in the United States. A series of systematic questions were sent to respondents including 619 National and 405 Southwestern samples. The result of the study provided an overview of characteristics that are significantly related to support or opposition to large-scale solar projects, which are project size, proximity, and visual impact. Later, another survey research from Carlisle, et al. [32] was published. This time, it focused more in detail on public preferences for buffer distance between the solar facility and nine distinct land features. With this quantitative result, Brewer, et al. [22] were able to apply it as a socio-cultural criterion in their site suitability analysis for utility-scale solar power in the Southwestern United States. Another example is an approach to conceptualizing social impact offered by Tello [33]. It describes the connection between solar development and its effects on community issues. Initially, four parameters including; health, crime, green spaces, and real estate values, were suggested. Each of them can be assessed by different indicators which are health index, crime rates, the amount of green space, and property values respectively. At the conclusion, additional parameters that could be converted into numbers, are recommended in order to enhance the effectiveness of the module.

In terms of environmental constraints, a general method is to observe the impact of the solar field through changes in the existence or behaviors of specific fauna or flora nearby [34, 35]. Due to their living adaptation ability, these ecological changes are anticipated in response to human intervention. One of this kind of study is the Mojave Desert Ecoregional Assessment by Randall, et al. [36]. They identified a distribution of biodiversity conservation values across the Mojave desert region in the United States. A conservation value map was created by using the conservation planning software Marxan and a variety of conservation species targets. Finally, the map's regions were classified into four categories (Ecologically core, Ecologically intact, Moderately degraded, and Highly converted). This map was then applied by Cameron, et al. [37] as an environmental criterion in the site suitability analysis of solar energy development in the Mojave desert. Another alternative study was performed by Hernandez, et al. [38]. Their multiple criteria model called the Carnegie Energy and Environmental Compatibility Model (CEEC), takes into account ten different land cover types, such as grassland, open space, forest, etc., in the analysis. A result of their study is a three-classed spatial compatibility map (Compatible, Potentially compatible, and Incompatible) for solar energy development in California.

Even though a few initiative approaches have been proposed to address the lack of environmental and social criteria consideration in the site suitability analysis, they are still not widely implemented. One major drawback of these techniques is that they require great effort to conduct the study. In the case of a survey study, a certain number of respondents would be needed to assure the results. Or, in the case of wildlife observation, it would be difficult to periodically locate and monitor them. Moreover, the proposed approaches in some literature were not clarified in sufficient detail, making them not practical to follow. For this reason, the study in this report will tackle the issue of environmental criterion, as it is one of the research gaps in the MCDA for solar energy development.

1.2 Area of Study

This research is concerned with the entire of the Netherlands as its study region. The country locates in northwestern Europe and shares borders with Belgium to the south, Germany to the east, and the North Sea to the north and west as depicted in Figure 1-3. The main characteristic of the Netherlands' topography is a flat terrain, most of which lies below sea level [39].

Regarding climate conditions, the country spots in a temperate zone in the Northern Hemisphere, which is an area in the middle latitudes between the equator and the North polar region, hence, the temperature swings throughout the year. The mean temperature ranges from 3°C to 18°C during the winter and summer seasons respectively [40]. For wind speed conditions, it is prominent since statistical data collected in the period 1991-2020 [41] shows that the average wind speed can increase from 5 m/s (yearly average) to beyond 20 m/s during the windiest hour.

Figure 1-3: The country of the Netherlands [42].

Moving on to the renewable energy technology preference, wind energy is a majority followed by solar energy because of the high wind speed condition in the Netherlands. There were 2,606 wind turbines realized at the end of 2020, with approximately 80% located on land, and 20% at sea [43]. To compare the extent of different types of RET, the amount of generated electricity from each source was investigated. Figure 1-4 (upper) demonstrates the statistical data of the net electricity production[1] from *Centraal Bureau voor de Statistiek* (CBS) [44]. The energy is categorized into four main renewable sources; hydropower[2], wind energy, solar energy, and biomass during the year from 2013 to 2022. This data is duplicated in Figure 1-4 (lower) but presented in another form of a percentage share of all renewable electricity production.

[1] The electricity production excluding self-consumption
[2] Net electricity production by hydropower is relatively small, hence the scale might be too low to be seen from the figure

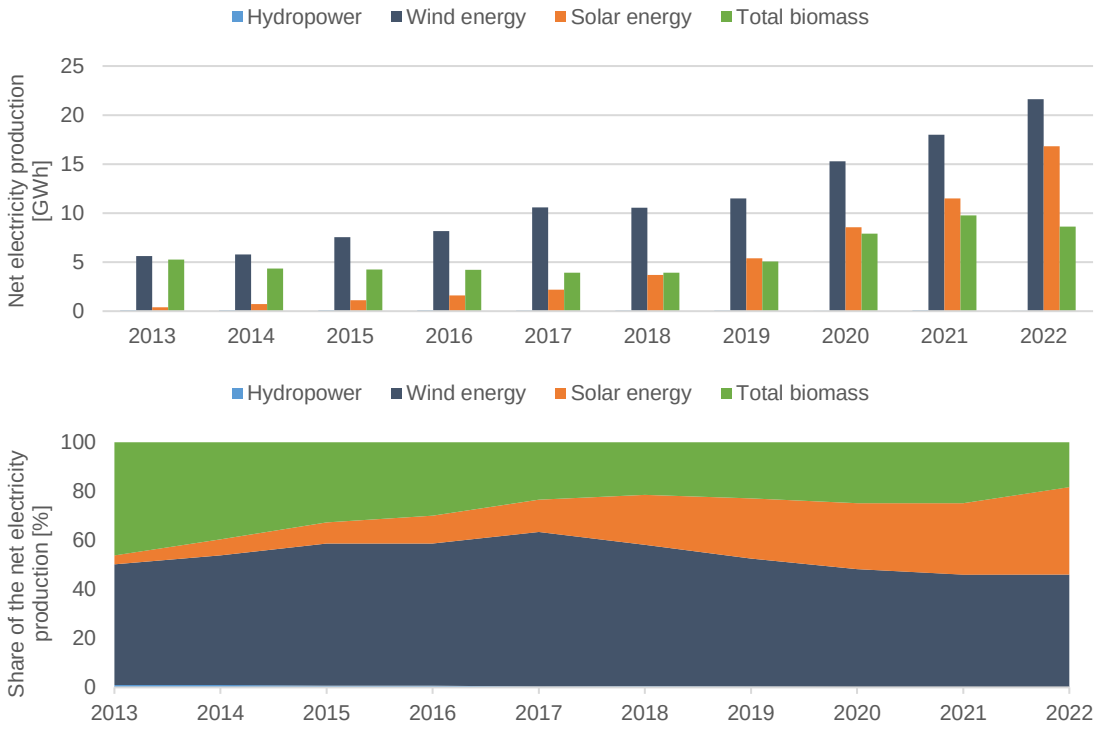

Figure 1-4: (Upper) Net electricity production, presented in GWh, from four renewable sources in the Netherlands (hydropower, wind energy, solar energy, and total biomass); (Lower) The same net electricity production presented as a percentage share. Data taken from *Centraal Bureau voor de Statistiek* (CBS) [44].

These graphs reveal that although wind energy is the superior renewable energy source to others, solar energy has a significant potential to be an alternative source as well. This can be seen from the trend in the graph that the amount of net electricity generated from wind turbines increased steadily every year (navy plot), while the electricity from solar technology rose exponentially since 2018 (orange plot). As a result, the percentage share of solar energy became greater in the last five years, from 13% in 2017 to 36% in 2022. This evidences great attention on solar energy development in recent years.

As far as the spatial issue is concerned in this study, It is beneficial to review the current function of an area in order to understand the mainland features in the Netherlands. According to the database from CBS in 2017 [45], the proportion of eight forms of land use is displayed in Figure 1-5. It shows three main uses of the land including 19% of water bodies (all shades of blue), 12.6% of the areas that are highly intervened by humans (all shades of red), and 14.7% of the natural areas with 53.7% of agricultural land (all shades of green). It can be seen that around half of the country's land is dedicated to agricultural activities; if renewable energy technologies could be implemented on parts of this landscape, they would provide a great deal of potential.

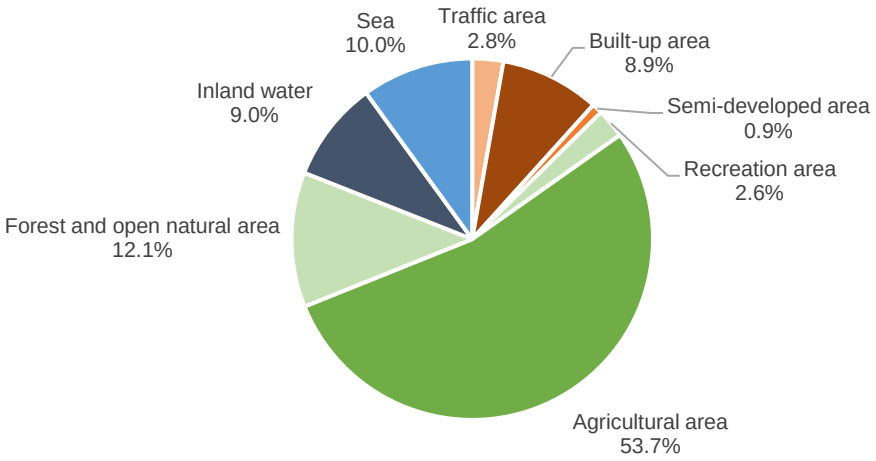

Figure 1-5: The proportion of land use in the Netherlands in 2017, categorized into three main features: water (all blue shades), developed areas (all red shades), and green areas (all green shades). Data taken from *Centraal Bureau voor de Statistiek* (CBS) [45].

1.3 Objectives of Study

This research aims to conduct the site suitability analysis for ground-based solar energy technology in the Netherlands and advance a suitability model by incorporating the environmental criterion in the assessment. Four basic steps are being adopted in the study. One is to perform a literature review on the solar siting analysis. Next, an indicator representing environmental criterion will be established. It is so-called the compatibility index. Then, other available factors will be together assessed with the environmental constraint in order to create an index that is able to identify the level of suitability of an area in the Netherlands for solar energy development. Lastly, the suitability model developed in the previous step will be applied to the locations of existing solar projects for further analysis. Overall, this study embarks with a main research question:

Which type of land features are suitable for ground-based solar energy development in the Netherlands?

Certain milestones were set to narrow down the analyzing process. This has been done through three sets of objectives which are;

1. To explore available and significant factors related to the environmental aspect
2. To develop a model that can identify the level of suitability of an area for ground-based solar energy projects
3. To examine the relationship between the proposed suitability model and existing solar energy locations

The report is organized through five chapters including the first introduction chapter. Assumptions, input data, and the method used to conduct the study will be covered in Chapter 2. The outcomes of the analysis will be illustrated through figures with explanations and discussions in Chapter 3. Finally, all findings linked to the research question and sub-objectives mentioned above will be concluded in Chapter 4, whereas the limitations of this study, as well as recommendations for further improvements, will be addressed in Chapter 5.

2
METHODOLOGY

This research was conducted mainly using a particular software called ArcGIS Pro. The term “GIS” refers to Graphical Information System. This software is a desktop application for data analytics and visualization in 2D, 3D, and 4D (dimensions). The most advantage of using it is that it provides effective toolsets for editing, customizing, and evaluating the spatial database. The version of the software supplied by the Delft University of Technology is ArcGIS Pro 3.0.3.

Beginning with the characteristics of databases used in ArcGIS Pro (2.1) and the research’s assumptions (2.2), this chapter describes a main procedure that can be divided into four phases. **Phase 1** explains in detail how to compute the compatibility index (2.3) as well as how to validate it (2.4). This index was then combined with the other six layers in **Phase 2** to construct the suitability index (2.5). A selected method to combine all these layers together is called the Analytical Hierarchy Process (AHP) (2.6). Following this, five suitability maps were created by sensitivity analysis (2.7) based on the different interests in each input component. Moving on to **Phase 3**, the locations of existing solar projects in the Netherlands were examined and linked with the proposed suitability model, leading to an additional suitability index (2.8). Then, all results were finalized by excluding areas that have been exploited for other purposes (2.9). Finally, **Phase 4** concludes with a case study demonstrating the implications of applying these results to the renewable spatial policy (2.10).

2.1 Databases

Among various opened data sources that have been reached during an assessment, the most widely used one in this study is the so-called **Geobasic registration**. It was developed by the Netherlands’ government in collaboration with numerous partners and specialists from multiple organizations. This database contains detailed digital data images with essential information which have served for the provision of government services and policies, for example, population data, addresses of locations, office buildings, land features, etc. This data source includes six location-related elements (Table 2-1), each of which contributes a different characteristic of a location. All of

them are periodically monitored and updated by the relevant department. Apart from these six databases, there are additional free-access databases from other sites such as transmission line data from the grid operator, TenneT, and demographic data by CBS.nl. They will be referenced individually in subsequent sections discussing input data.

Table 2-1: The perspective of six geobasic registrations [46].

	Abbreviation	Full name (in Dutch)	Observed Details
1	BGT	*Basisregistratie Grootschalige Topografie*	Physical objects: Buildings, Roads, Water, and Green
2	BRT	*Basisregistratie Topografie*	Topographic elements
3	BRK	*Basisregistratie Kadaster*	Immovable properties, Pipelines and Cable networks
4	BAG	*Basisregistratie Adressen en Gebouwen*	Addresses and buildings
5	BRO	*Basisregistratie Ondergrond*	Soil and Subsurface properties
6	WOZ	*Waarde Onroerende Zaken*	Value of immovable property

Turning now to the data format, common cartographic data that are going to be projected in the ArcGIS Pro, can be allocated into two types [47]. The first one is ***vector*** data. It represents point, line, and polygon features. The second one is ***raster*** data. An example of these features is illustrated in Figure 2-1. Further details will be briefly discussed as follows [48].

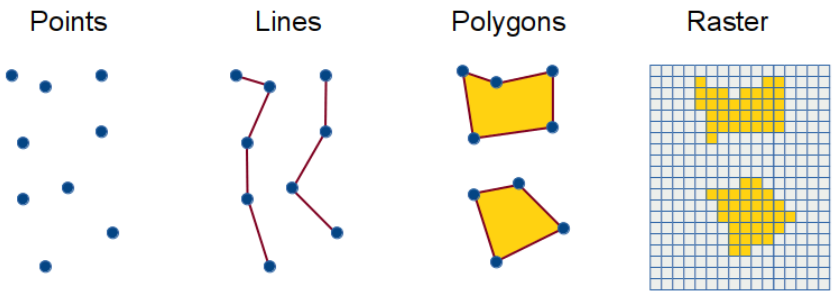

Figure 2-1: Common cartographic format data: Vector (points, lines, polygons) and Raster types [47].

A point feature holds only pairs of x- and y-coordinates without length and area. It is used to model features that don't require those lines and areas to convey the meaning. For instance, addresses, solar park locations, and high voltage mast.

A line feature could be either straight or curved line segments connected between two vertices. The length of each segment is stored as additional data. Features that are usually modeled in this format are roads, railways, streets, and streams.

A polygon feature is a fully enclosed plane territory comprising more than two line segments. The information about an area is attached to each territory. Examples include building footprints, agricultural areas, and demographical data.

Raster is a matrix of cells (or pixels) in which each of them represents only one value at a time. A complete set of data is portrayed through the whole grid. Raster format type can render both discrete and continuous data, for example, land use, surface elevation, images from satellites, digital pictures, or temperature.

Raster data grants additional advantages for a wide range of applications. To begin with, its data structure is simple with only the grid cells and their values. Spatial and statistical analysis would be operated faster with this format. It also has the ability to store those features with any vector types (points, lines, polygons) as well as image and surface data with smaller space requirements [49]. For these reasons, raster data has been extensively used in many kinds of geographical studies including the one conducted in this research.

On the other hand, there is a limitation on raster cell dimensions which might turn the preference to the vector type. This is because the shape of the grid cells has to be square, thus, if the size is too large, it would lose accuracy at the edge of the spatial data. This can be noticed from a dissimilarity among the three raster dimensions in Figure 2-2. To smoother the edge, the raster size needs to be reduced. However, the number of pixels could be significantly increased resulting in more storage space demand and a longer analyzing process. It is necessary to determine how coarse or fine the raster should be to adequately convey the meaning of the data in the analysis. Therefore, an assumption of reasonable raster dimension shall be made.

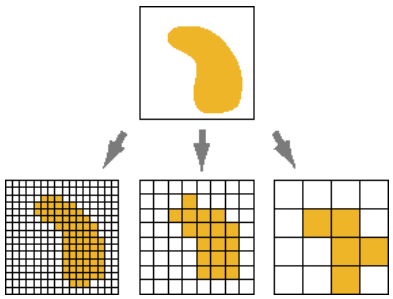

Figure 2-2: An example of the outputs of converting an image to a raster format with three different dimensions [49]. The smaller the pixel size, the better to represent the picture, but it results in a significant increasing in the number of pixels.

2.2 Assumptions

Three main assumptions have been made at the beginning of the study. The first one is a dimension of raster data. It is a critical point that can affect the interpretation of the data results. The other two are related to the scope of the study. A clarification will be declared on which type of solar technology does not include in the analysis. Similarly, the boundary of this research will be addressed in that it does not include a comprehensive design of solar applications in a particular area. The details are as follows.

1. **90 x 90 meters dimension**
   Characterizations of an area within a raster cell are assumed to be the same. Although previous studies generated other resolutions, 5m [13], 10m [22, 26], 1km [23], and 1.5km [50], the grid size of 90 by 90 meters was selected in this study based on the literature from Stoms, et al. [51]. This size is equivalent to a football field. Moreover, it is compatible with the specification of the data processor and storage capacity of the author's computer.

2. **Ground-based solar energy development**
   One of the solutions to tackle the limitations of land use for RET is to consider the space from the sea or water parts. This concept implies floating solar technology in which solar panels are installed on a water surface instead of the ground. However, the focus of this study is on solar projects implemented on land, hence this particular floating solar type is not included. With this assumption, the water availability within the study area was omitted from the analysis.

3. **Quality-based design exclusion**
   The attempts to mitigate the negative impacts of solar facilities on the surroundings have been conducted through several aspects. One solution addresses how the solar parks can be configured to contribute multifunction use of land by adding the function of energy production to the land's original purpose, e.g., food production, transportation, and dwelling. Agrivoltaics [52-54] is a good example of this aspect. It revises a conventional design of solar parks with optional modifications, such as, increasing the panel's height, widening the gap between the arrays, reducing the panel's size, or using vertical bi-facial solar panels, so that there is enough space for crops or grassland to grow in the same area. Other configuration designs [55] based on different land features were also proposed, for instance, an installation of solar panels under the road surface, along with the road sound barrier, or on the dike slope. For some designs, improvements were suggested from an aesthetic point: how could the panels be more colorful, or how to create a wave shape from the solar field [56]? Such propositions could be considered as quality-based designs, which are beyond the scope of this research. Generally, this study was conducted for prospection analysis rather than plant design.

Phase 1

2.3 Procedure – Compatibility Index

The objective of this section is to establish a variable representing the environmental aspect of the sustainable energy landscapes framework. It was first carried out based on a study from Stoms, et al. [51] where an initiative approach of compatibility indicator was introduced. A principal logic is that degraded areas close to the existing infrastructure would have the least potential value for nature and biodiversity, thus these sites are more compatible with solar energy development. Yet, this approach is not a comprehensive assessment of an exact biodiversity value. There are no biological observations or species conservation models performed [51].

According to the Intergovernmental Panel on Climate Change (IPCC) report [57], degraded areas are defined as places both directly and indirectly intervened by human-induced activities, resulting in a negative trend in land quality. They include the change in climate conditions caused by humans, and also the loss of biological productivity, ecological integrity, and values to humans.

An index was established by applying a score to the compatibility concept which could be perceived as described in the equation below. It is the intention of this approach not to exclude natural places such as national parks, recreation areas, and forests, from the decision-making process. Rather a lower score would be assigned for these areas. By doing so, it would be beneficial for the model to reveal the level of environmental significance based on its physical condition. All in all, it is preferred to select the locations for solar parks farther away from natural areas and close to the city.

Higher score = more compatible = more likely suitable for solar development *[58]*

Regarding the compatibility index in this report, three components were considered. The first two are Native Cover and Fragmentation. They were computed by the techniques adopted from the literature [58]. While the third one, named Green, is an additional adjustment to the approach. An average of them will result in the compatibility index. Individual descriptions of each component will be briefly provided in the next part, whereas the details of setting parameters and analyzing steps will be put in Appendix A.

2.3.1 Native Cover component

This component determines the degraded areas based on the removal of vegetative cover which causes the loss in biological productivity. Stoms, et al. [58] differentiate the extent of degraded areas regarding the existing land use in relation to the vegetative cover. In the case of urban development involving massive construction, such as neighborhoods, industrial sites, or transportation routes, a vast majority of ground space would be utilized, leaving no space for plants to grow, thereby resulting in highly degraded areas. On the other hand, in the case of rural or agricultural areas where the land has not been completely disturbed, it is likely that the vegetation would recover after a certain period of time, defining this type of terrain as moderately or lightly degraded.

The Native Cover map was developed by analyzing three spatial data inputs (Table 2-2). An overview of them in the software is illustrated in Figure 2-3. Starting with a layer of terrains from the BRT, all ground areas in the Netherlands were classified into 21 land types. In “grassland” category, it includes agricultural areas as well as other parts with some amount of grass, for example, small gardens, city parks, front lawns, and backyards. However, only agricultural land is considered because it covers more than half of the country's area (Figure 1-5). Another registered database called *Basisregistratie Percelen* (BRP) was then placed on the BRT layer to inspect the exact agricultural fields. This resulted in the addition of 5 more categories of land types, bringing the total to 26. Subsequently, an urbanization level was considered to be associated with an extent of land degradation. In other words, the degree of degradation for a particular land type may change depending on its location, for example, residential areas in metropolitan tends to be more degraded than those in rural districts. Thus, five urbanization levels, which are stored in the demographic statistics of the Netherlands were added as another layer. They were estimated based on the density of addresses in each neighborhood [59].

Table 2-2: The data inputs of the Native Cover component.

	Data	Database	Data provider	Taken date	Format	Remarks
1	Terrains	BRT	PDOK [60]	14/02/23	Polygon	-
2	Agricultural areas	BRP	PDOK [61]	14/03/23	Polygon	-
3	Urbanity levels	CBS	ESRI NL [62]	14/03/23	Polygon	-

(1) Terrains (2) Agricultural areas (3) Urbanity levels

Figure 2-3: An example of three input layers for the Native Cover component projected on the base map of the aerial photograph [63].

Consequently, a 26x5 matrix of the Native Cover map was formed by merging 26 land types with 5 urbanization levels. The final step is to assign a discreet score to the matrix (Appendix A.1). It should be highlighted that a given set of scores is consistent with the study of Stoms, et al. [58].

2.3.2 Fragmentation component

Habitat fragmentation refers to a disconnection of native ecosystems. When linear infrastructure, such as streets, highways, motorways, or canals, is constructed through large and contiguous natural habitats, it fragments these areas into smaller, more isolated ones [64].

Lack of habitat connectivity can lead to a decrease in biodiversity in many ways [65, 66]. It does not only reduce the size of habitats, but also affects the physical conditions in these areas considering air quality, noise pollution, or the change of water flow. Some local species with low adaptation ability will be sensitive to these changes and finally become endangered. Therefore, habitat fragmentation is another dominant component in determining the degraded areas.

The Fragmentation map was modeled through four polyline layers (Table 2-3). They comprise surface transportation networks (roads and railroads), transmission lines (both overhead and underground lines), and artificial waterways (canals and ditches) from OpenStreetMap (OSM) database. Obstacles in water streams (dams and weirs) were also included as they could obstruct the migration of marine species. Figure 2-4 displays an example location for these features. The complete selection of features in the waterways layer can be found in Appendix A.2.

Table 2-3: The data inputs of the Fragmentation component.

	Data	Database	Data provider	Taken date	Format	Remarks
1	Roads	BRT	PDOK [60]	14/02/23	Polyline	-
2	Railroads					-
3	Waterways	OSM	ESRI NL [67]	07/04/23	Polyline	Table A-2
4	Transmission lines	TenneT	TenneT [68]	14/02/23	Polyline	-

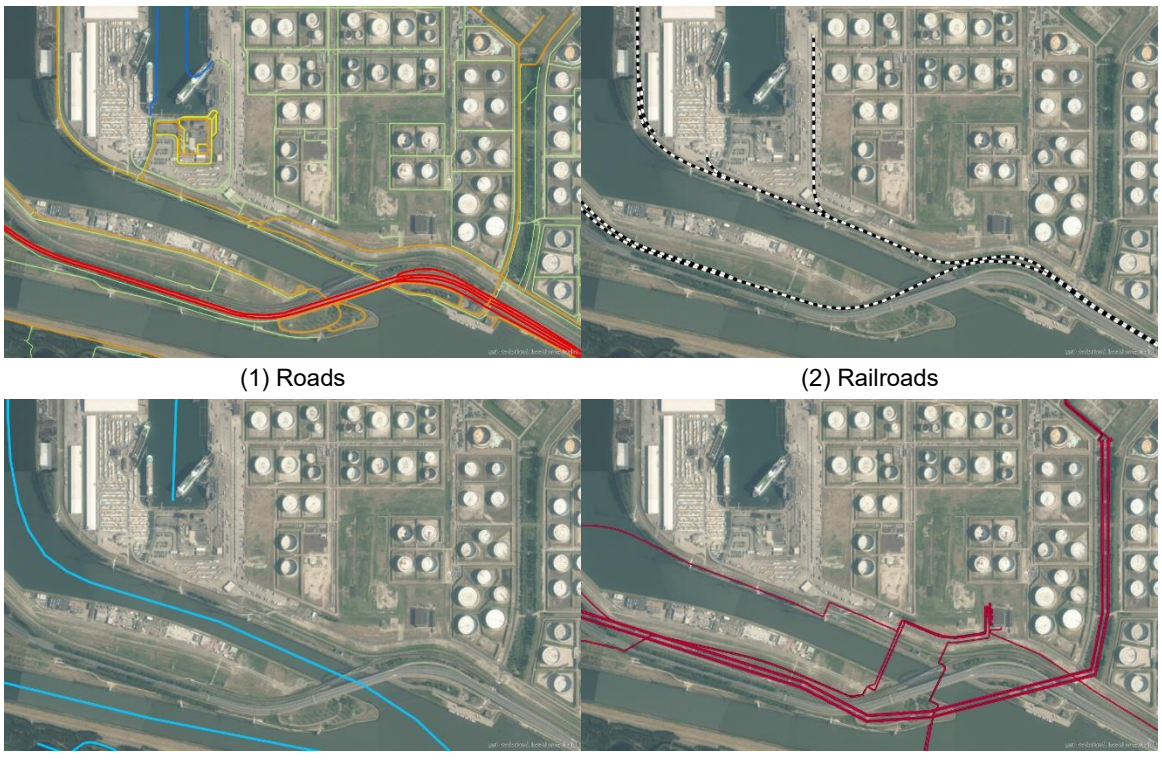

(1) Roads (2) Railroads

(3) Waterways (4) Transmission lines

Figure 2-4: An example of four input layers for the Fragmentation component projected on the base map of the aerial photograph [63].

In principle, the concept is to observe all these line features in each raster cell. The greater the number of lines, the more fragmented it is. The fragmentation score was indicated by the line density value expressed in kilometers per square kilometer (km/km^2). In addition, according to Stoms, et al. [51], specific weights were assigned to each line feature in the line density calculation as indicated in Table 2-4. This is because the degree of fragmentation is proportional to the type and scale of the infrastructure. In conclusion, the fragmentation values from those four layers were combined using the maximum logic, selecting the highest values among them.

Table 2-4: Weights for the linear features in the Fragmentation component [51].

Linear features	Weight
Motorway	9
Highway	6
Regional Road	4
Local Road	3
Street	1
Other	1
Airport	6
Airport Runway	6
Ferry connection	0
Railroad	5
Waterways	5
Transmission line	1

2.3.3 Green component

As previously stated, the Green map is an additional component of the compatibility model. It was proposed by the realization that there are small parks or green areas in the city that could have been habitats for specific living creatures, considering ducks residing along the canal, birds nesting on trees, ants colonizing underground, and flowers or shrubs growing beneath the shade of tall trees. This enhances the quality of the local ecological system.

In this context, the vegetative cover refers to land features under the overgrown and bare terrain databases, which consists of various types of natural landscapes, such as spontaneously flourishing mixed forests, dunes or sand along the coastline, small grassland, bushes, and trees in urban areas. However, it does not include agricultural or arable land types, as they are already accounted for in the Native Cover component. The concept of this component could be interpreted as a contrast to the Native Cover component, as it focuses on the vegetative cover of an area rather than its degradation.

Four layers displayed in Table 2-5 and Figure 2-5 were employed to construct the Green map. It begins with the *"Groen per buurt"* layer by the Climate Impact Atlas [69], which provides an overview of green features (trees, grass, and shrubs) in the form of the area percentage per neighborhood. Although these data might have been used directly for the Green map because they were consistent with the concept of the vegetative cover, the scale of the neighborhood is too coarse in comparison to the raster resolution of 90 meters to adequately portray the green coverage. For this reason, more specific indicators, *"Begroid"* and *"Onbegroid"* terrain from BGT [70], are required to add on top of it. Further details on the selected features of these databases can be found in Appendix A.3. With these two additional layers, the proportion of green coverage per raster pixel

was calculable. These values will subsequently be converted back into a score (the higher the green percentage, the lower the score of the compatibility is). Lastly, the presence of water bodies from the BRT database was indicated in this component. This layer received a score of zero (indicating incompatibility) since the water part is not within the scope of the study, as mentioned in the assumption. For a conservative result, all layers were combined using the minimum value selection.

Table 2-5: The data inputs of the Green component.

	Data	Database	Data provider	Taken date	Format	Remarks
1	*Groen per buurt*	Basiskaarten	Climate Effect Atlas [69]	02/03/23	Polygon	-
2	*Begroid terrein*	BGT	PDOK [70]	14/03/23	Polygon	Table A-3
3	*Onbegroid terrein*					Table A-3
4	Water bodies	BRT	PDOK [60]	14/02/03	Polygon	-

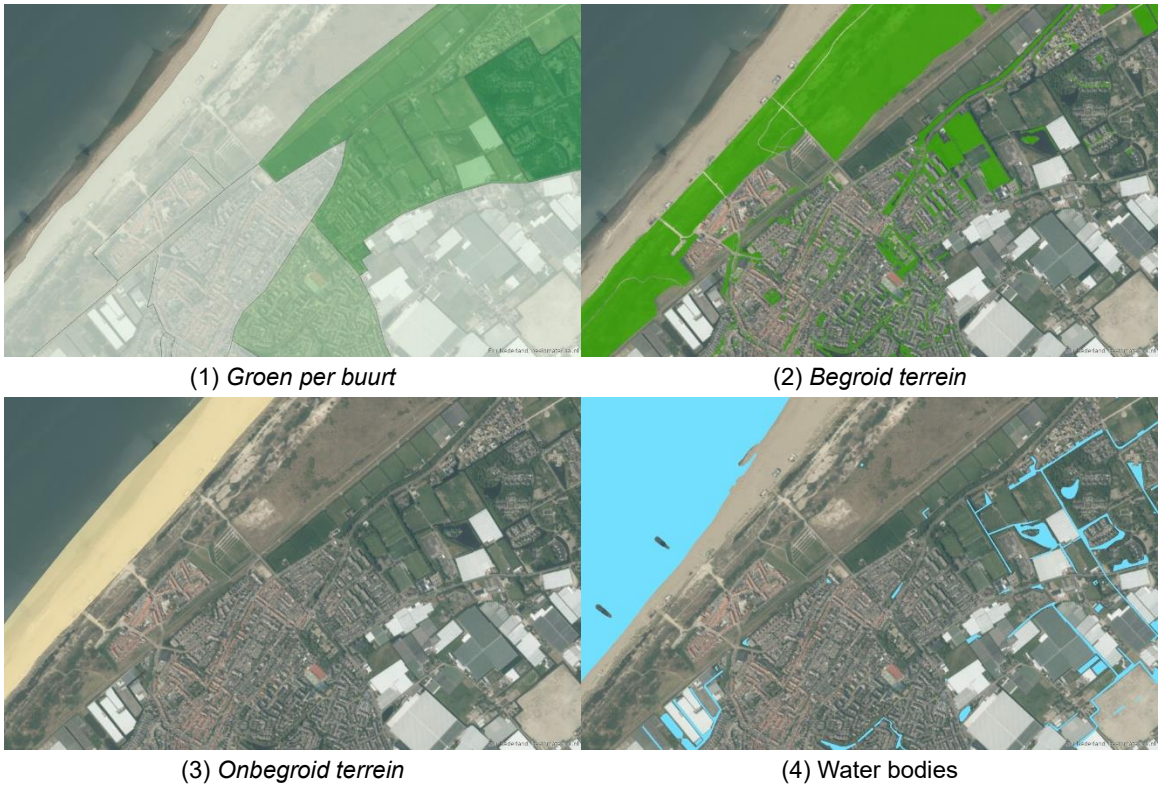

(1) *Groen per buurt* (2) *Begroid terrein*

(3) *Onbegroid terrein* (4) Water bodies

Figure 2-5: An example of four input layers for the Green component projected on the base map of the aerial photograph [63].

2.4 Map Validation

Since the compatibility approach was adopted and modified from the study of Stoms, et al. [58], it is essential to validate whether or not the model result conforms to the concept of a degraded area. This was carried out by comparing compatibility scores in designated natural zones in the Netherlands. A rationale behind the validation process is that these regions hold a high biodiversity value [71], and hence are incompatible with solar installations. Therefore, low compatibility scores could be expected from them.

There are different kinds of protected nature areas in the Netherlands, each of which contributes unique perspectives to the preservation of natural value [71]. The main one that was used in the validation process is from a nature conservation policy called the Netherlands Nature Network (NNN) [72]. It was developed based on the previous policy, the National Ecological Network (NEN) [73], in 2013 by shifting a number of tasks related to spatial planning, the economy, and nature conservation from the national level to the provincial level [74]. However, its principle remains in focusing on larger natural areas both landscapes and waterscapes, that are connected in a coherent network, so that the exchange of various animal populations would occur resulting in higher biodiversity value [71]. Figure 2-6 illustrates designated areas under the NNN (dark green color), which encompass numerous environmental regions of the country, such as national parks, new recreational areas, significant lakes and rivers, and places under Natura 2000 areas [75]. In addition to the NNN, another four protected sites were compared to the compatibility map. They accounted for national parks, national landscapes, geologically significant places, and the Natura 2000 areas. A brief description of them can be found in the reference pamphlet [71] and the figures demonstrating areas under each database will be provided in Appendix A.4. As an overview, Table 2-6 summarizes all databases utilized in the validation process.

Table 2-6: The reference database of natural areas for the validation process.

	Database	Data provider	Taken date	Format	Remarks
1	Netherlands Nature Network	PDOK [72]	05/04/23	Polygon	-
2	National parks	PDOK [76]	05/04/23	Polygon	Figure A-7
3	National landscapes	PDOK [77]	05/04/23	Polygon	Figure A-7
4	Geological values	PDOK [78]	05/04/23	Polygon	Figure A-7
5	Natura 2000	PDOK [79]	05/04/23	Polygon	Figure A-7

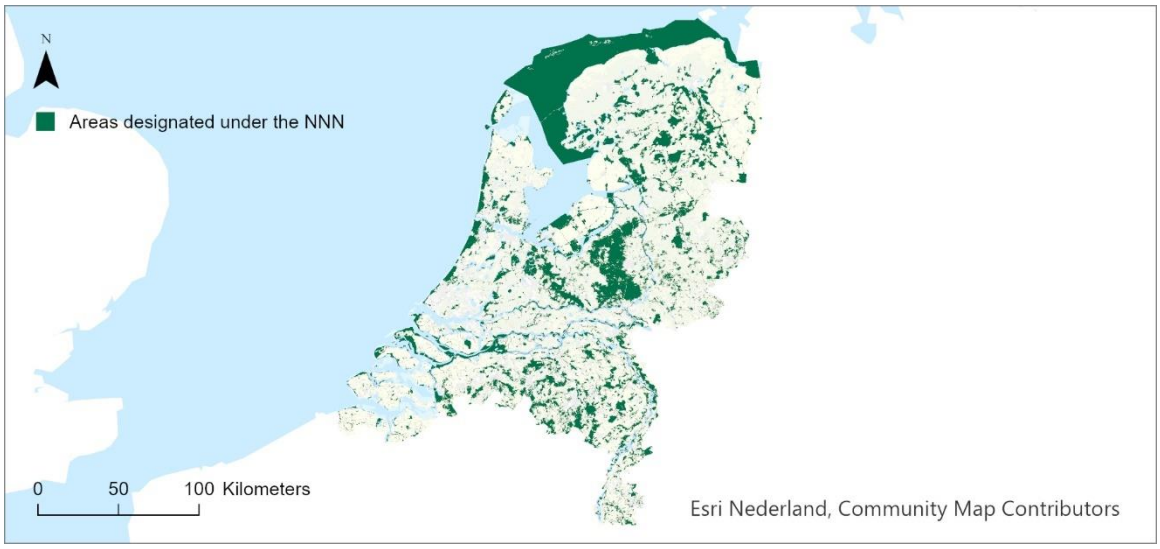

Figure 2-6: Areas under the Netherlands Nature Network (NNN) [72].

Phase 2

2.5 Procedure – Suitability Index

The suitability index is the main result of this research. In general, it indicates which sites are more compliant with all input constraints than others. Throughout this thesis, these constraints correspond to factors under the sustainable energy landscapes framework [16], which applies four primary aspects: Sustainable technical, Economical, Environmental, and Socio-cultural. Examples of typical evaluation factors from each aspect can be found in the study of Wang, et al. [13].

In this study, there are seven factors contributing to the suitability index. The one that was already discussed in the previous phase, the compatibility index, falls under the environmental aspect. For the sociocultural aspect, it will be excluded from the analysis because it requires public opinion, which was unavailable at the time this research was being conducted. The rest of them were identified by a literature review, as reported in Table 1-2. From the data, it can be inferred that slope and solar resources were selected mostly for a technical aspect, whereas proximity to public roads, railways, water bodies, and power lines, as well as the land prices, were favored for an economical aspect.

Hereby, only significant attributes of those factors were included in the suitability index. For this reason, the road feature was filtered for highways and motorways in response to major transportation. Train stations were considered instead of railways since these are the precise locations from which commuters depart. For water parts, the selection has been made on two conditions: the width of the water stream and the coverage area of water bodies. An area specification was roughly drawn from the National Oceanic and Atmospheric Administration (NOAA) guideline [80]. So, the one with a width greater than 12 meters or an area greater than 4,000 square meters will be accounted for.

Besides, three remarks have been made on specific factors. First, The distance to water bodies will be reorganized into the same group as the compatibility index under the environmental aspect. Second, the average house values (*gemiddelde woningwaarde*) from the CBS database will substitute for the land prices. This database provides information sorted into three tiers including neighborhoods (*buurten*), districts (*wijken*), and municipalities (*gemeenten*), ranging from the most fined to coarse data. Third, slope data will be omitted, as the Netherlands' landscape is dominantly flat. In a nutshell, all seven factors were summarized in Table 2-7.

Table 2-7: Seven factors included in the analysis to construct the Suitability Index.

	Data	Database	Data provider	Taken date	Format	Remarks
1	Photovoltaic Electricity Potential	Global Solar Atlas 2.0	Solargis [81]	04/05/23	Raster	kW/kW$_p$
2	Major Roads	BRT	PDOK [60]	14/02/23	Polyline	Highways & Motorways
3	Traffic & Transport	OSM	ESRI NL [82]	21/03/23	Point	Train stations
4	House values	CBS	ESRI NL [83-85]	20/03/23	Polygon	Average House Value
5	Transmission lines	TenneT	TenneT [68]	14/02/23	Polyline	
6	Compatibility Index	Refers to Chapter 2.3 Procedure – Compatibility Index				
7	Water bodies	BRT	PDOK [60]	14/02/23	Polygon	Rivers width > 12 m Water area > 4000 m^2

At this stage, a hierarchy of components for the suitability model can be generated as depicted in Figure 2-7. They can be categorized into two tiers. The first level is from the sustainable energy landscapes framework consisting of three aspects excluding the sociocultural criterion. The second level contains factors that correspond to those aspects. The original map data of each factor can be found in Appendix B.2. Overall, this hierarchy illustrates how the suitability index was built over multi-layers.

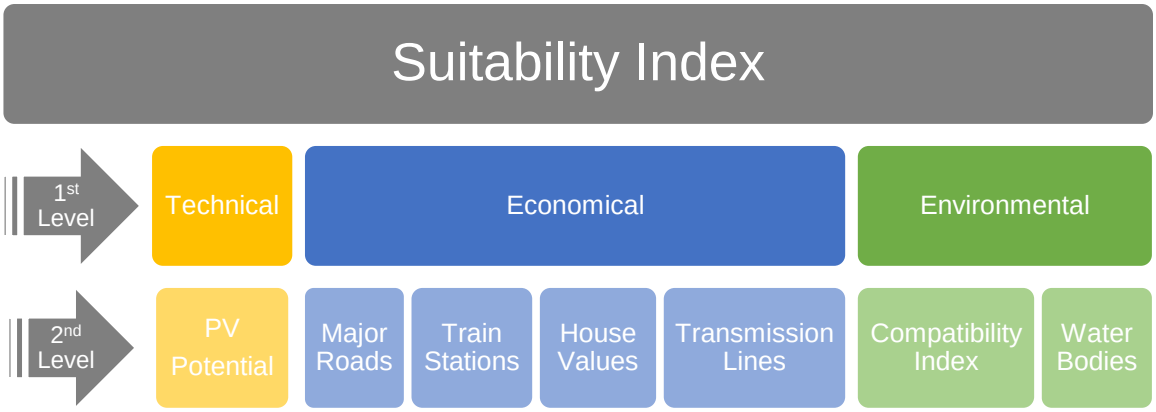

Figure 2-7: Hierarchical multicriteria model of the Suitability Index. It consists of two levels in which the first layer is associated with three aspects of the energy landscapes framework [16], and the second layer is the corresponding selected factors in this study.

The index of suitability was constructed by overlaying these seven input layers together. In terms of value interaction, a linear-relationship formula has been employed to score the suitability map (Equation 2.1). In this sense, the unit of each criterion should be aligned identically. However, factors from these three aspects typically have different units, which makes them unable to directly be applied to the equation. For this reason, the normalization method will be used in this study to standardize the units.

$$A_m = W_1 C_1 + W_2 C_2 + \cdots + W_n C_n \qquad 2.1$$

where
n is a number of criteria
m is a number of alternatives
W_n is the weight of criterion *n*
C_n is the criterion *n*
A_m is the final score of the suitability index of alternative *m*

To transform the original data values into a normalized form, two equations (Equation 2.2 - 2.3) were applied. The decision between them depends on whether the correlation between the data meaning and the concept of suitability is positive or negative. If it is positive, for example, the greater amount of solar resources, the more suitable area for the development, then Equation 2.2 would be adopted. Alternatively, if it is negative, for instance, the closer (lower) the distance to the road, the more beneficial the project receives, and the higher the suitability, thus Equation 2.3 would be utilized. The result of this normalization process of each factor will be provided in Figure B-3.

$$C_n = \frac{x - \min(x)}{\max(x) - \min(x)} \qquad 2.2$$

$$C_n = \frac{\max(x) - x}{\max(x) - \min(x)} \qquad 2.3$$

where
n is a number of criteria
C_n is the criterion n
x is the value of C_n *in each raster cell*

The next step is to estimate the criteria weights, W_n in Equation 2.1, in order to achieve the final score, A_m, of the index. It was accomplished by implementing a particular mathematical technique known as Analytical Hierarchy Process (AHP), which will be detailed in the following section. As a result, the final suitability index score will vary from 0 to 100.

2.6 Analytical Hierarchy Process (AHP)

AHP is an effective tool to derive a hierarchy of alternatives in the decision-making problem. The theory was introduced by Saaty [86] in 1980. It is the most popular technique for RET site suitability analysis because of its simplicity of the weighted sum method [13]. Different determination methods such as fuzzy logic quantifiers, the Best-Worst Method (BMW), Criteria Importance through Intercriteria Correlation (CRITIC), etc., have also been tested in a range of academic papers [12, 20, 87, 88]. They all demonstrated that each technique has its own benefits and drawbacks to compose the suitability map. These were discussed briefly in the study of Wang, et al. [13] and Wu, et al. [89]. Choosing one of them may depend on the study's objectives. Since the effect of weight calculating techniques is irrelevant to the purpose of this research, the most promising one, AHP, was then adopted.

A key notion of AHP is to interpret the importance of each factor into a priority weight that is always summed up to 100% of the consideration. This can be done by comparing all factors for every possible match and assessing them in pairs to determine to what extent one is more/less important than the other. By doing this, a pairwise comparison matrix has to be developed.

The characteristic of the matrix is that a list of factors in the analysis is arranged in rows and columns, resulting in a square matrix. The values within the matrix represent relative importance judgments. Note that a comparison of the same pair should return the same value, but in a transpose form if their order is reversed. For example, if the relative importance of A compared to B is a_{AB}, then this value for B relative to A will be a_{BA} or $1/a_{AB}$. Because of this, only half of the matrix must be completed, as the other half will be in an inverse form. Lastly, the diagonal values are always equal to one because any component compared to itself should be of equal importance. An example of this matrix with seven factors was displayed in Table 2-8.

Table 2-8: An example of a pairwise comparison matrix with seven factors.

Factors	1	2	3	4	5	6	7
1	1	a_{12}	a_{13}	a_{14}	a_{15}	a_{16}	a_{17}
2	$a_{21} = 1/a_{12}$	1	a_{23}	a_{24}	a_{25}	a_{26}	a_{27}
3	$a_{31} = 1/a_{13}$	$a_{32} = 1/a_{23}$	1	a_{34}	a_{35}	a_{36}	a_{37}
4	Inverse form			1	a_{45}	a_{46}	a_{47}
5					1	a_{56}	a_{57}
6						1	a_{67}
7							1

Although It may be straightforward to compare two factors and indicate which one is more or less significant, it is fairly difficult to describe the degree of this relative. Accordingly, a set of absolute scales ranging from 1 to 9 has been proposed in Table 2-9 by Saaty [90] for preliminary

input in the matrix. This is a crucial step in quantifying the relative importance by its definition. The scales can also be turned to a finer number for a particular purpose.

However, the selection of these scores may be arbitrary because it is based on an individual judgment. It is recommended to review the final version of the comparison matrix with other specialists who share the same field of study, to generate a reliable input for AHP.

Table 2-9: An absolute scale for the relative importance with the definition [90].

Intensity of importance	Definition
1	Equal importance
3	Moderate importance of one over another
5	Essential or strong importance
7	Very strong importance
9	Extreme importance
2, 4, 6, 8	Intermediate values between the two adjacent judgments

Prior to examining the AHP result, it is necessary to check the Consistency Ratio (C.R.) of the input whether it is in an acceptable range or not. This issue relates to the transitive property of value. Supposing A is more significant than B, and B is more significant than C, then logically A would be more significant than C. This is true in theory, but it may not always be valid in a real case, especially when there are multiple factors to compare. There may be some perspectives that could influence the significance of C to be more than A. This causes a contradiction with the AHP input. Following the logic, this discrepancy should be lowered as much as possible. In fact, Saaty [90] suggested that it is fair enough to allow some inconsistencies in the comparison matrix, as they could reflect knowledge or information to the preference. In conclusion, the author set a 10% tolerance of the consistency ratio as a threshold. An example of basic AHP calculation will be provided in Appendix B.1.

Having explained what is meant by AHP and the importance of the consistency ratio, this section will now move on to discuss the method to calculate the priority weight. Theoretically, the priorities ought to be approximated using the eigenvector derivation method. All relevant principles and equations behind this method can be found in the literature of Saaty [90]. In comparison to the eigenvector approach, the author suggested two additional simple procedures for estimating the weights. It could be either simplified by normalizing only the geometric means of the matrix's rows. Or the other way is to normalize the elements in each column of the matrix and then average over each row. Nevertheless, these techniques are only applicable when the number of criteria does not exceed three. Hence, for important applications involving several criteria, the original eigenvector method should be used.

Regarding this report, AHP calculations were performed with the help of an open-sourced online template [91]. It was developed by Goepel [92] on the basis of the eigenvector approach. The results were examined and they conformed to the examples in the original paper of Saaty [90].

In terms of the C.R., it can be calculated by two parameters: the Consistency index (C.I.) and the Random Consistency index (R.I.). The first component, C.I., is a number indicating the difference between our comparison matrix and the consistent matrix [93]. This term was mathematically defined by Saaty [90] as a function of the largest eigenvalue and a number of input criteria given in Equation 2.5. The latter component, R.I., is an average consistency index derived from a randomly generated matrix with 500 sample sizes using the absolute scale presented in Table 2-9 [90]. The result of R.I. depending on the number of criteria is indicated in Table 2-10. Finally, Saaty [90] suggested that the consistency ratio can be determined by comparing these C.I. and R.I. as shown in Equation 2.4.

$$Consistency\ Ratio\ (C.R.) = \frac{Consistency\ Index\ (C.I.)}{Random\ Consistency\ Index\ (R.I.)} \quad 2.4$$

$$C.I. = \frac{(\lambda_{max} - n)}{(n-1)} \quad 2.5$$

Where
n is a number of criteria
λ_{max} is a maximum eigenvalue obtained from the AHP eigenvector method

Table 2-10: An index of Random Consistency [90].

n	1	2	3	4	5	6	7	8	9	10
Random consistency index (R.I.)	0	0	0.58	0.90	1.12	1.24	1.32	1.41	1.45	1.49

Returning to this research, three comparison matrices were created by analyzing the relative important values of those seven factors in Table 2-7 from existing studies [19-27]. Determining the values by judging from them as a reference case could benefit the integrity of the input for AHP calculation (less subjective). The matrix in Table 2-11 was applied to the first level of the suitability index hierarchy (Figure 2-7), which includes three criteria; technical, economical, and environmental. The remaining two matrices (Table 2-12 and Table 2-13) evaluate the factors at the second level of the hierarchy, with the exception of the PV potential factor, which is the only one factor under the technical aspect. As a result, these matrices altogether with their final weights and C.I. were shown in the Tables below.

Table 2-11: Pairwise comparison matrix of the Suitability Index calculated by an online template [91].

Suitability Index	Technical	Economical	Environmental	Priority
Technical	1	1/2	2	**0.297**
Economical	2	1	3	**0.540**
Environmental	1/2	1/3	1	**0.163**

C.R. = 1%

Table 2-12: Pairwise comparison matrix of Economical criterion calculated by an online template [91].

Economical criterion	Roads	Train Stations	House Values	Transmission Lines	Priority
Major Roads	1	3	1/3	1/2	**0.156**
Train Stations	1/3	1	1/7	1/5	**0.058**
House Values	3	7	1	3	**0.532**
Transmission Lines	2	5	1/3	1	**0.254**

C.R. = 2.7%

Table 2-13: Pairwise comparison matrix of Environmental criterion calculated by an online template [91].

Environmental criterion	Compatibility Index	Water Bodies	Priority
Compatibility Index	1	9	**0.9**
Water Bodies	1/9	1	**0.1**

C.R. = 0%

2.7 Sensitivity Analysis

At the end of the AHP calculation, sensitivity analysis was conducted to evaluate the impact of each major criterion on the suitability index. Five scenarios were generated (Table 2-14) by varying the relative importance inputs in the first comparison matrix (Table 2-11) including three criteria: technical, economical, and environmental aspects. It begins with a base case for which the priority weights were derived from the literature review (the results are as same as indicated in Table 2-11). The next scenario implements an equal priority distribution where all criteria are of equal importance which is equal to 33.3%. The last three cases are developed on the hypothesis that only one aspect is threefold as significant as the others; hence, the highlighted component accounts for 60% of the total, while the other components account for 20%. Nonetheless, the aggregate of these priority weights from three inputs in every situation is 100.

Table 2-14: Summary of the priority weights in the first hierarchy of the Suitability Index. Five scenarios were generated by shifting the focus among three criteria, with the first base case derived from the literature review, the second case being an equal weight distribution, and the last three scenarios emphasizing a single criterion by assigning it a value three times greater than the others.

Scenario	1	2	3	4	5
Level 1 Priority Weight [%]	Base case from literature	Equal weight distribution	Technical highlight	Economical highlight	Environmental highlight
Technical criterion	29.7	33.3	60	20	20
Economical criterion	54.0	33.3	20	60	20
Environmental criterion	16.3	33.3	20	20	60

In addition, the relative importance of factors at the second level of the hierarchy (Table 2-12 and Table 2-13) can also be modified to provide more scenarios. However, the focus of this study is only the effect of the primary criteria. As a result, the priority weights of the seven sub-criteria factors were maintained throughout all scenarios as they were in the first case (Table 2-12 and Table 2-13).

Table 2-15: Summary of the priority weights in the second hierarchy of the Suitability Index. According to this study, they were kept constant as the same as the first base case for all scenarios.

Scenario	1	2	3	4	5
Level 2 Priority Weight [%]	Base case from literature	Equal weight distribution	Technical highlight	Economical highlight	Environmental highlight
PV Potential	100				
Major Roads	15.6				
Train Stations	5.8				
House Values	53.2				
Transmission Lines	25.4				
Compatibility Index	90				
Water Bodies	10				

In summary, the final priority weight (parameter W_n) in Equation 2.1 can be obtained by multiplying the priority weights of these two levels (values in Table 2-14 and Table 2-15). As a result of the sensitivity analysis, there are five sets of them. All were presented in accordance with each scenario in Table 2-16 below. In any case, the summation of the weights of all factors would equal 100.

Table 2-16: The final priority weights of selected seven factors in the suitability analysis for five scenarios.

Scenario	1	2	3	4	5
Final Priority Weight [%]	Base case from literature	Equal weight distribution	Technical highlight	Economical highlight	Environmental highlight
PV Potential	29.70	33.33	60.00	20.00	20.00
Major Roads	8.42	5.20	3.12	9.36	3.12
Train Stations	3.13	1.93	1.16	3.48	1.16
House Values	28.73	17.73	10.64	31.92	10.64
Transmission Lines	13.72	8.47	5.08	15.24	5.08
Compatibility Index	14.67	30.00	18.00	18.00	54.00
Water Bodies	1.63	3.33	2.00	2.00	6.00
Total	100	100	100	100	100

Phase 3

2.8 Existing solar energy projects

According to the information on large-scale solar energy projects in the Netherlands from ROM3D [94], another branch of spatial analysis can proceed. This source provides a data set containing an overview of solar energy supporting schemes (SDE+, SDE++, etc.) with reference numbers for each project, the capacity in megawatts (MW), types of construction, the status of the project, the year it was realized, and the coordination of its location. The document was up to date as of March 27, 2023. There are 979 solar projects in total including both that were completed and in planning phases. Filtering the data for those ground-based project locations which have been realized and consistent with the aerial photographs [63], only 582 projects were selected. The distribution in locations of these projects was illustrated on the map of the Netherlands in Figure 2-8 below.

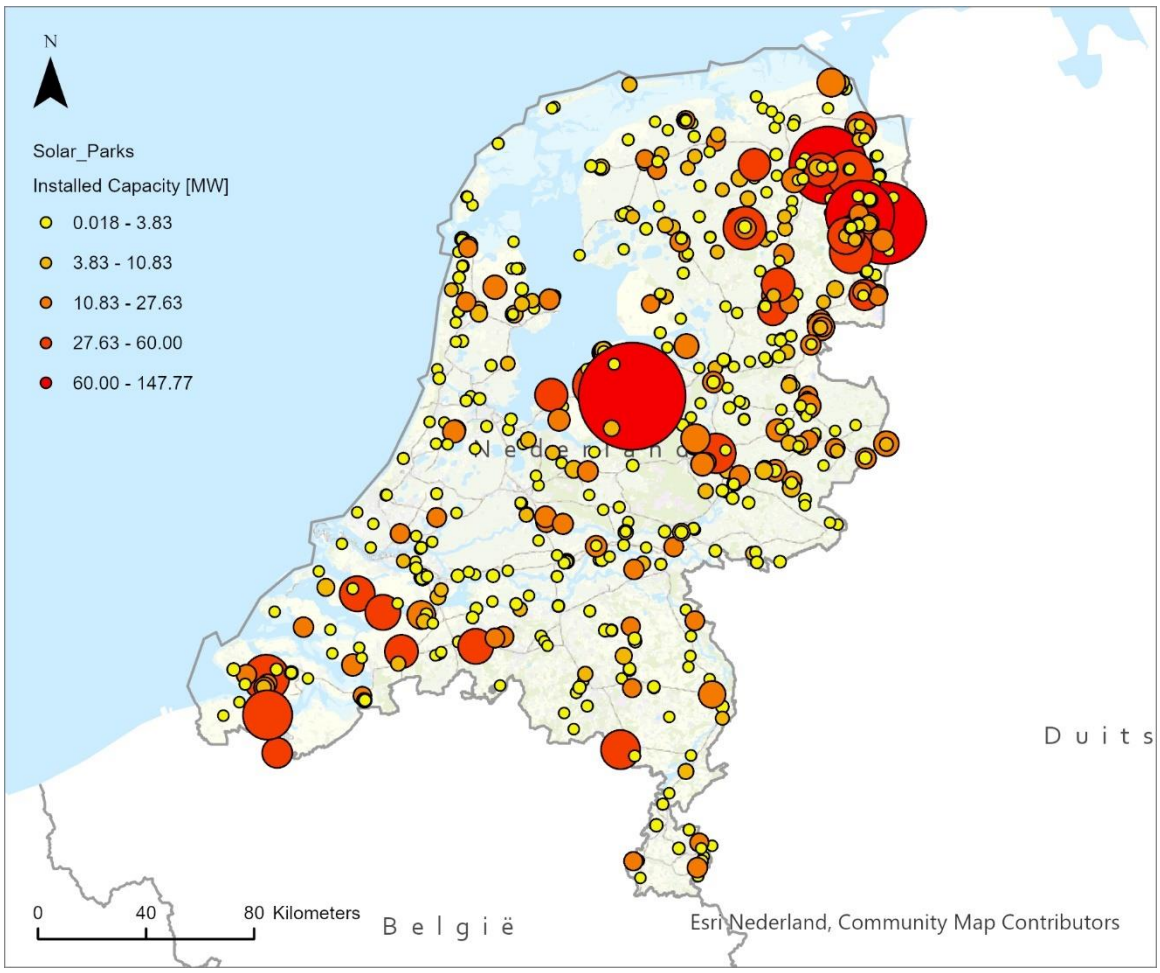

Figure 2-8: The selected solar projects from the ROM3D database [94]. Each circle indicates the location of a single project.

To combine these selected projects with the suitability model (comprised of three major criteria with seven input layers), their locations were used to extract the values from each layer. This leads to 7 groups of 582 scores for each factor. The distribution of these scores per group is illustrated in a box plot (Figure 2-9). This graph illustrates the breakdown of the suitability score from the existing projects regarding the seven input components.

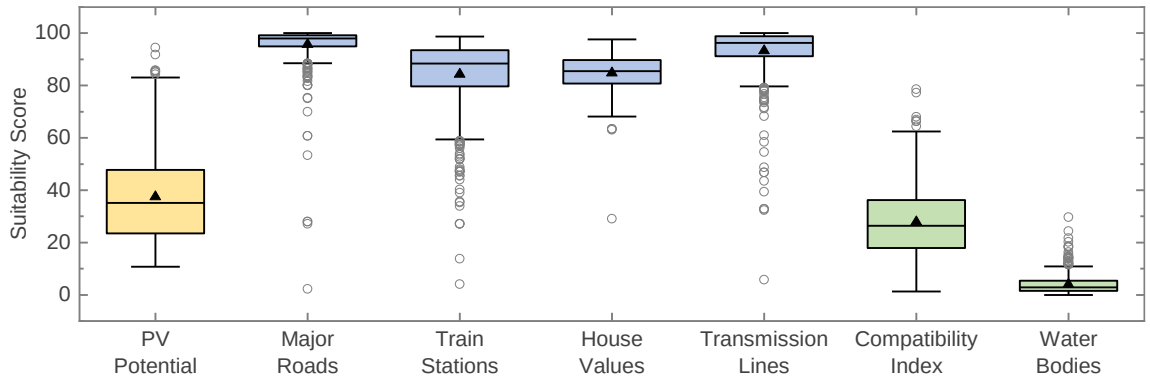

Figure 2-9: The score distribution of the seven input factors for the suitability index based on the locations of the selected solar projects. The triangle mark refers to the mean value of each distribution and the circles stand for data outliers.

From these data distributions, another set of priority weights can be generated. The figure demonstrates that the existing solar energy projects pay the most attention to an economic criterion as most of their locations receive a higher score in this constraint. On the contrary, the score distribution for a technical criterion has a mixed pattern varying from low to medium values, while those scores for an environmental criterion typically fluctuate within a lower score range. From this perspective, the graph reveals that the importance of an economic criterion should be greater than that of technical and environmental criteria. By performing a normalization on the mean value of each distribution, an additional priority weight can be obtained. Both the mean value and its associated normalized form are summarized in Table 2-17.

Table 2-17: The mean value and its normalized form of the score distribution of seven input factors in the suitability analysis, extracted from the locations of the selected existing solar projects.

Factors	PV Potential	Major Roads	Train Stations	House Values	Transmission Lines	Compatibility Index	Water Bodies
Mean Value	37.47	95.71	84.24	84.78	93.22	27.80	3.99
Normalized Mean	**8.77**	**22.40**	**19.72**	**19.85**	**21.82**	**6.51**	**0.93**

The sixth scenario from this section was added to the sensitivity analysis. The final weights from the previous five study cases are repeated in Table 2-18, along with an additional weight derived from the selected existing solar energy projects. These data will then be employed to construct six suitability maps that will be presented in the following Chapter 3.

Table 2-18: The final priority weights of selected seven factors in suitability analysis for five scenarios with an additional case of existing solar projects.

Scenario	**1**	**2**	**3**	**4**	**5**	**6**
Final Priority Weight [%]	Literature review	Equal distribution	Technical highlight	Economical highlight	Environmental highlight	**Existing projects**
PV Potential	29.70	33.33	60.00	20.00	20.00	**8.77**
Major Roads	8.42	5.20	3.12	9.36	3.12	**22.40**
Train Stations	3.13	1.93	1.16	3.48	1.16	**19.72**
House Values	28.73	17.73	10.64	31.92	10.64	**19.85**
Transmission Lines	13.72	8.47	5.08	15.24	5.08	**21.82**
Compatibility Index	14.67	30.00	18.00	18.00	54.00	**6.51**
Water Bodies	1.63	3.33	2.00	2.00	6.00	**0.93**
Total	100	100	100	100	100	**100**

2.9 Excluded areas

Exclusion areas are an additional layer to add on top of the suitability map. This layer was formed based on a realization that it is unlikely for the projects to be constructed on existing well-developed locations such as city centers, or surface transportation. Moreover, the water part was also neglected from the analysis according to the second assumption indicating that this study considers merely ground-based solar energy projects.

This layer was modeled through a group of factors (Table 2-19) from the BRT database. They can be classified into three steps. First, they are built-up areas or spaces that have been substantially exploited by human activities. Examples of them are widely diverse, such as accommodation, industrial areas, markets, sports fields, military training grounds, educational institutions, museums, etc. Thus, four databases were taken to cover them as much as possible. Second, it is an on-land transportation channel. Since a polygon format is available, the road and railroad databases were utilized in this instance. Lastly, it is a significant water component. This is the same database used by the water distance layer which is one of the seven factors constituting the suitability index (Table 2-7). Overall, these excluded areas discussed in this section are projected on the map as a dark color in Figure 2-10. Further details on how to build this layer was provided in Appendix B.3.

Table 2-19: The inputs of the excluded layer.

	Data	Database	Data provider	Taken date	Format	Remarks
1	City boundaries	BRT	PDOK [60]	14/02/23	Polygon	-
2	Places					-
3	Functional areas					Table B-2
4	Buildings					-
5	Roads					-
6	Railroads					-
7	Water bodies					Rivers width > 12 m Water area > 4000 m^2

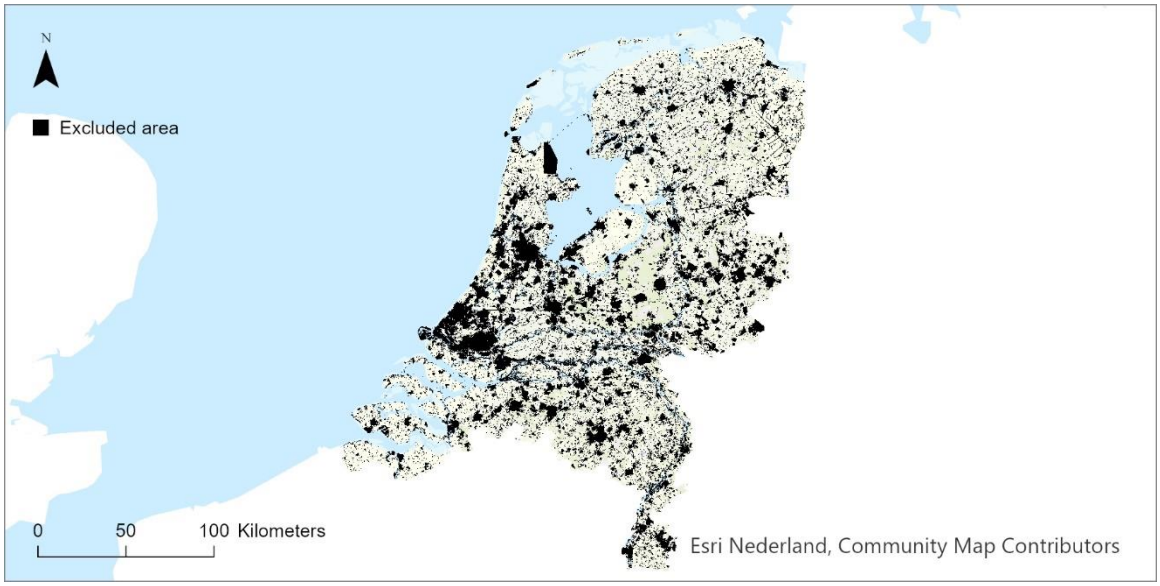

Figure 2-10: Areas that were excluded from the suitability analysis.

Phase 4

2.10 Potential energy generation

The last section of this Chapter describes the method how to apply the results from site suitability analysis. Recalling Regional Energy Strategies (RES) [9], mentioned in the introduction Chapter, it is a national program that intends to create a collaboration between thirty regions in the Netherlands in order to manage the land strategically for the purpose of 35 TWh energy generation by 2030 (one of the measures from the Climate Agreement [4]). Nonetheless, the suitability index developed in this research deals only with land management in the country and does not provide insight into energy outcomes. In order to advance the result by coupling it with this energy target, this section describes the process to calculate the energy generation from the selected locations by the model.

The solar resource map [81] was used to determine an approximation of the solar energy generation potential. The cell values contained in this map represent the average annual electricity production relative to the installed capacity of solar photovoltaic (PV) power plants [kWh/kW_p] [81]. These values have already accounted for important parameters related to a conventional PV system, such as its configuration, optimal tilt angle, solar radiation, air temperature, energy losses due to dirt and soiling, and other conversion losses from the balance of the system (inverters, cables, transformer, etc.).

The next step is to estimate the average installed capacity per pixel of solar PV power plants (kW_p/pixel). This is because the unit of the value in each pixel of the solar map is in the form of kWh/kW_p. Thus, an intermediate calculation is required to eliminate the term "kW_p" out of each pixel, resulting in the energy unit (only kWh). Since the map was reprojected into a raster with a 90 x 90 meters dimension to match the assumption, the area per pixel is equal to 8100 square meters. Therefore, the term kW_p/pixel can be converted to kW_p/m^2 using this factor.

However, determining the average value of kW_p/m^2 for solar projects in the Netherlands is quite challenging because the information provided by the ROM3D database [94] does not specify the occupied area. Besides, since all datasets were projected onto the map in point format, the coverage area cannot be calculated from the ArcGIS program. Fortunately, a layer of *functional areas* from the BRT database (Table 2-19) offers some masked areas of solar parks, but without the installed capacity. By matching the capacity information from the ROM3D database with the masked areas from the BRT of the solar projects at the same location (a few examples are shown in Figure 2-11), the average term of kW_p/m^2 for ground-based solar projects can be achieved. This results in 0.09 kW/m^2 which is equivalent to around **730 kW/pixel**.

The final step is to filter the suitable locations for solar energy projects with the help of the suitability map. Potential areas can be selected by setting a threshold of the suitability score. The total energy production could then be simply calculated by summing all values from the solar resource map inside the selected areas and multiplying this summation value by the average capacity obtained in the previous paragraph. Also, the calculation was taken into account an additional 10% of the required land derived from the needed space around the field. In the end, the relationship between the generated energy and the suitability index from this research has been established, and further discussions of the results will be elaborated in the following chapter.

Figure 2-11: Examples of solar fields in the Netherlands specified by the ROM3D database (point format), and the BRT database (yellow polygon format) projected on the base map of the aerial photograph [63].

3

RESULTS & DISCUSSIONS

This chapter discusses the outcomes of the previous chapter. The first one (3.1) will offer a compatibility map which is an initial result for addressing an environmental aspect in the solar suitability analysis. This map will next be validated with the designated natural locations. Subsequently, it will be combined with the other six layers described in the methodology chapter in order to construct the suitability index (3.2). Regarding this, six suitability maps have been developed as a consequence of the sensitivity analysis. Later, the discussion turns to an evaluation of the available data on existing solar project locations in the Netherlands (3.3), followed by an application of these suitability maps to the spatially-related energy policy (3.4).

3.1 Compatibility Index

The compatibility map (Figure 3-1) portrays the distribution of the environmental compatibility level of on-land solar energy development in the Netherlands through a score ranging from 0 to 100 (least to greatest compatible). The scores were classified into five bins by applying a geometric method[1] from the ArcGIS tool. The visualization of the map was designed with yellow representing a range of greatest scores and dark blue symbolizing the lowest.

By its concept, the high score can be interpreted as highly degraded areas, and vice versa. Hence, the map would also reflect the gradient of developed areas such as cities, densely populated places, as well as rural, and natural regions across the country. In short, the map was developed by mathematically averaging the score values of three sub-maps (Native Cover, Fragmentation, and Green) whose images are presented through Figure A-2, Figure A-4, and Figure A-6 respectively in Appendix A.

[1] The class width is defined mathematically based on a geometric series. Additional information is available on an online manual [95].

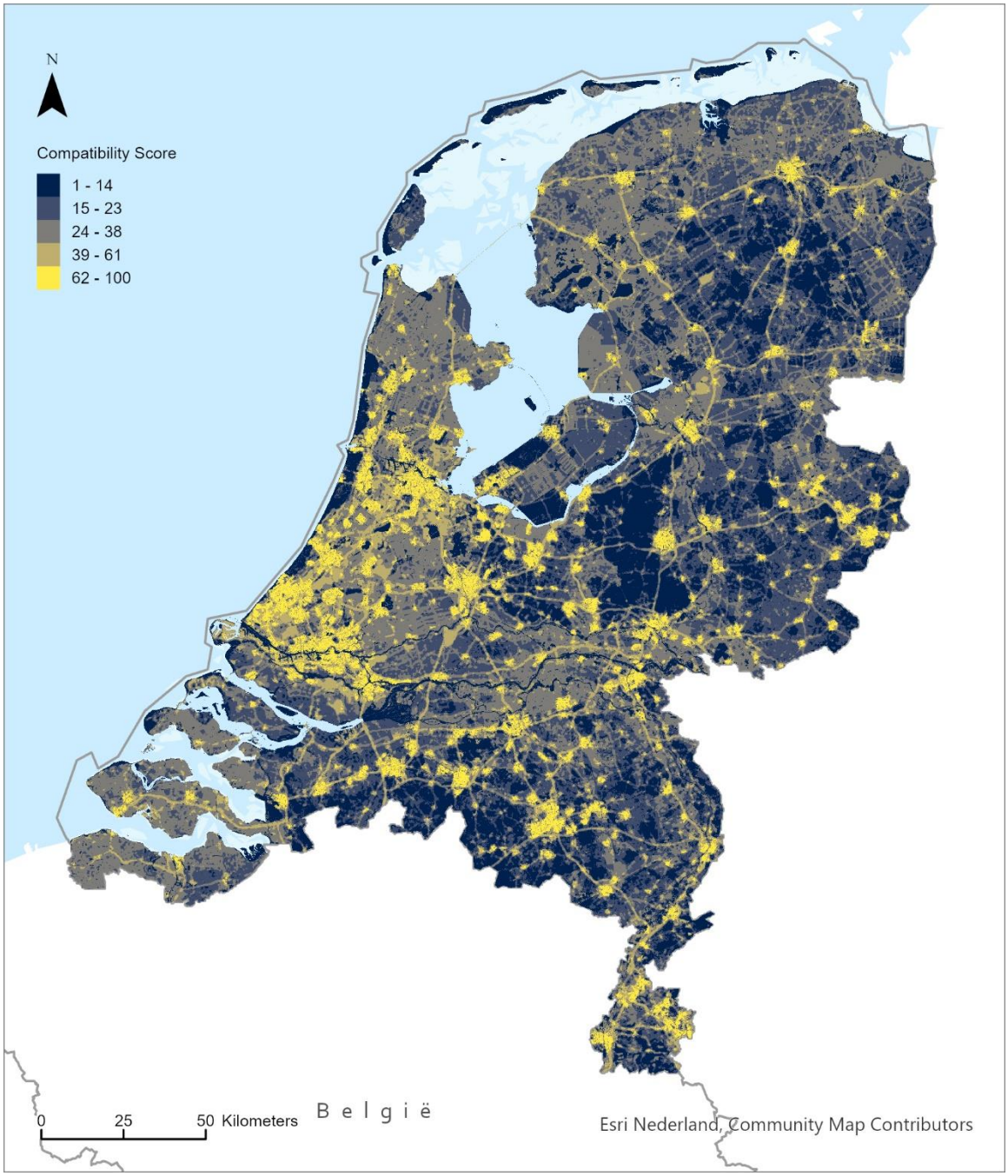

Figure 3-1: Compatibility Index. The pattern of bright yellow areas resembles anthropogenic areas such as cities, villages, railways, and major roads, while dark blue areas match the natural spaces and regions with less human population.

In terms of statistics, the score distribution was plotted in the histogram (Figure 3-2) between the number of raster pixels (y-axis) and a corresponding range of scores (x-axis). There is a peak in the lower score range between 20 to 30, indicating that the majority of the country consists of lightly degraded land. Conversely, the number of pixels with compatibility scores of 40 and above is relatively insignificant, suggesting that only a small portion of space was intensively degraded. The average value of the compatibility score for the entire country is 26.9.

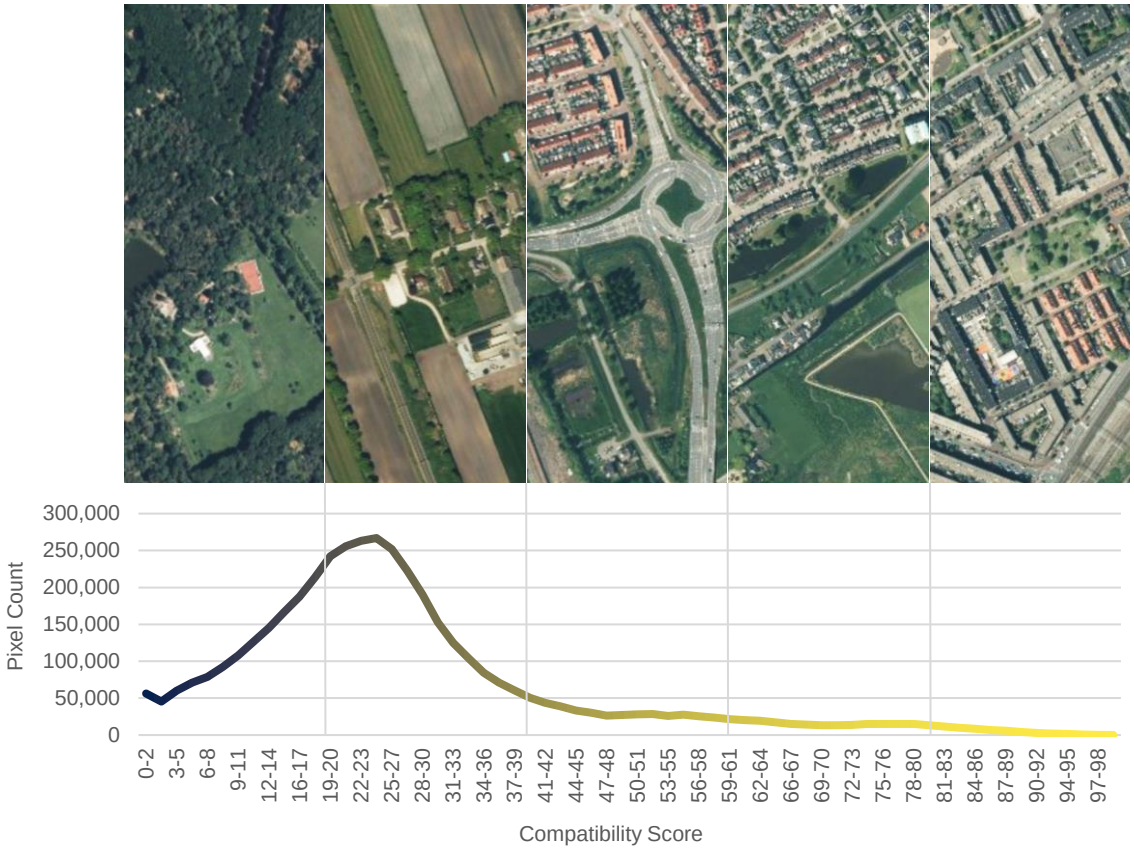

Figure 3-2: The distribution of compatibility scores over the entire country counted per raster pixel. It is portrayed with an example of five land features from aerial photographs [63], that are indicative of each score range. The line color matches the legend of the map in Figure 3-1.

Attached to the above figure are five example images of land features along with the score range. Increasing from low to high compatibility score, there are forests where there are little to non-inhabitants, agricultural fields where more people and local streets are presented, motorways junctions that fragment green terrain into small isolated spaces, the edges of the city where the boundary between urban and natural area can be distinctly outlined, and the city centers where there is a combination of dense population, a variety of transportation routes, and urban environment.

Note that these examples merely present the comparison between the compatibility score and actual land features in order to illustrate what the compatibility index implies. It is possible, for example, that road intersections would obtain a higher score if there were adjacent villages or inhabited communities, or that urban areas would receive a lower score if a large number of local nature parks existed within. In any case, the index is genuinely established by the contributions of three inputs: Native Cover, Fragmentation, and Green. Thus, the extent of the final score does depend upon the presence of these three components at specific locations and does not dedicate to one particular land feature.

To assure that the compatibility index adheres to its concept, preferring the degraded areas for solar projects, the map needs to be validated. Even though this approach was examined and accepted in the original work [58], not all of the calculation steps were followed by this study, and certain modifications were made. Therefore, it is necessary to examine the result before proceeding to the next phase of analysis.

Validation Result

Figure 3-3 exhibits the compatibility scores of designated locations within the Netherlands Nature Network (NNN). The majority of these areas are depicted on the map with a dark blue color, suggesting a relatively low score (1-23 refers to the map legend). This finding can also be drawn from a histogram (Figure 3-4), which shows a left-skewed score distribution (high amount of pixels with a lower score). Further clarification could be interpreted from a cumulative function that was indicated in the same figure. A corresponding score of 80% cumulative is approximately 22. This implies that 80% of all protected nature areas in the NNN were indexed with low compatibility scores below 22.

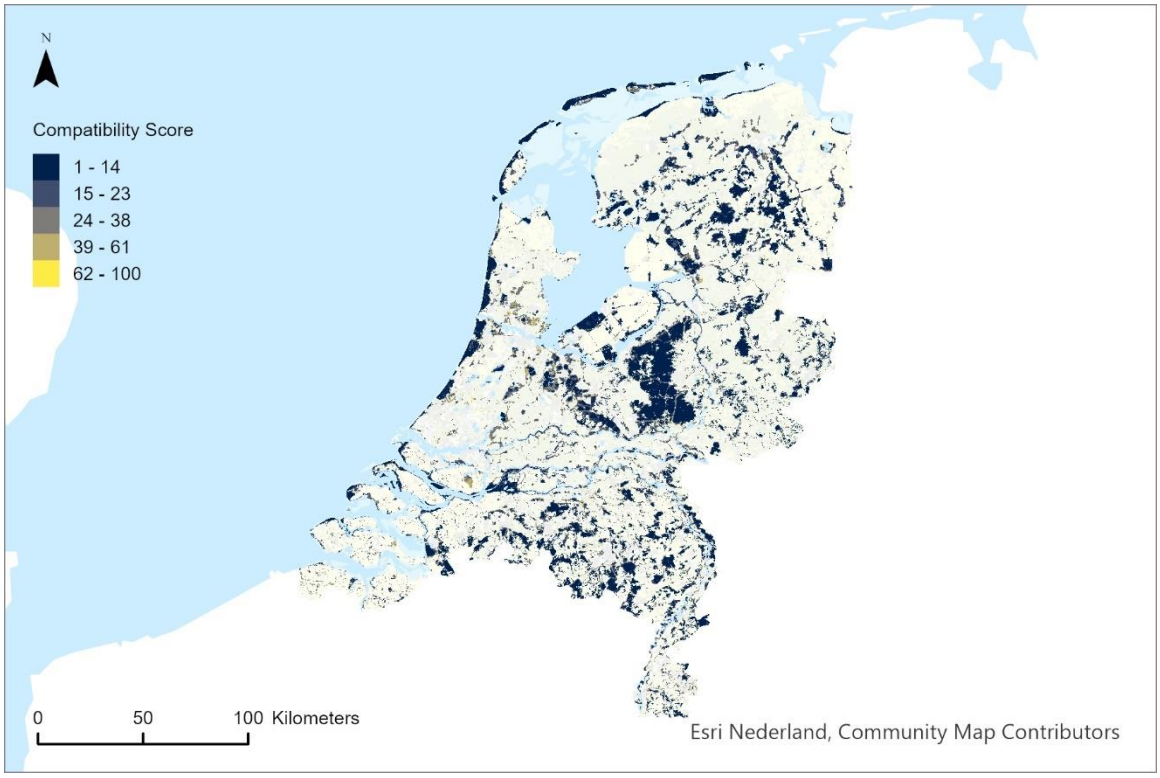

Figure 3-3: A segment of the compatibility map masked with the NNN**.** The range of scores and color scheme are consistent with the compatibility map. However, as the model identifies the natural regions with low score ranges, most of the masks are displayed in dark blue.

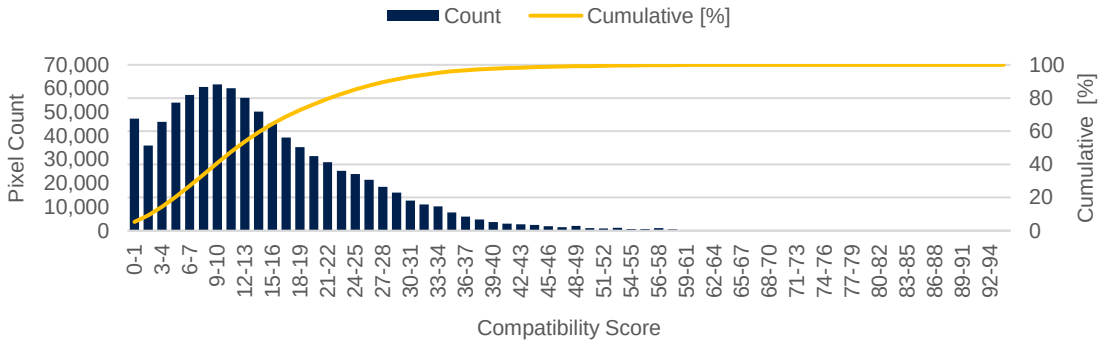

Figure 3-4: The distribution of compatibility scores over the NNN depicted with the cumulative function.

Two observations might be made regarding the validation process based on Figure 3-4: why do the protected nature areas have certain levels of compatibility, and why are there few of them with high scores (for example more than 50)? An answer to these remarks lies in the concept of degraded areas which is an approach to constructing the compatibility index. All buildings and infrastructure are considered to be the cause of vegetation loss, thus increasing their compatibility scores. It is normal for the module to allocate a score to the most of regions, including the designated natural areas, given that such constructions, particularly the road network, have been extensively developed across the nation. Figure 3-5 (left, middle) demonstrates that, although being labeled as a part of the NNN areas, the area is nonetheless marginally degraded due to the presence of surrounding communities and local roads.

Another remark highlights conflicting natural places with a particularly high compatibility score. This may occur in case these places were in close proximity to highly degraded areas, so their ratings were greatly affected. Figure 3-5 (right) depicts a local park in the city center that could serve as an instance of this circumstance. Overall, it is important to note that the compatibility index was developed from an evaluation of the physical conditions of land features from a perspective of land degradation, which differs from the basis for constructing the NNN map, a connection between large nature areas

[71].

(1) the NNN area within 5-15 compatibility score range | (2) the NNN area within 20-30 compatibility score range | (3) the NNN area within 80-90 compatibility score range

Figure 3-5: Three examples of locations from the aerial photograph [63] under the NNN area [72] with a specific compatibility score range: (1) a forest in a rural area, (2) a green field between residential and industrial districts, and (3) a city park.

As stated in the Methodology chapter, there are four additional maps besides the NNN area that indicate the natural sites based on different perspectives (individual Figures provided in Appendix A.4). With these maps, the validation procedure of the compatibility index was repeated and the results of score distribution extracted from each map including the NNN were plotted and compared in Figure 3-6. They all show a similar pattern in which most areas have a low score range, with a slight deviation in statistical values. Then, the same remarks and explanations discussed in the previous paragraphs could also be applied to them. This suggests that the compatibility approach is practical in a way that it is able to distinguish these natural spaces with a range of lower scores, which could be advantageous to the site suitability analysis, rather than excluding them.

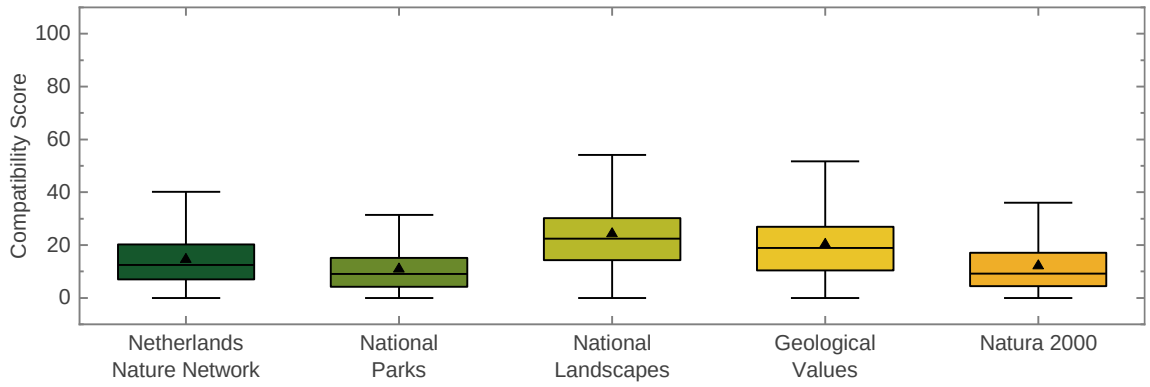

Figure 3-6: The distribution of compatibility score over the nature areas designated by five databases: the Netherlands Nature Network [72], National Parks [76], National Landscapes [77], Geological Values [78], and Natura 2000 [79]. The triangle mark refers to the mean value of each distribution.

In conclusion, the compatibility index which is regarded as a factor from the environmental aspect in the site suitability analysis has been completed. However, employing only this component as a basis for evaluating potential locations of renewable energy development would be insufficient. Hence, additional parameters are required for this kind of analysis, the results of which will be presented in the next section.

3.2 Suitability Index

The Suitability Index in this research delivers a perception of how relatively suitable an area is for solar energy development compared to the other parts of the study's areas based on selected seven input constraints. There are six maps (Figure 3-7) developed from six different scenarios in the sensitivity analysis (Table 2-18). A raster pixel in each map carries a value that is the result of the weighted sum calculation of the seven input layers. It varies from 0 to 100 denoting the least to most suitable area. Additionally, all locations specified in the exclusion layer were removed from the final map (black space on the map). All suitability maps were visualized by the same application of the color stretch function with the "Minimum Maximum" method[1] [96]. Referring to this, blue and red colors were assigned to symbolize the minimum and maximum scores respectively, with yellow color representing the middle score.

Followed by the map is the suitability score distribution of each scenario displayed via six histogram plots (Figure 3-8). The mean value of each distribution was indicated by a navy solid line with number identification. The scale of both x- and y-axis of all graphs were aligned to be the same for better visual comparison. These statistical results reflect the effect of the main criteria (technical, economical, and environmental) on the final suitability score.

Considering the map, it provides an overview of the suitability score distribution across the Netherlands. Depending on different sets of priority weights, each scenario contributes its own suitability index, hence the color shadings. For some cases (scenarios 1, 4, and 6), they portray a more red tone color than others (scenarios 2, 3, and 5), indicating that most regions in the country from these schemes received a higher score. However, it can be noticed that the distribution of individual map scores follows a similar pattern; extensive natural areas in Gelderland province (center of the country) and underpopulated places in Friesland and Drenthe provinces (north and northeast of the country) have a lower score range than the rest of the country.

[1] This technique enhances the appearance of the figure by linearly stretching the statistics from a raster to match the color ramp value, i.e., 0 to 255 for 8-bit color.

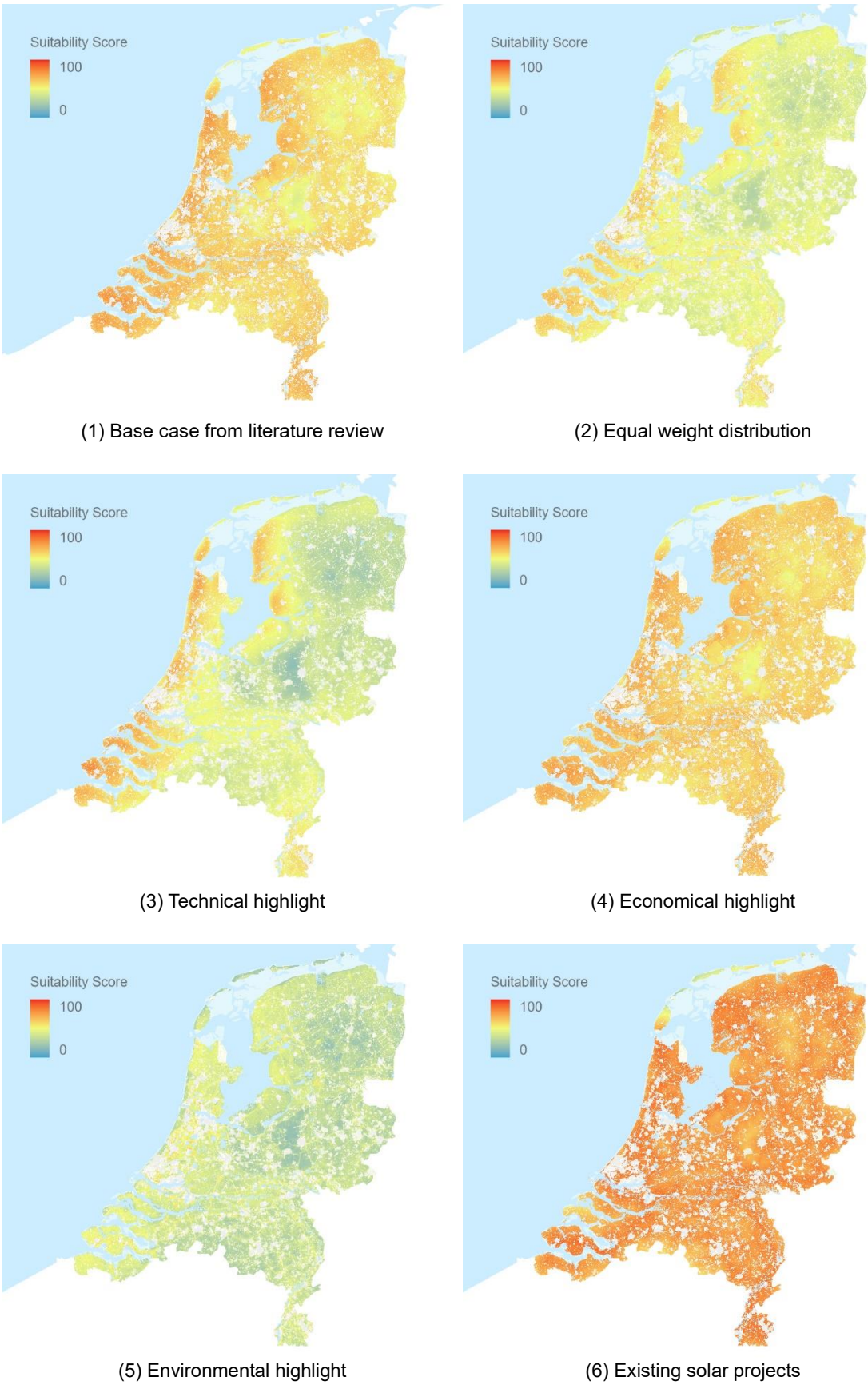

(1) Base case from literature review

(2) Equal weight distribution

(3) Technical highlight

(4) Economical highlight

(5) Environmental highlight

(6) Existing solar projects

Figure 3-7: The final six suitability maps resulting from the sensitivity analysis.

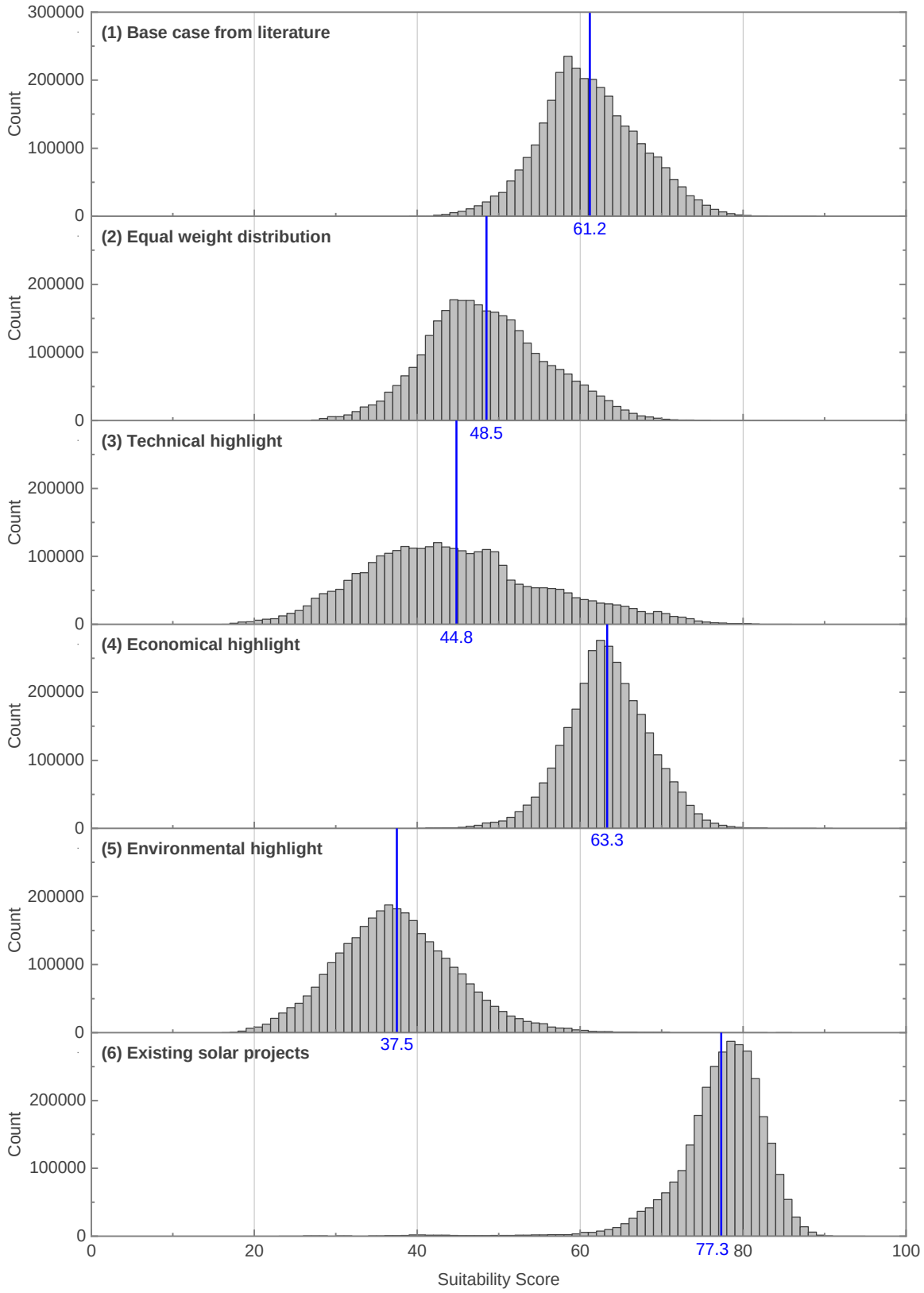

Figure 3-8: The distribution of suitability score across the Netherlands counted per raster pixel. Six histograms were plotted with the indication of the mean value (blue line) in accordance with each scenario of the suitability map results.

The suitability score of **Case 1** and **Case 4** demonstrates a similar distribution pattern across the country. This is because these cases highlight an economical aspect (Table 2-14), which considers the proximity of a specific region to public transport systems, e.g., road networks, train stations, or transmission lines. Since these facilities have been broadly installed throughout the country, they contribute significantly to the suitability score. For **Case 2**, it shows a mixed result in which a range of high scores locate on the western side of the country as a result of greater solar resources, moderate scores cluster around the area near the city districts and major roads, and low scores appear in natural areas. Compared to **Case 3** in which the scores align distinctively from high to low in the direction from west to east of the country due to the focus on solar energy resources, **Case 5** produces a map with overall lower scores because it emphasizes an environmental aspect that mainly seeks degraded areas for a higher suitability score. However, those highly degraded areas such as urban areas, industrial districts, and major transportation networks were already excluded from the map, resulting in a reduction in the suitability score for the remaining land. Finally, **Case 6** is an extreme scenario extracted from the locations of existing solar projects in the Netherlands [94]. Considering the priority weights for this scenario as given in Table 2-18, it greatly concentrates on the economic aspect, which accounts for 84% of the priority weight. Therefore, the result should likely be the same as in Case 4 but would be more intense in terms of the final suitability scores.

Considering the different priority weights and the mean value of suitability scores (Figure 3-8) in each scenario, the effect of three main criteria (technical, economical, and environmental aspects) on the suitability level of an area can be examined. From the values indicated in Table 2-18, it can be noticed that the weights of the economical term for scenarios 6, 4, 1, and 2 were allocated as 84%, 60%, 54%, and 33% accordingly, while scenarios 3 and 5 were appointed the same lowest weight of 20%. The same order of these scenarios can also be extracted from the consideration of the mean value of the suitability score; 77.3, 63.3, 61.2, 48.5, 44.8, and 37.5 for scenarios 6, 4, 1, 2, 3, and 5 respectively. This indicates that the economical criterion and the suitability index have a positive relationship. In addition, the mean value of scenario 5 is less than that of scenario 3 because most areas with high suitability scores in scenario 5 were defined as highly degraded areas by the compatibility approach, and these areas were already excluded from the map. Then, the remaining land in scenario 5 possesses only low to medium scores. Given the aforementioned, it could be inferred from this suitability model that the higher the weights on an economical criterion, the greater the suitability index, however the higher the weights on an environmental criterion, the lower the scores.

3.3 Solar projects on the map

This section reviews the ROM3D database [94] which provides information on existing solar projects in the Netherlands. This could be regarded as a supplementary result for the site suitability analysis as it is advantageous to explore how such projects have developed so far in the country, where the energy transition has been well recognized, and how the Solar Ladder campaign (discussed in the introduction Chapter) influences this development. As a preliminary step, 582 out of 979 data points were chosen and projected onto the map as seen in Figure 2-8. A few spots were magnified to provide the detailed configuration as an example in Figure 3-9.

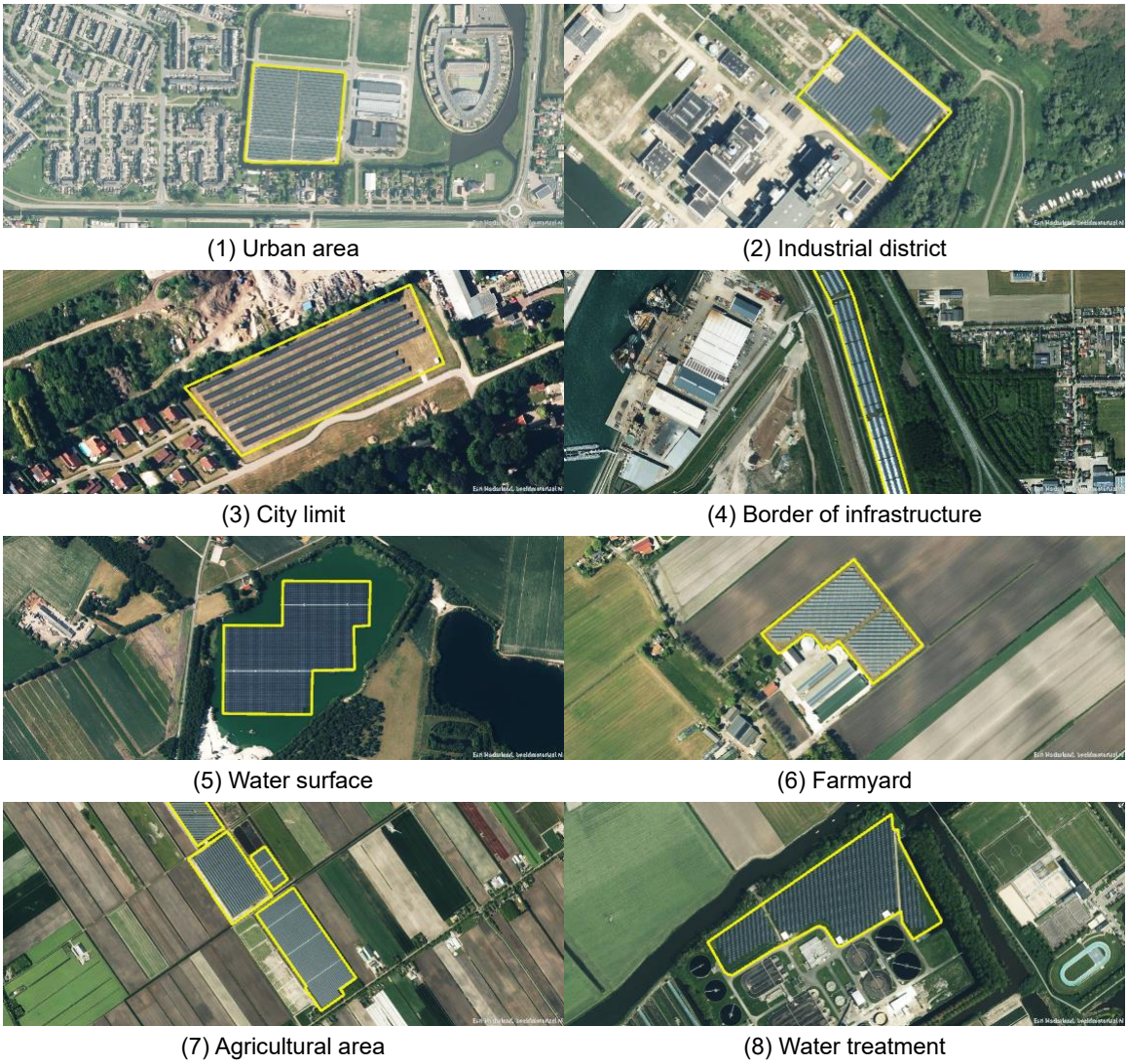

(1) Urban area (2) Industrial district

(3) City limit (4) Border of infrastructure

(5) Water surface (6) Farmyard

(7) Agricultural area (8) Water treatment

Figure 3-9: Examples of existing solar parks (images from the aerial photograph [63]) specified by ROM3D [94]. Below each picture is an identification of a configuration category based on the land feature by this study.

An assessment of these data points was performed via Figure 3-10. They were plotted from the same database, but their attributes were presented differently. Figure 3-10 (left) displays the annual number of completed solar projects, whereas Figure 3-10 (right) indicates their capacity in megawatts (MW). Moreover, all data were grouped into eight categories according to their configuration: urban areas, industrial districts, city outskirts, water surfaces, farmyards, agricultural areas, and water treatment fields.

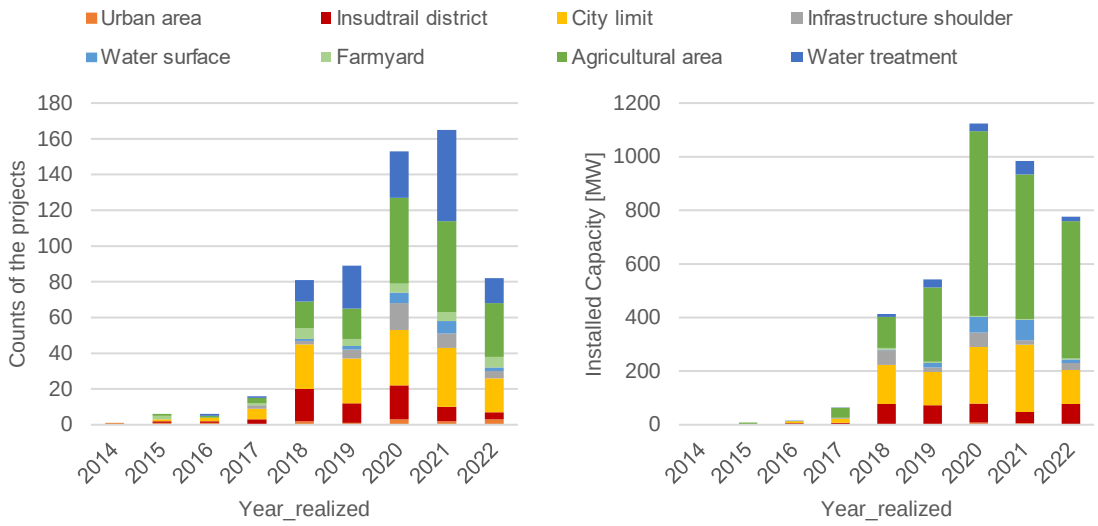

Figure 3-10: The statistical plots of the selected existing solar projects in the Netherlands (582 projects in total) classified by eight land feature configurations. The left graph depicts the number of projects completed each year between 2014 and 2022, while the right graph displays their installed capacity in MW.

These graphs demonstrate that solar energy development in the Netherlands has been hugely invested since 2018. The total capacity of completed projects rocketed up from approximately 60 MW in 2017 to slightly above 400 MW in 2018, and even surpassed 1000 MW in 2020. A similar trend can be taken from the other graph, where the number of completed projects rose from 17 to 81 to 155 in 2017, 2018, and 2020 respectively.

In contrast, there is a significant decrease in numbers for both graphs from 2021 to 2022. The reasons could be varied and are outside the scope of this report. Nonetheless, an intriguing part of this shift is that the total capacity decreased linearly, although the number of completed projects dropped by half between those years. This disproportion reduction represents large-scale project implementation during this period.

The last discussion for these results focuses on the impact of the Solar Ladder campaign on the development of solar energy technology. In brief, this program, which was introduced in 2019 [7], encourages the combined use of land for new solar projects, so that extra space would not be required. It gives priority to solar energy configurations on existing infrastructure, for example, rooftops, road network surroundings, landfill sites, and urban areas. The agricultural area is also included in this preference but with low priority. Regarding this, the presence of solar projects with these configurations should become more prevalent after the published year of this campaign, 2019. However, it does not necessary for the trend to be seen directly after 2019, as it could take a long time to complete such projects from the design phase to the first electricity generation, or there could be a delay in the construction phase resulting in a delay in the year realized.

Applying the notion of the Solar Ladder campaign to Figure 3-10, an explanation can be retrieved in two points. For the first case, it is apparent that the number of solar projects at water treatment sites has doubled in 2021 with 51 projects completed compared to 25 projects realized in the year of 2019. Also, the number of solar fields installed around the city limits has been steadily increasing since 2019. For the second point, it shows a contradiction of projects in agricultural areas, which should be expectedly less executed, on the other hand, several projects under this category were completed from 2020 onwards. This might be because of the focus on large-scale solar projects which require a vast bare space from the agricultural land type. Thus far, these results prove that the campaign does affect solar energy development in the country by driving it in a direction that is more space-efficient in the Netherlands.

3.4 Research Application

After completing the suitability maps, it is interesting to apply these results to the existing spatial policies and assess the potential benefits they could offer to the decision-makers. By evaluating the suitability score, it is possible to determine which regions are optimal for solar energy projects. Then, the potential energy generation of these selected locations can be approximated using the solar resource map [81]. However, the score on each suitability map is subjectively determined by its specific conditions. In other words, a score in one particular scenario does not have the same relevance as the same score in another scenario. To avoid arbitrarily setting the suitability score, one practical procedure for applying these maps would be to first identify the energy requirement and then iteratively determine which score in each scenario may achieve this target.

A case study was created by choosing *Regional Energy Strategies* (RES) program as a reference. Of particular interest are the goal of generating 35 TWh from renewable sources on land by 2030 and the remark by Cornax, et al. [5] mentioning that 10 TWh of solar energy would require 166.5 km^2 of agricultural land. As a result, the case study was conducted in two steps: first, it was determined if the areas required by our model for 10 TWh of solar energy were consistent with what was mentioned above, and second, it was examined which types of potential land would be necessary if all 35 TWh was realized by solar energy.

1st step: 10 TWh

The purpose of this step is to verify that the amount of land identified by the suitability model for a 10 TWh energy target is aligned with the statement made in the report by Bosch & van Rijn [5]. This was done by adjusting the suitability score with intervals of 1 until the 10 TWh energy target was met. Following this, the number of raster cells on the suitability map with greater or equal to this score was counted and multiplied by its size (8100 square meters) resulting in the total areas. Table 3-1 below shows both results of total energy production and requisite land space for each of the six scenarios (referred to the suitability analysis).

Table 3-1: The potential solar energy generation and the amount of ground space required in response to the threshold suitability score as a minimum, for achieving 10 and 35 TWh energy demand targets. The threshold score on each scenario is subjectively determined by its specific conditions; hence, they do not have the same relevance and cannot be compared to each other.

Scenarios	1 Literature review	2 Equal distribution	3 Technical highlight	4 Economical highlight	5 Environmental highlight	6 Existing projects
10 TWh energy demand target						
Threshold suitability score	77	68	74	76	59	87
Potential energy generation [TWh]	10.43	10.00	12.16	12.59	11.44	15.88
Required land space [km^2]	115.8	111.6	133.5	142.1	131.1	180.9
35 TWh energy demand target						
Threshold suitability score	74	64	70	74	55	86
Potential energy generation [TWh]	46.89	48.22	45.94	36.69	36.08	35.79
Required land space [km^2]	523.6	540.0	508.2	414.6	414.7	409.4

According to the suitability model, the area required to generate 10 TWh of solar energy ranges from 110 to 180 km^2. This 70 km^2 variation could be visualized as three times the size of Delft (24 km^2), or nearly the size of the Hague district (86 km^2) [85]. Referring to the statement of 166.5 km^2 in the report [5], it is important to note that their value was computed using different assumptions and methods compared to this study, for example, they considered only the agricultural land feature, whereas this research evaluated a variety of land types based on the suitability perception. Therefore, it is not necessary for the results to be identical, but at least it should not be that significant difference. Reasons for these lower required areas from our estimate could be an overestimation of the average installed capacity, failure to account for other energy losses, etc. The key essence of this comparison is that there is no significant discrepancy, and thus it supports the viability of our model.

2nd step: 35 TWh

The same procedures as explained in the previous section were repeated, with a change in energy requirement, to 35 TWh. The required areas for this quantity of energy as a minimum condition were also estimated and shown in Table 3-1, to give an idea of how it increases from the previous case of 10 TWh.

The location distribution of these required areas throughout all scenarios was examined and plotted in Figure 3-11. Generally, it can be seen that these areas are concentrated on the western and southern sides of the country. This is because most of the fields in these regions are well-developed, thus the topography has been significantly changed to accommodate supporting infrastructure such as housing, roads, railroads, power lines, etc. Moreover, solar irradiance is stronger in the western side of the country. This may also contribute to favorable conditions for solar energy projects.

Nonetheless, a slight deviation can be observed in these distributions. It is apparent in scenario 3 that almost all of these preferable areas are spot only in the West since this case emphasizes the technical aspect. While other scenarios (1, 2, 4, 5, and 6) produce a variety of selected places in various regions of the country. Referring to this, scenarios 5 and 6 deliver the most widespread distribution over the country. This is because scenario 5 emphasizes an environmental aspect, which includes the compatibility index layer that assigns higher scores to cities, villages, and major roads where they were located all over the map. And scenario 6, which highlights the economical aspect, rates the scores based on house values and proximity to public transportation infrastructure. Since these facilities are extensively installed around the country, they increase the attractiveness of these areas by the model.

It is essential to note that the size of the orange dots in Figure 3-11 has no bearing on the amount of land space. Their size was enlarged just that it makes the map looks clearer to identify the distribution. Because of this, adjacent dots were overlapped to each other, reducing the amount of dots on the map. This means that although those preferable areas in scenario 5 seem to be greater than other scenarios, the overall land space is still more or less the same as indicated in Table 3-1.

To avoid a misinterpretation of Figure 3-1, the size of these preferable locations in each scenario was calculated per region and reported in Table 3-2. Similarly, it conveys the same meaning as the figure: the distribution of these selected areas in the Netherlands in terms of twelve regions. Therefore, more land would be reserved in the western regions of Zeeland, Zuid-Holland, and Noord-Holland, as well as in the southern region of Limberg. In addition, this value is dispersed more fairly to different regions in scenarios 4 and 6. The total amount of land space for each scenario is identical to what is presented in Table 3-1.

(1) Base case from literature review

(2) Equal weight distribution

(3) Technical highlight

(4) Economical highlight

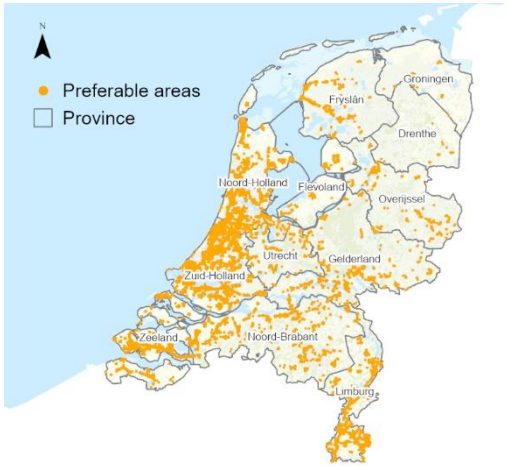

(5) Environmental highlight

(6) Existing solar projects

Figure 3-11: Preferable areas in each scenario for the requirement of 35 TWh solar energy generation. The orange dots on the map have been enlarged to provide a clearer representation of the location distribution; nevertheless, they do not reveal the amount of space they occupied. The figure shows that the western and southern sides of the country are the potential region that comply with all input constraints of the suitability model in this research more than other parts.

Table 3-2: The distribution of land space per region of preferable areas in each scenario for the requirement of 35 TWh solar energy generation.

Land space per region [km²]		1 Literature review	2 Equal distribution	3 Technical highlight	4 Economical highlight	5 Environmental highlight	6 Existing projects
1	Groningen	0.00	0.00	0.00	0.06	1.15	2.21
2	Fryslân	29.14	17.25	2.14	31.65	20.14	31.38
3	Drenthe	0.00	0.01	0.00	0.12	0.51	1.12
4	Overijssel	0.02	0.06	0.00	0.67	12.09	4.43
5	Flevoland	1.17	3.13	0.00	4.97	5.38	9.15
6	Gelderland	0.08	0.65	0.00	3.52	16.61	16.01
7	Utrecht	0.01	0.62	0.00	0.66	7.44	1.71
8	Noord-Holland	121.85	127.02	93.89	86.74	78.36	82.54
9	Zuid-Holland	101.61	144.67	121.97	87.03	158.29	77.61
10	Zeeland	248.06	215.71	290.20	141.94	50.95	89.87
11	Noord-Brabant	3.80	7.40	0.01	11.06	25.59	14.00
12	Limburg	17.87	23.48	0.00	46.18	38.21	79.36
SUM		**523.6**	**540.0**	**508.2**	**414.6**	**414.7**	**409.4**

Next, the focus of this section is shifting from the land's size to its characteristics. This was accomplished by comparing those selected areas with land categorization in the BRT database [60]. However, instead of selecting one of these scenarios as a reference for this analysis, it would be less subjective to identify promising locations that the suitability model has always chosen in every scenario. This was attained by intersecting all maps in Figure 3-11. The result was portrayed in Figure 3-12 below, along with the proportions of their corresponding landscape features.

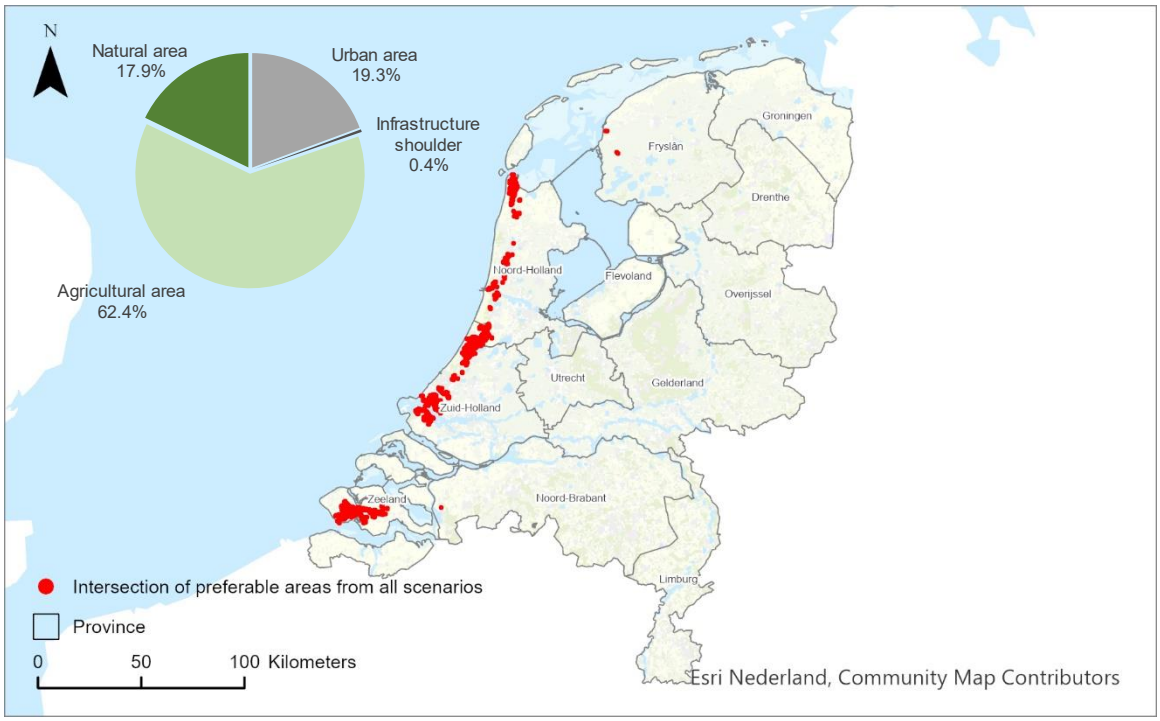

Figure 3-12: The intersection of preferred areas (red color) from all scenarios (six suitability maps filtered by the minimum score as indicated in Table 3-1, for the 35 TWh energy target). The map is accompanied by a pie chart displaying the portions of these intersecting land areas categorized by topography features from the BRT database [60].

Figure 3-12 demonstrates that the suitability index could be applied to determine the most likely regions for solar project realization on the premise of energy requirement. According to the map, mostly all intersection areas are found in the western part of the country, as they were restricted by scenario 3, which favors places with an excess of solar resources, which are normally located in the West. Potential solar energy generation from these areas was estimated to be 3.7 TWh. In terms of the pie chart, more than half of the total potential areas is agricultural area, accounting for 62.4%. The rest is distributed as 19.3% for urban areas, 0.4% for border of infrastructure, and 17.9% for natural areas.

A few particular sites were zoomed in as an example in Figure 3-13 to demonstrate a clear image of these preferred areas. They were generally favored at locations on the city's outskirts and along commuter routes. In some locations, these areas were even already realized by solar projects (blue mask on the map).

Figure 3-13: Examples of the intersection areas from Figure 3-12 masked by the yellow field on the map [63]. Existing solar projects were also marked with blue polygons, and their positions were indicated on a small grey map in the upper right corner.

Regarding the figure above, some flaws that the model situates the potential areas on existing buildings or settlements even though an exclusion layer was already applied, can be explained by two main reasons. The first one is related to the 90-meter raster resolution, which may be too coarse to correctly indicate some minor land features. Second is the input data accuracy. Even if the databases used here are from the government department [46], a national-scale analysis includes a variety of land attributes that could make it difficult to classify all the data. As a result, it is likely that some places might be neglected or mislabeled from the database.

In summary, this chapter has provided and discussed all results obtained from this study. They can be divided into four achievement levels. First is **the compatibility index** which is a factor representing an environmental constraint in the site suitability analysis. It indicates how compatible an area is for solar energy projects from an environmental perspective assessed by the concept of land degradation [58]. Next is the site suitability analysis which establishes **the suitability index** by combining seven factors (Table 2-7) including solar resources, the proximity to roads, train stations, transmission lines, water bodies, house values, and the previous result, the compatibility index. Nevertheless, the outcome of overlaying these seven layers could vary depending on the priority weight assigned to each of them. Thus, a sensitivity analysis was conducted to demonstrate five possible scenarios to construct the suitability map. Later in the third stage, information from ROM3D [94] regarding **existing solar projects** in the Netherlands was analyzed and coupled with the suitability model in this study in order to create an additional scenario (the sixth case). Also, a relationship between solar projects and their configuration was revealed at this step. Finally, an example of applying the suitability results was exhibited through **a case study** that considers the current energy-related spatial policy, RES [9]. Although this model is not an ultimate instrument that can be utilized solely to make a decisive judgment, all these results demonstrate that the model is helpful for the decision-maker in a way that it could preliminarily screen the potential locations for solar energy development from the entire country.

4

CONCLUSION

This report aimed to develop a model to assist in identifying suitable locations for ground-based solar energy projects in the Netherlands. It begins with an examination of four sustainability dimensions introduced by Stremke [16] consisting of technical, economical, environmental, and socio-cultural aspects. From a literature review, it was found that factors under the first two aspects were always taken into account in the site suitability analysis. However, natural regions were typically treated as restricted areas and were excluded from the map, and public opinion which represents a social aspect was usually neglected from the research due to the difficulty of collaborating with personnel from various sectors. As a result, this study was conducted through four phases in response to the main research question and three sub-objectives concluded as follows.

Sub-Objective 1: To explore available and significant factors related to the environmental aspect

The initial result of this study is a compatibility index. It was established by the concept of area degradation from the study of Stoms, et al. [58]. This index identifies a potential site for solar energy development that would have the least impact on the environment by considering existing land degradation; the more transformation of an area is, the more degraded area, and hence the more compatible it is for the solar projects. In this study, three components, comprising the Native Cover, Fragmentation, and Green map, were used to construct the compatibility index, whose score spans from 0 to 100 (least to greatest compatible area).

Considering the score distribution, it was found that the low score range (0-30) is dispersed across the majority of areas of the country, whilst the high score range (≥40) clusters around the cities and along main roadways. The mean value of this index for the entire country is approximately 26.9. This suggests that the land characteristic of the Netherlands is lightly degraded and still riches in natural spaces.

In addition, the index was validated with designated nature areas. The justification is that these natural areas possess different perspectives on natural preservation [71], thereby they are less compatible with solar energy development, hence, the compatibility score should be small. The validation process utilized five datasets including the Netherlands Nature Network (NNN) [72], national parks [76], national landscapes [77], places with geological values [78], and Natura 2000 [79]. A comparison of the mean compatibility score within these areas reveals that they all fall within the low range of 10 to 25, which conforms with the rationale mentioned above.

Sub-Objective 2: To develop a model that can identify the level of suitability of an area for ground-based solar energy projects

The second achievement is a suitability index developed from the linear combination of seven different factors, comprising solar energy resources, proximity to roads, train stations, transmission lines, and water bodies, housing values, and the compatibility index. By doing so, the Analytic Hierarchy Process [86] was applied to determine the priority weight of each factor. Since these priority values are directly related to the study interest, a sensitivity analysis was performed to assess the possible outcomes resulting from altering the importance level of three main aspects (technical, economical, and environmental). Referring to this, five scenarios were created; scenario 1 – values from the literature review, 2 – equal weight distributed, 3 – technical highlight, 4 – economic highlight, and 5 – environmental highlight.

With these indexes, locations in the country were appointed with a suitability score ranging from 0 to 100, allowing for the prioritization of suitable areas for solar energy development. The mean value of this index for each scenario, sorted from highest to lowest is 63.3, 61.2, 48.5, 44.8, 37.5 which corresponds to scenarios 4, 1, 2, 3, and 5. This could be interpreted that the more focus on an economical term in this suitability model, the higher the overall score. On the other hand, an environmental aspect limits the suitable level of an area, hence restricting the installation of solar panels in many locations.

Sub-Objective 3: To examine the relationship between the proposed suitability model and existing solar energy locations

The third phase analyzes how existing solar energy projects in the Netherlands (582 selected projects in total, data provided by ROM3D [94]) could be perceived from the suitability model. In order to connect these features, the process of constructing the suitability model was reversed by first positioning all 582 points on the map and then extracting the score from each of the seven suitability inputs pertaining to these points. This would result in the breakdown of the suitability score regarding the seven input components. By normalizing the mean value of these score distributions, an additional priority weight can be generated and set as the sixth scenario for another suitability map, with the relative importance of 84%, 9%, and 7% for economical, technical, and environmental aspects respectively. With such an intense weight on the economic term, this scenario provided the highest suitability score among other scenarios with a mean value of 77.3.

Research question: Which type of land features are suitable for ground-based solar energy development in the Netherlands?

An application of the suitability index from this research was demonstrated through a case study associated with a spatial energy campaign called Regional Energy Strategies (RES) [9]. This campaign entails the energy target of 35 TWh from renewable sources by 2030. Assuming that this amount of energy is a minimum requirement that would be realized by solar energy, the preferable areas that need to be developed can be determined by screening the highest suitability score downwards until the potential energy generation satisfies the requirement. This process was followed for all six scenarios, which produce different patterns of selected locations.

The intersection areas from all scenarios revealed regions around the large cities and industrial districts that lie on the western side of the Netherlands. This result suggests the most potential areas that have always been chosen in every scenario in response to the 35 TWh energy target. In addition, further observation with the topography database showed that the land features of these areas include 19.3% of an urban area, 0.4% of the border of infrastructure, 17.9% of a natural area, and 62.4% of an agricultural area.

5
RECOMMENDATIONS

Although the suitability model has been developed systematically throughout the course of this research, there are still a few parts that can be improved to enhance its validity. Accordingly, four recommendations were given in this final chapter. Part of them deals with the limitations of the study as outlined in the assumptions, while the other part addresses methodological issues. They are described as follows.

1. **To involve floating solar-type in the analysis**

It would be more beneficial for the suitability model if its scope could be extended to this floating configuration by taking into account large water bodies or lakes that provide sufficient conditions for the construction and energy production of solar PV panels on the water surface. Referring to this, another interesting data source, besides the Geobasic data, that could be useful for this branch of analysis is the Basic Map Aquatic database by PBL [97]. In short, it provides a spatially detailed geographical map with an insight into the characteristics and typology classification of surface water in the Netherlands.

2. **To involve social-cultural aspect in the analysis**

This is one of the four main criteria of the sustainable energy landscapes framework defined by Stremke [16]. Hence, it is a significant aspect that could considerably influence the decision-making process. Nonetheless, acquiring public opinion through the survey is admittedly challenging, both in terms of designing the questionnaire and gathering the data results from respondents. Therefore, it is strongly recommended to incorporate this criterion into the suitability model for more realistic results.

3. To scale down the study area

The third suggestion concerns the study area. In this research, the entire Netherlands was examined, which might be too large for a fined-grained analysis. To improve the accuracy of the suitability model, the study area should be reduced to a provincial or regional scale, then the raster resolution can be resized to be lower than 90 meters. With smaller pixel dimensions, the model will be able to distinguish the land features more effectively. Moreover, reducing the study area would also minimize the complexity of conducting the public survey since the target group is scoped down.

4. To recreate the Native Cover map with a continuous score distribution

The final recommendation addresses the score distribution of the Native Cover map, which is one of the three components constructing the compatibility index. The map was attached with five discrete values that correspond to the reference study of Stoms, et al. [58]. A sharp distinction in value between different land features might cause an inconsistency in the compatibility index. The Kernel Density calculation [98] for the Native Cover score is suggested as a solution to this issue. It is a part of the ArcGIS program's density toolset. This tool calculates the density of features (lines or points) using a probability kernel function, a statistical technique for smoothing the estimation of neighboring values around those features [99]. Therefore, the value will be slightly changed based on the distance to the input features, resulting in continuous data distribution.

An example of this proposal was tested by recreating the Native Cover map determined by the presence of buildings in a given area. Figure 5-1 compares the revised Native Cover score distribution obtained by applying the kernel function to the density calculation of these buildings' locations (Figure 5-1, right) to the prior result of this study (Figure 5-1, left). It can be seen that the score is now distributed continuously, and the map can also identify the areas that are close to the city. This might be helpful for the compatibility index. Nevertheless, further analysis is advised to evaluate how this method affects the overall compatibility index.

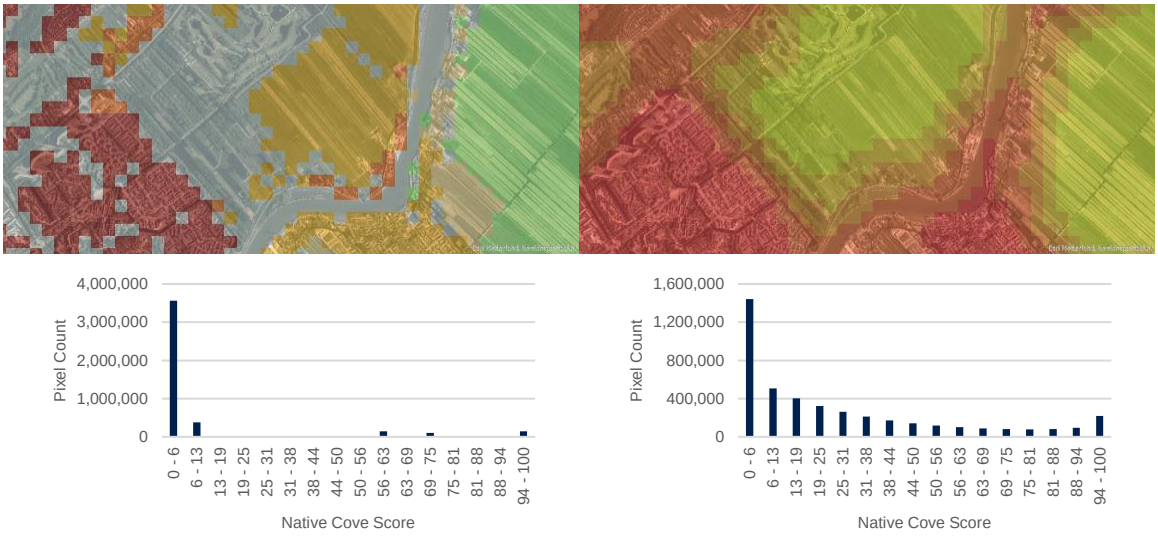

(1) the Native Cover map by ordinal value method (2) the Native Cover map by Kernel Density method

Figure 5-1: A comparison of the Native cover score distribution derived from (1) the method used in this study (ordinal value), and (2) the Kernel Density of buildings proposed in this section (continuous value). The graphs are demonstrated with a corresponding photograph of the edge of the city [63], where the left image depicts the sharp distinction between different land features, e.g., city, agriculture, and forest, and the right image provides a gradient of colors indicating the slight change in the score when these areas are located further away from the building zones.

Appendix

A

DETAILED INSTRUCTION – COMPATIBILITY INDEX

A.1 The Native Cover map establishing steps

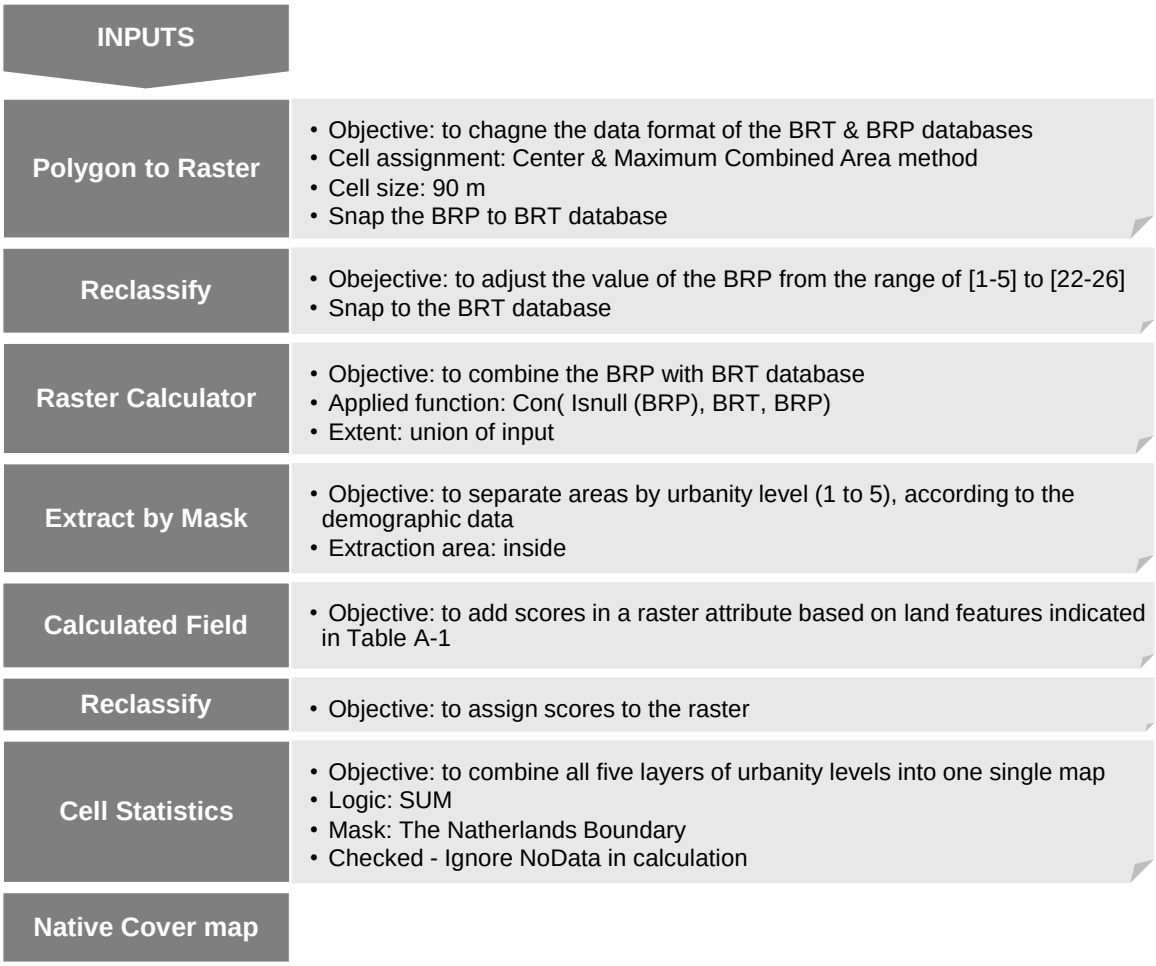

Figure A-1: Process for constructing the Native Cover map. The figure demonstrates the ArcGIS Tools (left) that were utilized for this component and arranges them in ascending order with justification and relevant configuration settings (right).

Table A-1: The score contributed to the Native Cover map. A set of values refers to the study of Stoms, et al. [58], and they were assigned based on two perspectives: 26 different land types from the BRT [60] and BRP [61] databases and a specification of 5 urbanity levels by CBS.nl [59].

		Land types	Urbanity level 1	Urbanity level 2	Urbanity level 3	Urbanity level 4	Urbanity level 5
			Highest populated				Lowest populated
BRT	0	**NoData**	0	0	0	0	0
	1	**Forest: mixed forest**	0	0	0	0	0
	2	**Forest: coniferous forest**	0	0	0	0	0
	3	**Forest: deciduous forest**	0	0	0	0	0
	4	**Forest: willow**	0	0	0	0	0
	5	**Coton wood**	0	0	0	0	0
	6	**Shrubland**	0	0	0	0	0
	7	**Sand**	0	0	0	0	0
	8	**Dune**	0	0	0	0	0
	9	**Basalt blocks, Stone slopes**	8	8	8	1	1
	10	**Jetty**	70	70	57	8	8
	11	**Fruit farm**	70	70	57	8	1
	12	**Orchard**	70	70	57	8	1
	13	**Nursery**	100	70	57	8	1
	14	**Cropland**	70	70	57	8	1
	15	**Graveyard with forest**	57	57	8	1	1
	16	**Graveyard without forest**	70	70	57	8	1
	17	**Fallow land**	100	100	70	57	8
	18	**Built-up area**	100	100	70	57	8
	19	**Railroad**	100	100	70	57	8
	20	**Other**	100	100	70	57	8
	21	**Grassland**	0	0	0	0	0
BRP	22	**Agricultural area: farmland**	70	70	57	8	1
	23	**Agricultural area: fallow land**	70	70	57	8	1
	24	**Agricultural area: grassland**	70	70	57	8	1
	25	**Natural area**	0	0	0	0	0
	26	**Other natural areas**	0	0	0	0	0

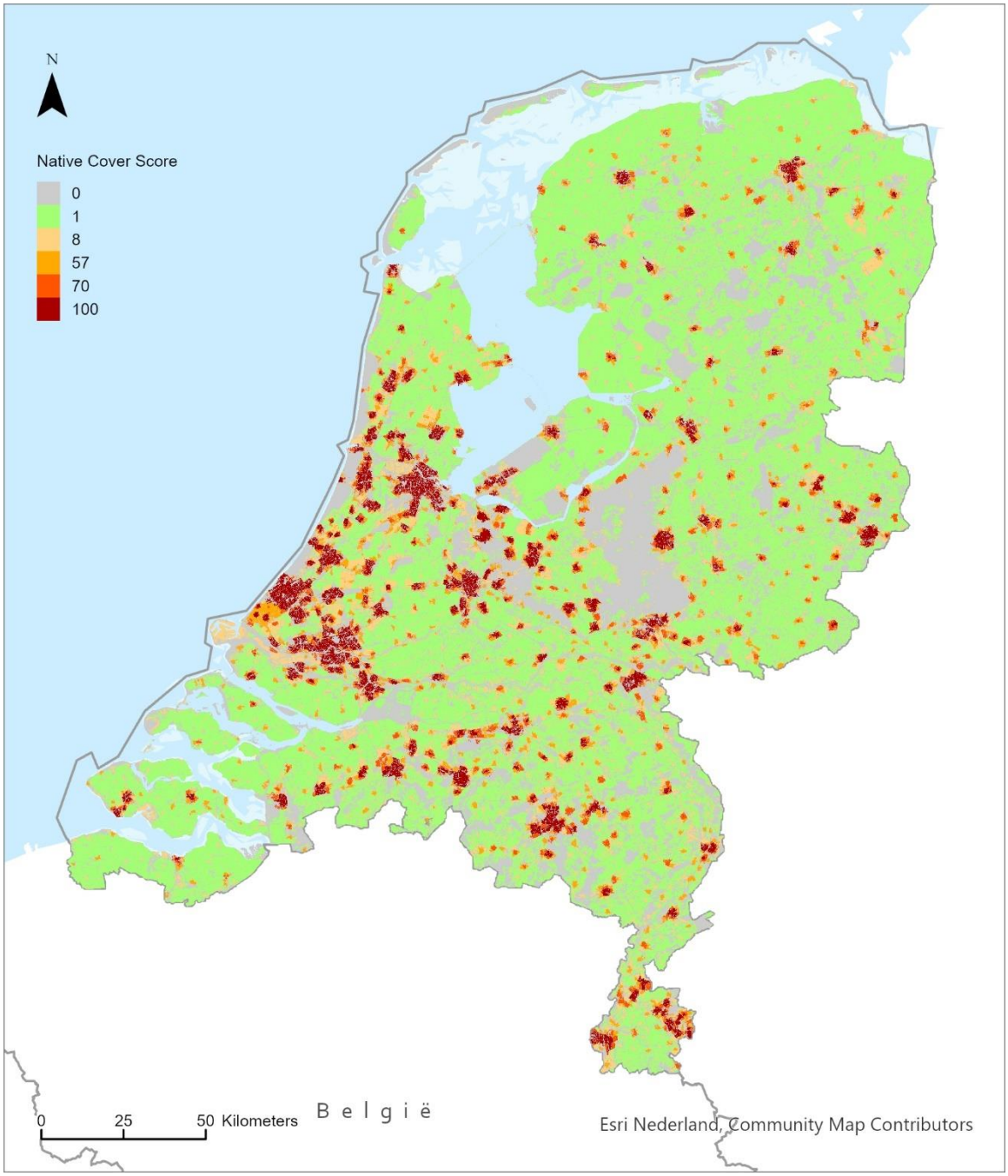

Figure A-2: The Native Cover Map. In this figure, five discrete values were adopted from the study of Stoms, et al. [58] with the zero value representing the natural regions defined by the BRT & BRP databases [60, 61]. The corresponding land features to each score are displayed in Table A-1.

A.2 The Fragmentation map establishing steps

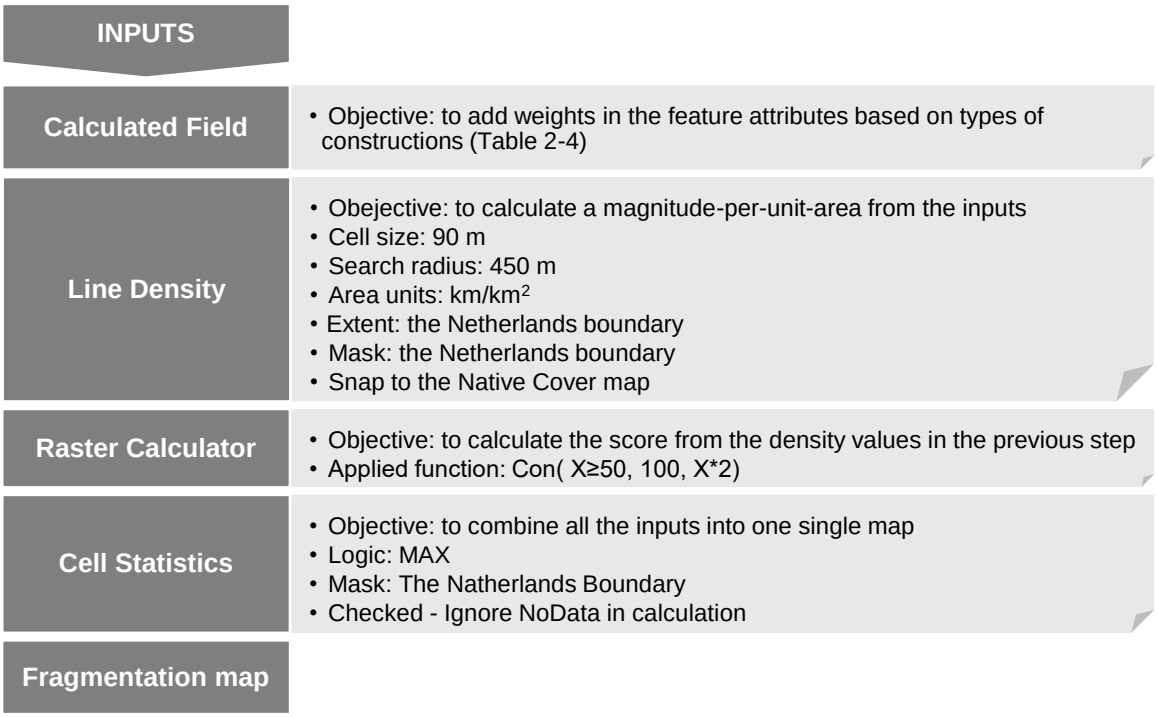

Figure A-3: Process for constructing the Fragmentation map. The figure demonstrates the ArcGIS Tools (left) that were utilized for this component and arranges them in ascending order with justification and relevant configuration settings (right).

Table A-2: The waterways selected attributes. The information in the list below is drawn from OpenStreetMap waterways data for Europe [67], collected on April 07, 2023. The selection process is based on the interpretation of each feature that might contribute to habitat fragmentation by comparing them with the map image [63].

	Features	Select		Features	Select		Features	Select
1	Artificial	✓	16	Drainage_channel	×	32	Rapids	×
2	Basin	✓	17	Dryriver	×	33	River	×
3	Blocked	✓	18	Fairway	×	34	Safe_water	×
4	Boat_lift	×	19	Fender	×	35	Security_lock	✓
5	Boom	✓	20	Fish_pass	×	36	Sluice	×
6	Brook	×	21	Floating_barrier	×	37	Stream	×
7	C+	×	22	Flow_control	×	38	Tidal_channel	×
8	Canal	✓	23	Gate	×	39	Tree_row	×
9	Construction	✓	24	Jetty	×	40	Tunnel	×
10	Culvert	×	25	Lock	✓	41	Virtual	×
11	Dam	✓	26	Lock_gate	✓	42	Wadi	×
12	Dept_line	✓	27	Lock_NHW	×	43	Water_inlet	×
13	Derelict_canal	✓	28	Portage	×	44	Water_outlet	×
14	Ditch	✓	29	Pressurized	×	45	Waterfall	×
15	Drain	✓	30	Proposed	×	46	Weir	✓
			31	Pumping_station	×	47	Yes	×

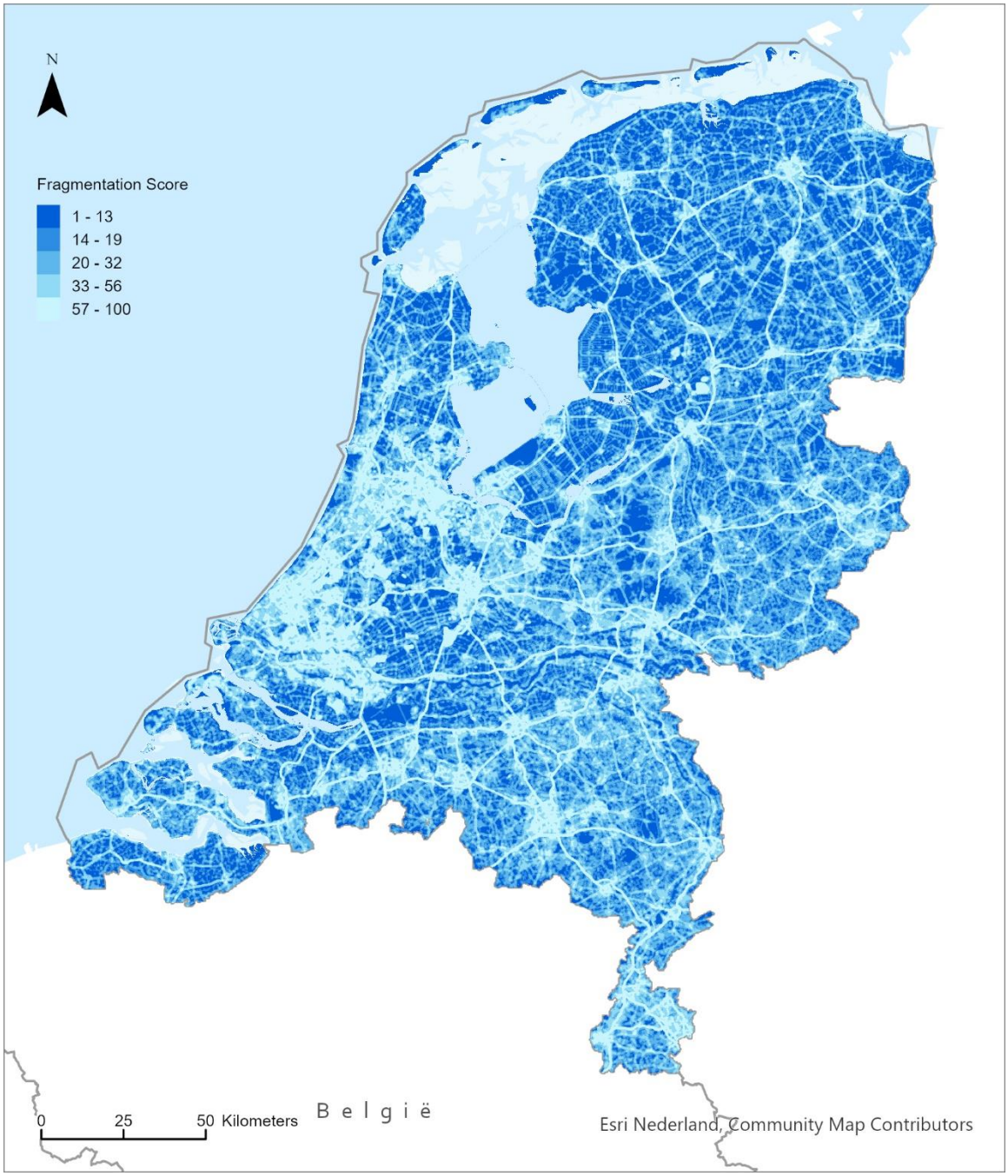

Figure A-4: The Fragmentation Map. The score was calculated based on the density of linear features including roads, railroads, waterways, and transmission lines. It was classified into five bins by applying a geometric method[1] from the ArcGIS tool with the blue-white color code.

[1] The class width is defined mathematically based on a geometric series. Additional information is available on an online manual [95].

A.3 The Green map establishing steps

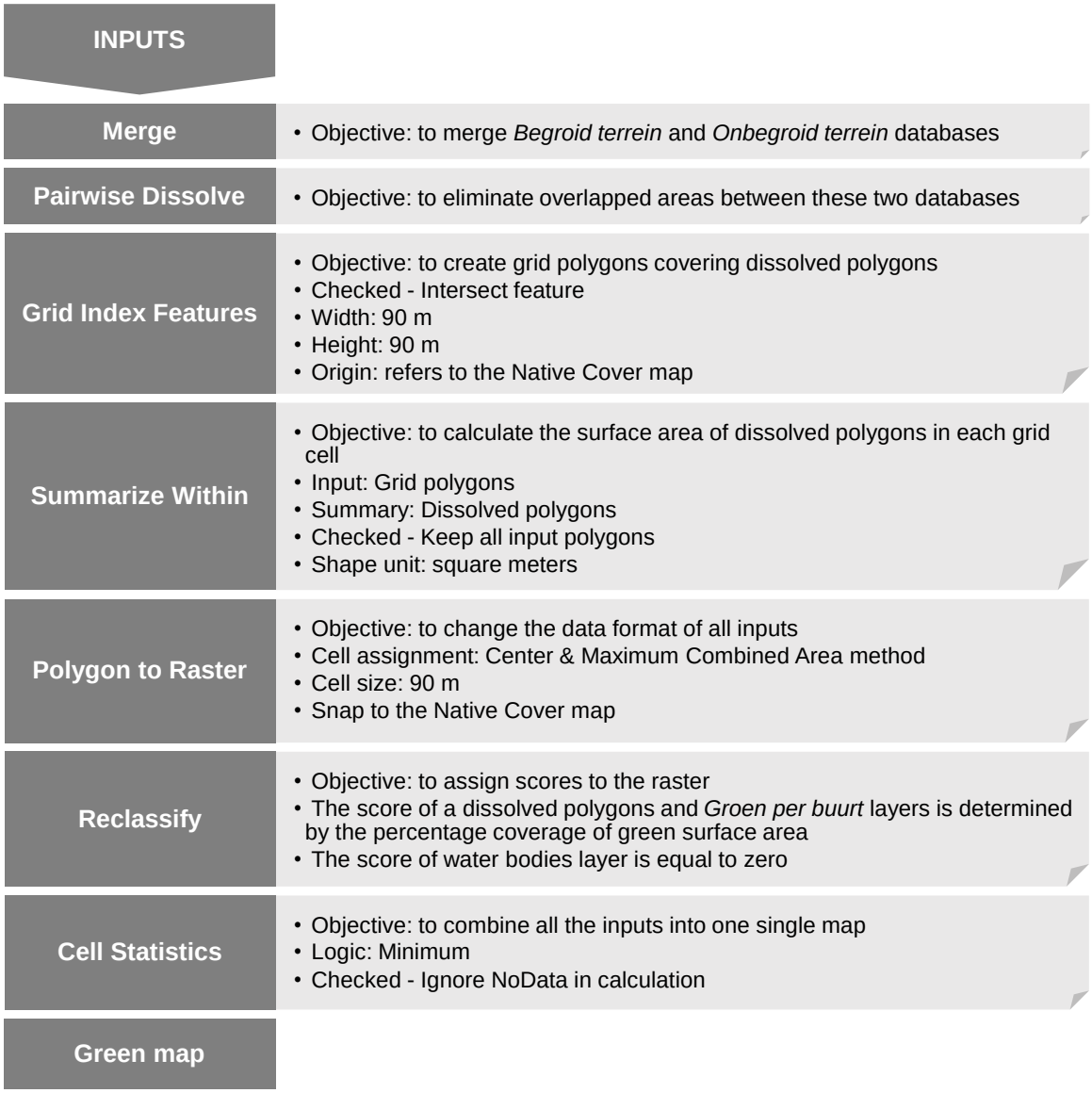

Figure A-5: Process for constructing the Green map. The figure demonstrates the ArcGIS Tools (left) that were utilized for this component and arranges them in ascending order with justification and relevant configuration settings (right).

Table A-3: The *Begroid terrein* and *Onbegroid terrein* selected attributes (in Dutch). The information in the list below is drawn from the *Basisregistratie Grootschalige Topografie* (BGT) database [70], collected on March 14, 2023. The selection process is based on the interpretation of each feature that might contribute to natural areas by comparing them with the map image [63].

		Label	Physical Appearance	Select
Begroid terrein	1	boomteelt	boomteelt	✗
	2	bouwland	bouwland	✗
	3	bouwland	bouwland: akkerbouw	✗
	4	bouwland	bouwland: bollenteelt	✗
	5	bouwland	bouwland: braakliggend	✗
	6	bouwland	bouwland: vollegrondsteelt	✗
	7	duin	duin	✓
	8	duin	duin: gesloten duinvegetatie	✓
	9	duin	duin: open duinvegetatie	✓
	10	fruitteelt	fruitteelt	✗
	11	fruitteelt	fruitteelt: hoogstam boomgaarden	✗
	12	fruitteelt	fruitteelt: klein fruit	✗
	13	fruitteelt	fruittelt: laagstam boomgaarden	✗
	14	fruitteelt	fruittelt: wijngaarden	✗
	15	gemengd bos	gemengd bos	✓
	16	grasland agrarisch	grasland agrarisch	✗
	17	grasland overig	grasland overig	✓
	18	groenvoorziening	groenvoorziening	✓
	19	groenvoorziening	groenvoorziening: bodembedekkers	✓
	20	groenvoorziening	groenvoorziening: bosplantsoen	✓
	21	groenvoorziening	groenvoorziening: gras- en kruidachtigen	✓
	22	groenvoorziening	groenvoorziening: heesters	✓
	23	groenvoorziening	groenvoorziening: planten	✓
	24	groenvoorziening	groenvoorziening: struikrozen	✓
	25	heide	heide	✓
	26	houtwal	houtwal	✓
	27	kwelder	kwelder	✓
	28	loofbos	loofbos	✓
	29	loofbos	loofbos: griend en hakhout	✓
	30	moeras	moeras	✓
	31	naaldbos	naaldbos	✓
	32	rietland	rietland	✓
	33	struiken	struiken	✓
	34	transitie	transitie	✗

Table A-3: The *Begroid terrein* and *Onbegroid terrein* selected attributes (in Dutch). The information in the list below is drawn from the *Basisregistratie Grootschalige Topografie* (BGT) database [70], collected on March 14, 2023. The selection process is based on the interpretation of each feature that might contribute to natural areas by comparing them with the map image [63]. *(Continued)*

		Label	Physical Appearance	Select
Onbegroid terrein	1	erf	erf	✗
	2	gesloten verharding	gesloten verharding	✗
	3	gesloten verharding	gesloten verharding: asfalt	✗
	4	gesloten verharding	gesloten verharding: cementbeton	✗
	5	gesloten verharding	gesloten verharding: kunststof	✗
	6	half verhard	half verhard	✗
	7	half verhard	half verhard: grasklinkers	✗
	8	half verhard	half verhard: gravel	✗
	9	half verhard	half verhard: grind	✗
	10	half verhard	half verhard: puin	✗
	11	half verhard	half verhard: schelpen	✗
	12	onverhard	onverhard	✗
	13	onverhard	onverhard: boomschors	✗
	14	onverhard	onverhard: zand	✗
	15	open verharding	open verharding	✗
	16	open verharding	open verharding: beton element	✗
	17	open verharding	open verharding: betonstraatstenen	✗
	18	open verharding	open verharding: gebakken klinkers	✗
	19	open verharding	open verharding: sierbestrating	✗
	20	open verharding	open verharding: tegels	✗
	21	transitie	transitie	✗
	22	zand	zand	✓
	23	zand	zand: strand en strandwal	✓
	24	zand	zand: zandverstuiving	✓

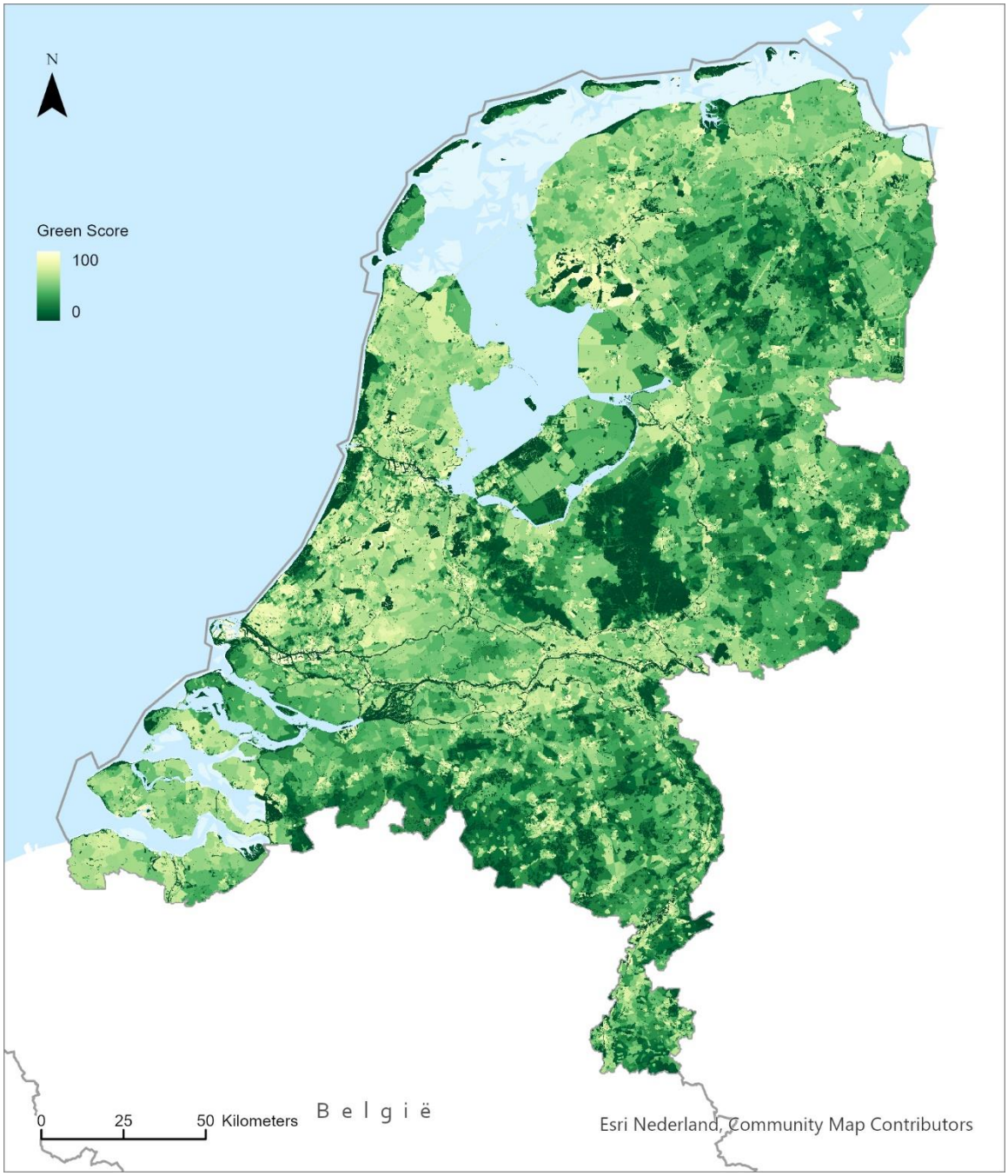

Figure A-6: The Green Map. The score was reversely calculated based on the surface area of the vegetative cover; the presence of natural objects such as trees, shrubs, and sand, will result in a lower score. This figure visualizes the score by the yellow-green color stretch function[1] with the “Minimum Maximum” method [96].

[1] This technique enhances the appearance of the figure by linearly stretching the statistics from a raster to match the color ramp value, i.e., 0 to 255 for 8-bit color.

A.4 Additional protected nature areas

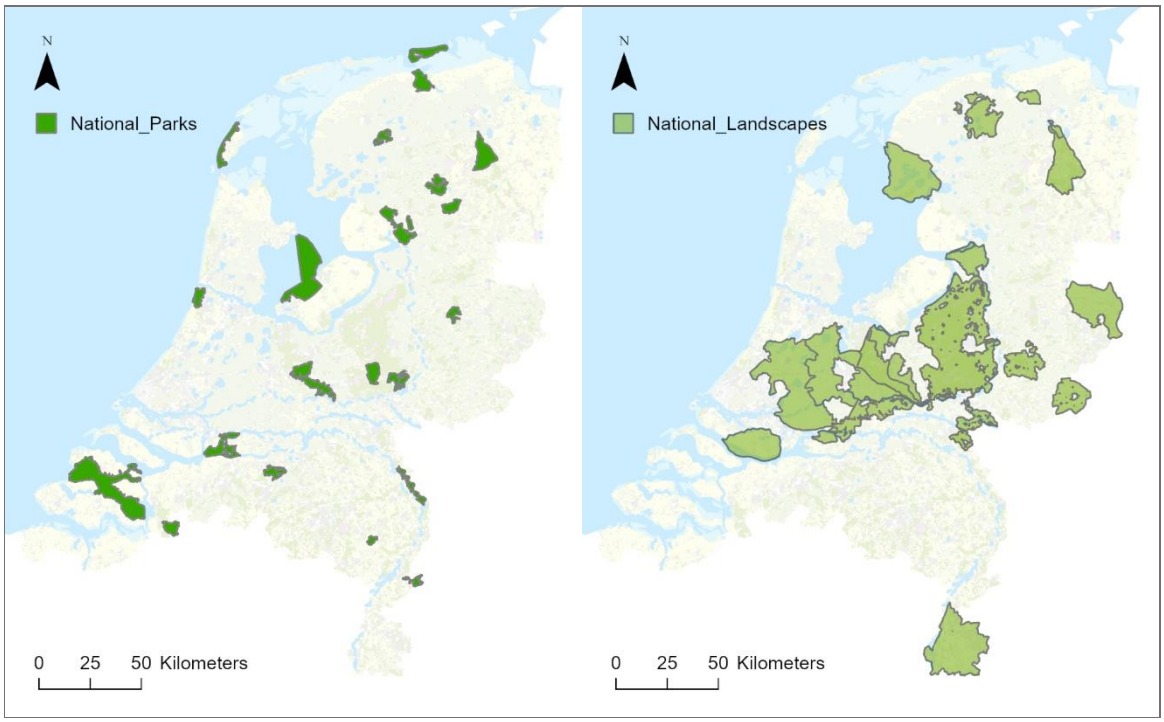

(1) National Parks (2) National Landscapes

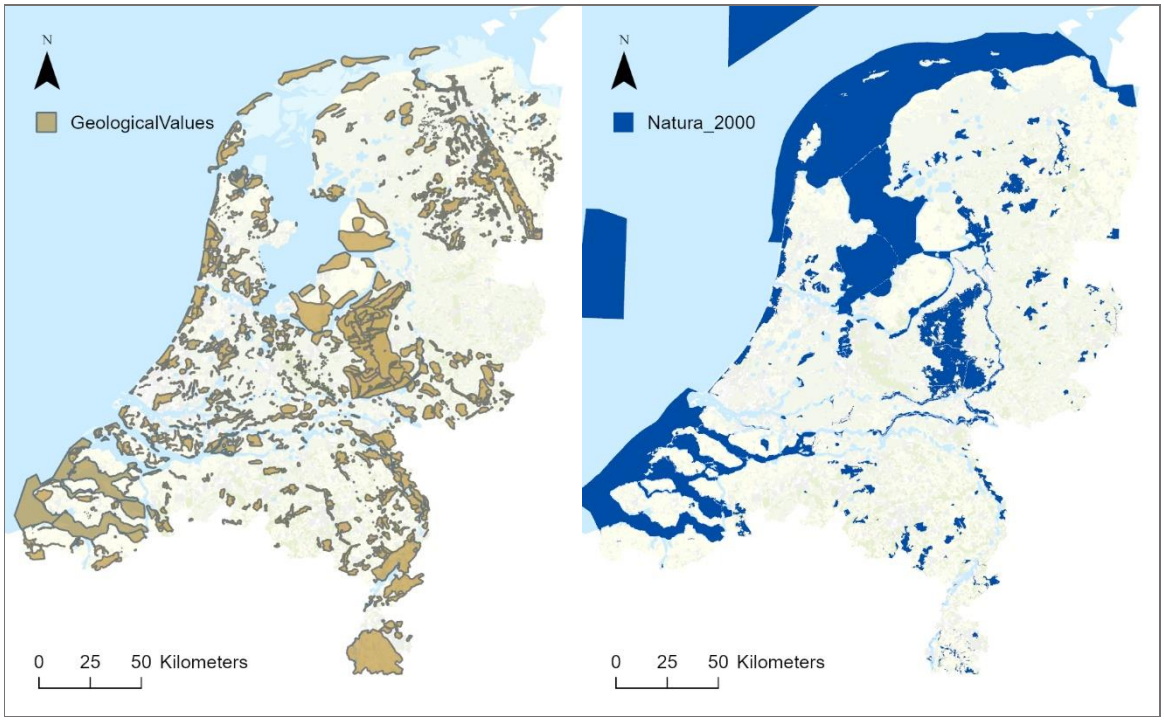

(3) Geologically places (4) Natura 2000

Figure A-7: Areas under four protected nature areas for the compatibility index validation: (1) national parks [76], (2) national landscapes [77], (3) geologically significant places [78], and (4) the Natura 2000 areas [79].

B

DETAILED INSTRUCTION – SUITABILITY INDEX

B.1 A basic example of Analytic Hierarchy Process (AHP)

For a better understanding of AHP calculation, two simple cases of the comparison matrix were given in the literature [90] (Figure B-1). The first example (Figure B-1, left) entails two criteria in which criterion A is three times more significant than criterion B. So the final weight for criterion A will be 0.75 and that for criterion B will be 0.25. The second case (Figure B-1, right) describes three criteria A, B, and C. The logic was put in a way that A is three times as important as B and half as important as C, whereas C is six times more important than B. This results in 0.3, 0.1, and 0.6 of the priority weight for criteria A, B, and C respectively.

RETURN	A	B	Priority
A	1	3	0.75
B	1/3	1	0.25

RETURN	A	B	C	Priority
A	1	3	1/2	0.30
B	1/3	1	1/6	0.10
C	2	6	1	0.60

Figure B-1: Two example cases of AHP calculation with priority results for 2 (left) and 3 (right) criteria [90].

The issue that was emphasized in this technique is that there might be some discrepancies among the input values in the matrix. From the latter example above, if criterion A is three times as important as B and half as important as C, it follows that C is six times as important as B. This is regarded as a value-transitive property. However, this is not always the case because in this technique every pair-wise must be evaluated separately. A different value, e.g. 4, can also be allocated to the pair of B to C instead of 6. And this mathematically contradicts with the property and affects the AHP results. By this means, Table B-1 repeats the calculation of the example above by changing the relative importance of B and C. The priority weight will then be 0.32 for A, 0.12 for B, and 0.56 for C, with an inconsistency value of 1.9%. As this is lower than the 10% threshold suggested by Saaty [90], the result is still acceptable for further analysis.

Table B-1: An alternate relative importance for the second case resulting in a change in priority weights and a certain degree of consistency ratio [91].

RETURN	A	B	C	Priority
A	1	3	1/2	**0.32**
B	1/3	1	**1/4**	**0.12**
C	2	**4**	1	**0.56**

C.R. = 1.9%

B.2 Additional input factors for the Suitability Index

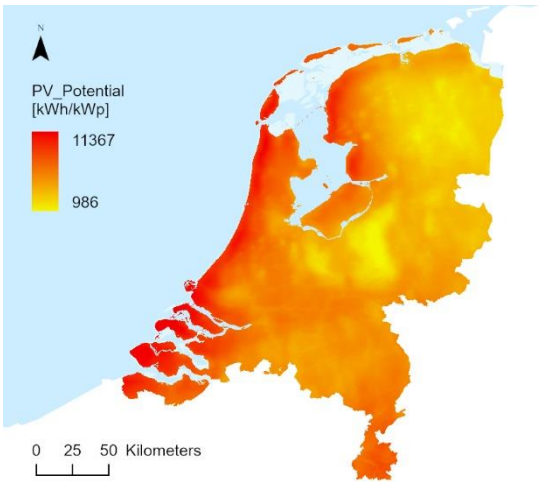

(1) PV potential [81]

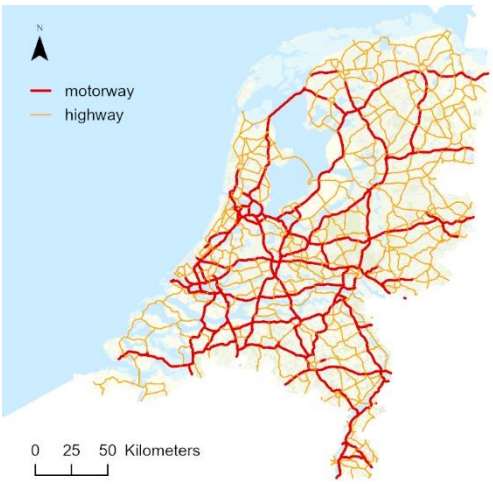

(2) Major Roads [60]

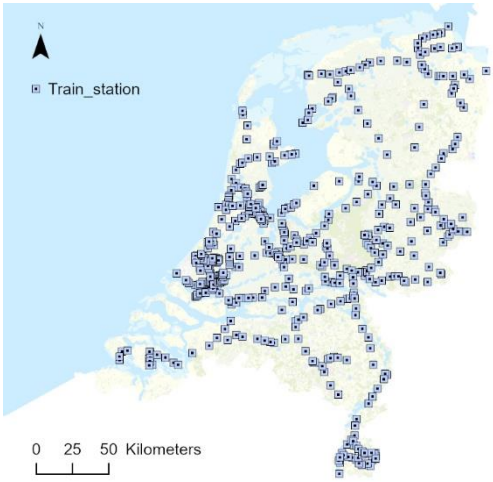

(3) Train Stations [82]

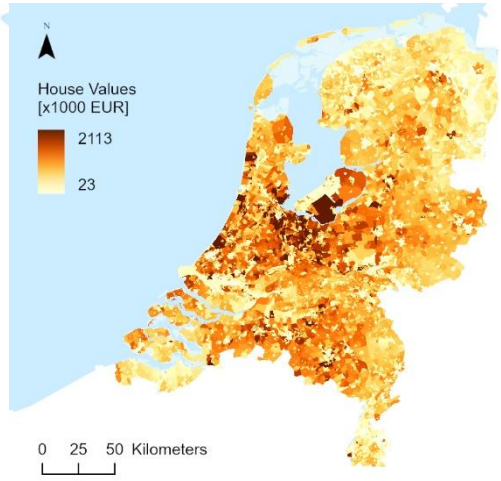

(4) House Values [83-85]

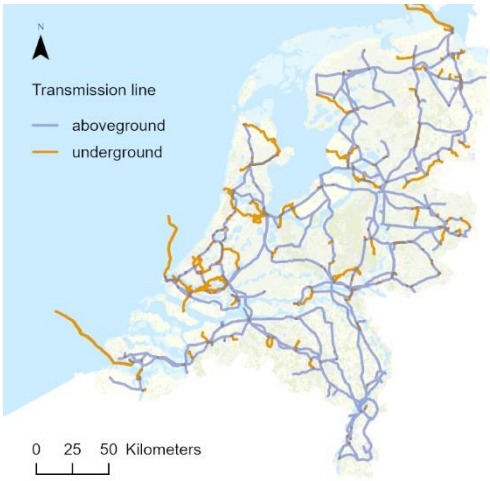

(5) Transmission Lines [68]

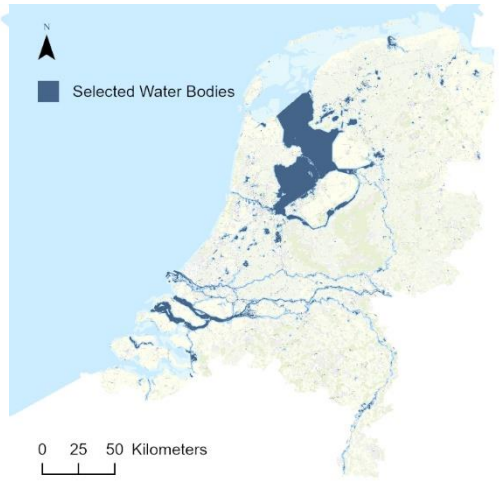

(6) Water Bodies [60]

Figure B-2: Original format of six input factors in the suitability model.

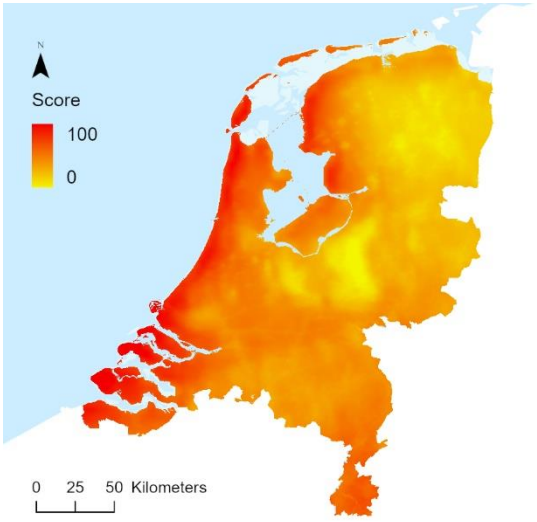

(1) normalized score of PV potential

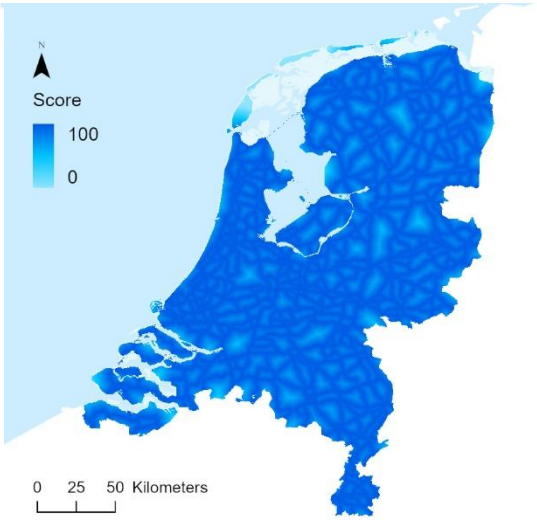

(2) normalized score of Major Roads

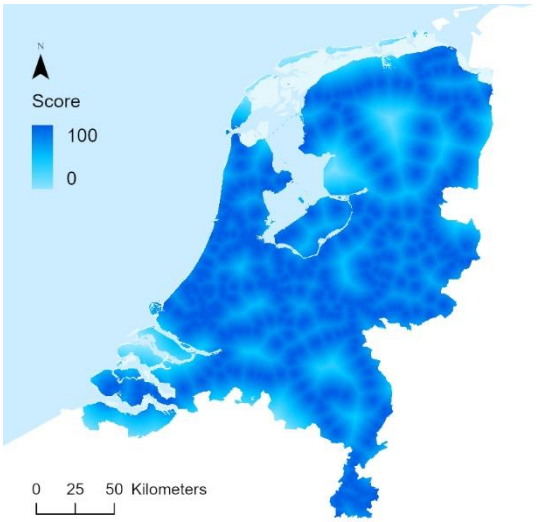

(3) normalized score of Train Stations

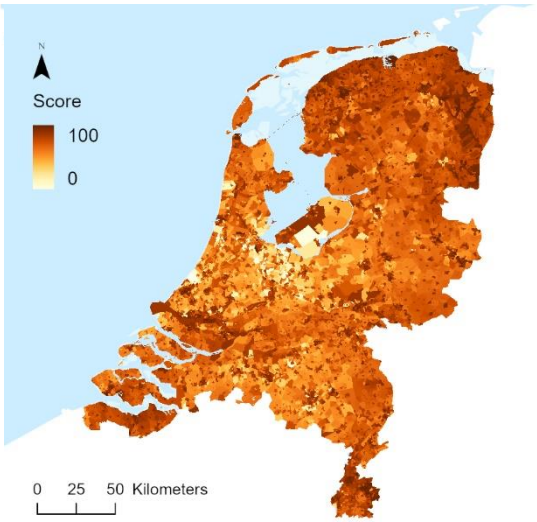

(4) normalized score of House Values

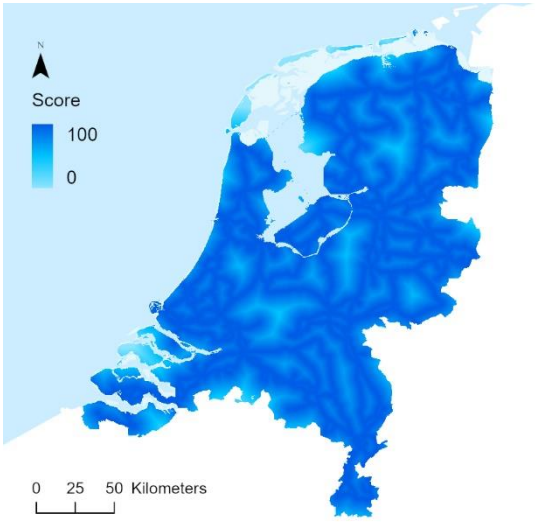

(5) normalized score of Transmission Lines

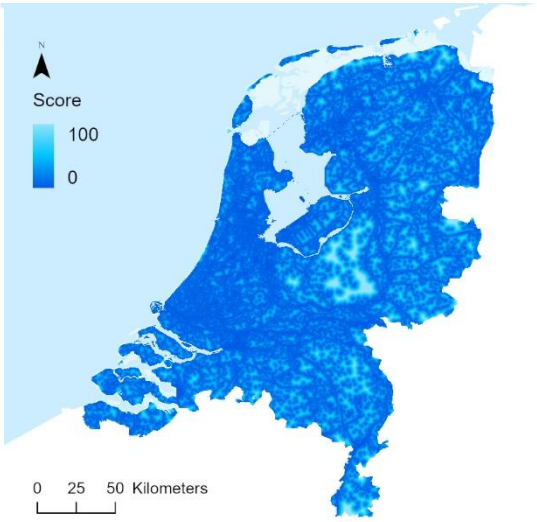

(6) normalized score of Water Bodies

Figure B-3: The result score of six input factors in the suitability model after the normalization process.

B.3 The exclusion map establishing steps

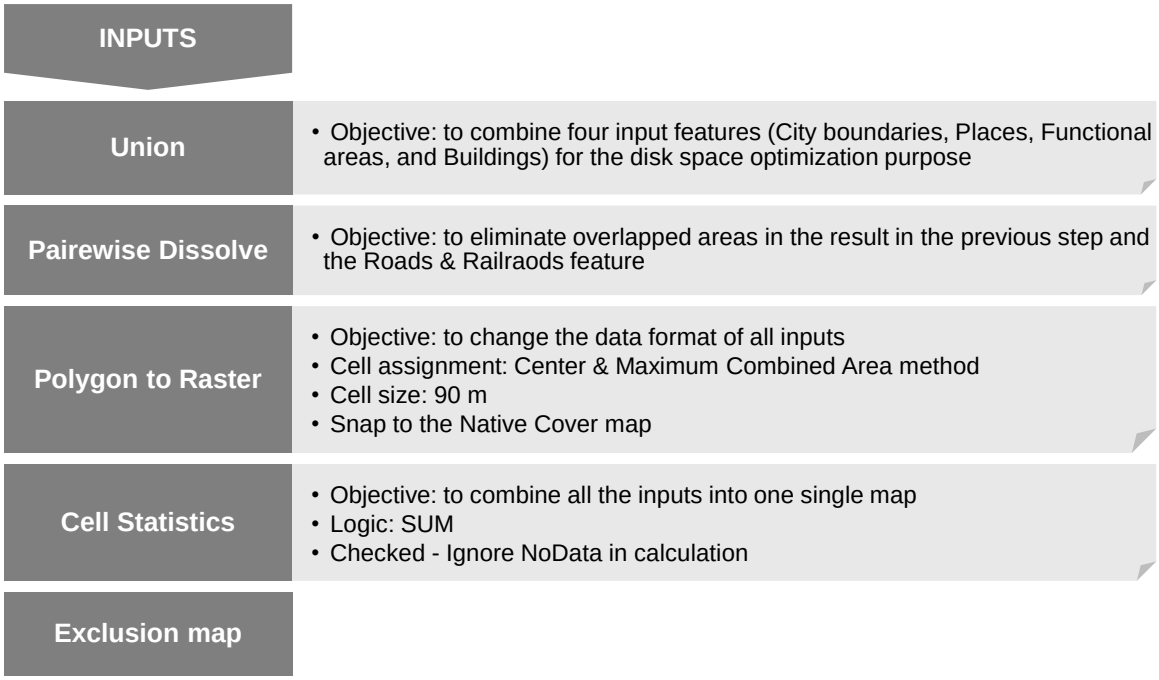

Figure B-4: Process for constructing the exclusion map. The figure demonstrates the ArcGIS Tools (left) that were utilized for this component and arranges them in ascending order with justification and relevant configuration settings (right).

Table B-2: The Funtional area selected attributes (in Dutch). The information in the list below is drawn from the *Basisregistratie Topografie* (BRT) database [60], collected on February 14, 2023. The selection process is based on the interpretation of each feature that might contribute to areas that are unlikely to be transformed due to renewable energy transition by comparing them with the map image [63].

	Features	Select		Features	Select
1	attractiepark	×	37	openluchtmuseum	✓
2	bedrijventerrein	×	38	openluchttheater	×
3	begraafplaats	✓	39	overig	×
4	botanische tuin	×	40	park	×
5	bungalowpark	×	41	plantsoen	×
6	camping, kampeerterrein	×	42	productie-installatie	✓
7	campus	×	43	recreatiegebied	×
8	caravanpark	✓	44	renbaan	×
9	circuit	×	45	skibaan	×
10	crossbaan	×	46	slipschool	×
11	dierentuin, safaripark	×	47	sluizencomplex	×
12	eendenkooi	×	48	sportterrein, sportcomplex	×
13	emplacement	×	49	stortplaats	×
14	erebegraafplaats	✓	50	tennispark	×
15	gaswinning	✓	51	transformatorstation	✓
16	gebied voor radioastronomie	✓	52	tuincentrum	×
17	gebouwencomplex	✓	53	vakantiepark	✓
18	golfterrein	×	54	verdedigingswerk	×
19	grafheuvel	×	55	verzorgingsplaats	✓
20	grindwinning	✓	56	viskwekerij	×
21	groeve	✓	57	visvijvercomplex	×
22	haven	✓	58	vliegveld, luchthaven	✓
23	heemtuin	×	59	volkstuinen	×
24	helikopterlandingsterrein	×	60	waterkering	×
25	ijsbaan	×	61	werf	×
26	infiltratiegebied	×	62	wildwissel	×
27	jachthaven	×	63	windturbinepark	×
28	kartingbaan	×	64	woonwagencentrum	✓
29	kassengebied	✓	65	zandwinning	✓
30	kazerne, legerplaats	✓	66	zenderpark	✓
31	milieustraat	×	67	ziekenhuiscomplex	✓
32	militair oefengebied, schietterrein	✓	68	zonnepark	×
33	mosselbank	×	69	zoutwinning	✓
34	nationaal park	×	70	zuiveringsinstallatie	✓
35	natuurgebied	×	71	zweefvliegveldterrein	×
36	oliewinning	✓	72	zwembadcomplex	×

Bibliography

[1] International Energy Agency. "Global Energy and Climate Model." IEA. https://www.iea.org/reports/global-energy-and-climate-model/net-zero-emissions-by-2050-scenario-nze (accessed June 07, 2023).

[2] International Energy Agency. "Renewable Electricity." IEA. https://www.iea.org/reports/renewable-power (accessed April 24, 2023).

[3] International Energy Agency. "Stimulation of sustainable energy production and climate transition (SDE++)." IEA. https://www.iea.org/policies/13639-stimulation-of-sustainable-energy-production-and-climate-transition-sde (accessed April 24, 2023).

[4] Netherlands Enterprise Agency. "Climate Agreement." RVO.nl. https://english.rvo.nl/sites/default/files/2020/10/National%20Climate%20Agreement%20The%20Netherlands%20-%20English_0.pdf (accessed April 24, 2023).

[5] L. Cornax, D. van Dyke, and R. van Rijn, "Beleidskaders zon-pv, Inventarisatie en analyse," March, 21 2019.

[6] T. Tamplin. "Economies of Scale." Finance Strategists. https://www.financestrategists.com/financial-advisor/economies-of-scale/?gclid=CjwKCAjw1YCkBhAOEiwA5aN4AUJnykbGegOGl9_7KQj-GGN8QZ660dFOvTxwg9QBvJRNvvF2UNVwvhoC1mMQAvD_BwE (accessed June 07, 2023).

[7] Ministerie van Economische Zaken en Klimaat. "Beantwoording moties Dik-Faber over een zonneladder als nationaal afwegingskader bij inpassing van zonne-energie." Rijksdienst voor Ondernemend Nederland. https://open.overheid.nl/documenten/ronl-98f56735-9cca-459b-b0db-15f6457bf167/pdf (accessed April 25, 2023).

[8] Het Nationaal Consortium. "Eco Certified Solar Parks." zon in landschap. https://zoninlandschap.nl/projecten/i358/ecocertified-solar-parks (accessed April 26, 2023).

[9] Nationaal Programma Regionale Energie Strategie. "Dutch National Programme Regional Energy Strategies." NP RES. https://www.regionale-energiestrategie.nl/home/default.aspx (accessed April 26, 2023).

[10] Stichting Solarpark De Kwekerij. "Photos." https://nlsolarparkdekwekerij.nl/fotos/ (accessed May 11, 2023).

[11] M. Enserink, R. Van Etteger, A. Van den Brink, and S. Stremke, "To support or oppose renewable energy projects? A systematic literature review on the factors influencing landscape design and social acceptance," *Energy Research & Social Science,* vol. 91, p. 102740, 2022/09/01/ 2022, doi: https://doi.org/10.1016/j.erss.2022.102740.

[12] S. Boroushaki and J. Malczewski, "Implementing an extension of the analytical hierarchy process using ordered weighted averaging operators with fuzzy quantifiers in ArcGIS," *Computers & Geosciences,* vol. 34, no. 4, pp. 399-410, 2008/04/01/ 2008, doi: https://doi.org/10.1016/j.cageo.2007.04.003.

[13] J.-J. Wang, Y.-Y. Jing, C.-F. Zhang, and J.-H. Zhao, "Review on multi-criteria decision analysis aid in sustainable energy decision-making," *Renewable and Sustainable Energy Reviews,* vol. 13, no. 9, pp. 2263-2278, 2009/12/01/ 2009, doi: https://doi.org/10.1016/j.rser.2009.06.021.

[14] P. Roddis, K. Roelich, K. Tran, S. Carver, M. Dallimer, and G. Ziv, "What shapes community acceptance of large-scale solar farms? A case study of the UK's first 'nationally significant' solar farm," *Solar Energy,* vol. 209, pp. 235-244, 2020/10/01/ 2020, doi: https://doi.org/10.1016/j.solener.2020.08.065.

[15] B. Frantál *et al.*, "Spatial targeting, synergies and scale: Exploring the criteria of smart practices for siting renewable energy projects," *Energy Policy,* vol. 120, pp. 85-93, 2018/09/01/ 2018, doi: https://doi.org/10.1016/j.enpol.2018.05.031.

[16] S. Stremke, "Sustainable Energy Landscape: Implementing Energy Transition in the Physical Realm (Encyclopedia of Environmental Management)," *Encyclopedia of Environmental Management,* vol. 2015, pp. 1-9, 08/18 2015, doi: 10.1081/E-EEM-120053717.

[17] C. Warren, C. Lumsden, S. O'Dowd, and R. Birnie, "'Green on Green': Public Perceptions of Wind Power in Scotland and Ireland," *Journal of Environmental Planning and Management,* vol. 48, pp. 853-875, 11/01 2005, doi: 10.1080/09640560500294376.
[18] J. A. Sward *et al.*, "Integrating social considerations in multicriteria decision analysis for utility-scale solar photovoltaic siting," *Applied Energy,* vol. 288, p. 116543, 2021/04/15/ 2021, doi: https://doi.org/10.1016/j.apenergy.2021.116543.
[19] J. Arán Carrión, A. Espín Estrella, F. Aznar Dols, M. Zamorano Toro, M. Rodríguez, and A. Ramos Ridao, "Environmental decision-support systems for evaluating the carrying capacity of land areas: Optimal site selection for grid-connected photovoltaic power plants," *Renewable and Sustainable Energy Reviews,* vol. 12, no. 9, pp. 2358-2380, 2008/12/01/ 2008, doi: https://doi.org/10.1016/j.rser.2007.06.011.
[20] Y. Charabi and A. Gastli, "PV site suitability analysis using GIS-based spatial fuzzy multi-criteria evaluation," *Renewable Energy,* vol. 36, no. 9, pp. 2554-2561, 2011/09/01/ 2011, doi: https://doi.org/10.1016/j.renene.2010.10.037.
[21] H. Effat, "Selection of Potential Sites for Solar Energy Farms in Ismailia Governorate, Egypt using SRTM and Multicriteria Analysis," *International Journal of Advanced Remote Sensing and GIS,* vol. 2, pp. 205-220, 01/22 2013.
[22] J. Brewer, D. P. Ames, D. Solan, R. Lee, and J. Carlisle, "Using GIS analytics and social preference data to evaluate utility-scale solar power site suitability," *Renewable Energy,* vol. 81, pp. 825-836, 2015/09/01/ 2015, doi: https://doi.org/10.1016/j.renene.2015.04.017.
[23] A. Alami Merrouni, F. Elwali Elalaoui, A. Mezrhab, A. Mezrhab, and A. Ghennioui, "Large scale PV sites selection by combining GIS and Analytical Hierarchy Process. Case study: Eastern Morocco," *Renewable Energy,* vol. 119, pp. 863-873, 2018/04/01/ 2018, doi: https://doi.org/10.1016/j.renene.2017.10.044.
[24] M. Giamalaki and T. Tsoutsos, "Sustainable siting of solar power installations in Mediterranean using a GIS/AHP approach," *Renewable Energy,* vol. 141, pp. 64-75, 2019/10/01/ 2019, doi: https://doi.org/10.1016/j.renene.2019.03.100.
[25] D. Messaoudi, N. Settou, B. Negrou, and B. Settou, "GIS based multi-criteria decision making for solar hydrogen production sites selection in Algeria," *International Journal of Hydrogen Energy,* vol. 44, no. 60, pp. 31808-31831, 2019/12/06/ 2019, doi: https://doi.org/10.1016/j.ijhydene.2019.10.099.
[26] T. Finn and P. McKenzie, "A high-resolution suitability index for solar farm location in complex landscapes," *Renewable Energy,* vol. 158, pp. 520-533, 2020/10/01/ 2020, doi: https://doi.org/10.1016/j.renene.2020.05.121.
[27] H.-W. Wang, A. Dodd, and Y. Ko, "Resolving the conflict of greens: A GIS-based and participatory least-conflict siting framework for solar energy development in southwest Taiwan," *Renewable Energy,* vol. 197, pp. 879-892, 2022/09/01/ 2022, doi: https://doi.org/10.1016/j.renene.2022.07.094.
[28] S. Carley, D. Konisky, Z. Atiq, and N. Land, "Energy infrastructure, NIMBYism, and public opinion: a systematic literature review of three decades of empirical survey literature," *Environmental Research Letters,* vol. 15, 09/01 2020, doi: 10.1088/1748-9326/ab875d.
[29] H. Boudet, "Public perceptions of and responses to new energy technologies," *Nature Energy,* vol. 4, p. 1, 05/01 2019, doi: 10.1038/s41560-019-0399-x.
[30] J. A. Gordon, N. Balta-Ozkan, and S. A. Nabavi, "Homes of the future: Unpacking public perceptions to power the domestic hydrogen transition," *Renewable and Sustainable Energy Reviews,* vol. 164, p. 112481, 2022/08/01/ 2022, doi: https://doi.org/10.1016/j.rser.2022.112481.
[31] J. E. Carlisle, S. L. Kane, D. Solan, M. Bowman, and J. C. Joe, "Public attitudes regarding large-scale solar energy development in the U.S," *Renewable and Sustainable Energy Reviews,* vol. 48, pp. 835-847, 2015/08/01/ 2015, doi: https://doi.org/10.1016/j.rser.2015.04.047.
[32] J. E. Carlisle, D. Solan, S. L. Kane, and J. Joe, "Utility-scale solar and public attitudes toward siting: A critical examination of proximity," *Land Use Policy,* vol. 58, pp. 491-501, 2016/12/15/ 2016, doi: https://doi.org/10.1016/j.landusepol.2016.08.006.
[33] M. A. Tello, "Conceptualizing social impact: A geographic perspective," *Journal of Business Research,* vol. 119, pp. 562-571, 2020/10/01/ 2020, doi: https://doi.org/10.1016/j.jbusres.2020.07.040.
[34] R. Chiabrando, E. Fabrizio, and G. Garnero, "The territorial and landscape impacts of photovoltaic systems: Definition of impacts and assessment of the glare risk," *Renewable*

and Sustainable Energy Reviews, vol. 13, no. 9, pp. 2441-2451, 2009/12/01/ 2009, doi: https://doi.org/10.1016/j.rser.2009.06.008.

[35] R. Chock *et al.*, "Evaluating potential effects of solar power facilities on wildlife from an animal behavior perspective," *Conservation Science and Practice,* vol. 3, 11/19 2020, doi: 10.1111/csp2.319.

[36] J. M. Randall *et al.*, " Mojave Desert Ecoregional Assessment," The Nature Conservancy, San Francisco, California, 2010. [Online]. Available: https://www.scienceforconservation.org/products/mojave-desert-ecoregional-assessment

[37] D. R. Cameron, B. S. Cohen, and S. A. Morrison, "An Approach to Enhance the Conservation-Compatibility of Solar Energy Development," *PLOS ONE,* vol. 7, no. 6, p. e38437, 2012, doi: 10.1371/journal.pone.0038437.

[38] R. R. Hernandez, M. K. Hoffacker, M. L. Murphy-Mariscal, G. C. Wu, and M. F. Allen, "Solar energy development impacts on land cover change and protected areas," *Proceedings of the National Academy of Sciences,* vol. 112, no. 44, pp. 13579-13584, 2015/11/03 2015, doi: 10.1073/pnas.1517656112.

[39] CountryReports. "Netherlands Geography." CountryReports. https://www.countryreports.org/country/Netherlands/geography.htm (accessed June 14, 2023).

[40] The World Bank Group. "Netherlands Climatology." Climate Change Knowledge Portal. https://climateknowledgeportal.worldbank.org/country/netherlands/climate-data-historical (accessed June 15, 2023).

[41] Koninklijk Nederlands Meteorologisch Instituut. Ministerie van Infrastructuur en Waterstaat. "Climate dashboard." KNMI. https://www.knmi.nl/klimaatdashboard (accessed July 20, 2023).

[42] Esri Nederland Community Map Contributors. Topo RD (vector tiled) [Online] Available: https://tudelft.maps.arcgis.com/home/item.html?id=38c4cfd9b72346c988be5fff1668ea79

[43] Centraal Bureau voor de Statistiek. "The Netherlands in numbers: How many wind turbines in the Netherlands?" CBS. https://longreads.cbs.nl/the-netherlands-in-numbers-2022/how-many-wind-turbines-in-the-netherlands/ (accessed June 15, 2023).

[44] Centraal Bureau voor de Statistiek. StatLine: Hernieuwbare elektriciteit; productie en vermogen [Online] Available: https://opendata.cbs.nl/statline/#/CBS/nl/dataset/82610NED/table?ts=1686823229192

[45] Centraal Bureau voor de Statistiek. StatLine: Bodemgebruik; uitgebreide gebruiksvorm, per gemeente [Online] Available: https://opendata.cbs.nl/statline/#/CBS/nl/dataset/70262ned/table?ts=1686842700288

[46] Ministerie van Binnenlandse Zaken en Koninkrijksrelaties. "Geobasisregistraties: Basisregistraties." BZK. https://www.geobasisregistraties.nl/basisregistraties/doorontwikkeling-in-samenhang (accessed June 16, 2023).

[47] L. Sharp. "Cartographic Design." ArcGIS StoryMaps. https://storymaps.arcgis.com/stories/58593bfc09c741a0b67dd81c22a914e3 (accessed June 16, 2023).

[48] ArcGIS Pro. "2D and 3D features." ESRI. https://pro.arcgis.com/en/pro-app/2.9/help/editing/introduction-to-creating-2d-and-3d-features.htm (accessed June 17, 2023).

[49] ArcGIS Pro. "What is raster data?" ESRI. https://pro.arcgis.com/en/pro-app/2.9/get-started/what-is-raster-data.htm#:~:text=In%20its%20simplest%20form%2C%20a,pictures%2C%20or%20even%20scanned%20maps. (accessed June 17, 2023).

[50] J. R. Janke, "Multicriteria GIS modeling of wind and solar farms in Colorado," *Renewable Energy,* vol. 35, no. 10, pp. 2228-2234, 2010/10/01/ 2010, doi: https://doi.org/10.1016/j.renene.2010.03.014.

[51] D. M. Stoms, S. L. Dashiell, and F. W. Davis, "Siting solar energy development to minimize biological impacts," *Renewable Energy,* vol. 57, pp. 289-298, 2013/09/01/ 2013, doi: https://doi.org/10.1016/j.renene.2013.01.055.

[52] ROM3D, "Grondgebonden zonneparken: Verkenning naar de afwegingskaders rond locatiekeuze en ruimtelijke inpassing in Nederland," De Rijksdienst voor Ondernemend Nederland, RVO.nl, September 2016. Accessed: March 16, 2023. [Online]. Available: https://www.rvo.nl/sites/default/files/2016/09/Grondgebonden%20Zonneparken%20-%20verkenning%20afwegingskadersmetbijlagen.pdf

[53] F. van der Zee, Bloem, J., Galama, P., Gollenbeek, L., van Os, J., Schotman, A., & de Vries, S., "Zonneparken natuur en landbouw," in "Wageningen Environmental Research rapport," Wageningen Environmental Research, Wageningen, April 2019. Accessed: March 03, 2023. [Online]. Available: https://edepot.wur.nl/475349

[54] I. Pettersson, Morell, K., Råberg, T. , van Noord, M., Zinko, U., Ghaem Sigarchian, and S. S., A., Unger, M., "Ecovoltaics och agrivoltaics - en handbok om solcellsparker som gynnar biologisk mångfald och ekosystemtjänster," RISE Research Institutes of Sweden, RISE, 2022. Accessed: October 10, 2022. [Online]. Available: https://www.ri.se/sites/default/files/2022-10/RISE_Ecogain_Eko-Sol_Handbok_2022-10-17_rev_0.pdf

[55] TKI Urban Energy and Generation Energy, "RUIMTELIJK POTENTIEEL VAN ZONNESTROOM IN NEDERLAND," ZON in landschap, topsectorenergie.nl, April 2021. Accessed: March 16, 2023. [Online]. Available: https://topsectorenergie.nl/documents/136/Ruimtelijk_potentieel_van_zonnestroom_in_Nederland.pdf

[56] Wageningen University and Research (WUR). "In my backyard please." ZON in landschap. https://zoninlandschap.nl/projecten/i174/in-my-backyard-please (accessed March 16, 2023).

[57] "Land degradation," in *Climate Change and Land: IPCC Special Report on Climate Change, Desertification, Land Degradation, Sustainable Land Management, Food Security, and Greenhouse Gas Fluxes in Terrestrial Ecosystems*, C. Intergovernmental Panel on Climate Ed. Cambridge: Cambridge University Press, 2022, pp. 345-436.

[58] D. M. Stoms, S. L. Dashiell, and F. W. Davis, "Mapping compatibility to minimize biodiversity impacts of solar energy development in the California Deserts," *Santa Barbara, Biogeography Lab, University of California Santa Barbara,* 2011.

[59] Centraal Bureau voor de Statistiek. Cijfers op de kaart: Stedelijkheid [Online] Available: https://www.cbs.nl/nl-nl/visualisaties/cijfers-op-de-kaart?subject=ST0001&year=2022&level=Gemeente

[60] Kadaster. TOP10NL Geopackage [Online] Available: https://service.pdok.nl/brt/topnl/atom/top10nl.xml

[61] Ministerie van Economische Zaken en Klimaat. Basisregistratie Gewaspercelen (BRP) (EPSG:28992) Geopackage [Online] Available: https://service.pdok.nl/rvo/brpgewaspercelen/atom/v1_0/basisregistratie_gewaspercelen_brp.xml

[62] Esri Nederland and Centraal Bureau voor de Statistiek. Buurten 2022 - CBS Wijk- en Buurtkaart [Online] Available: https://services.arcgisonline.nl/arcgis/rest/services/Demografie/CBS_WijkenBuurten_2022/FeatureServer/0

[63] Esri Nederland and Beeldmateriaal.nl. Luchtfoto actueel - 25 cm [Online] Available: https://services.arcgisonline.nl/arcgis/rest/services/Luchtfoto/Luchtfoto/MapServer

[64] H. B. Jackson and L. Fahrig, "Habitat Loss and Fragmentation," in *Encyclopedia of Biodiversity (Second Edition)*, S. A. Levin Ed. Waltham: Academic Press, 2013, pp. 50-58.

[65] L. Fahrig, "Effects of Habitat Fragmentation on Biodiversity," *Annual Review of Ecology, Evolution, and Systematics,* vol. 34, no. 1, pp. 487-515, 2003/11/01 2003, doi: 10.1146/annurev.ecolsys.34.011802.132419.

[66] N. M. Haddad *et al.*, "Habitat fragmentation and its lasting impact on Earth's ecosystems," *Science Advances,* vol. 1, no. 2, p. e1500052, doi: 10.1126/sciadv.1500052.

[67] OpenStreetMap contributors. OpenStreetMap Waterways for Europe [Online] Available: https://services-eu1.arcgis.com/zci5bUiJ8olAal7N/arcgis/rest/services/OSM_Waterways_EU/FeatureServer

[68] TenneT TSO B.V. TenneT Assets Hoogspanning [Online] Available: https://services-eu1.arcgis.com/WjozPuR5ROn6NZE8/arcgis/rest/services/TenneT_Assets_Hoogspanning/FeatureServer

[69] Climate Impact Atlas. Basiskaarten [Online] Available: https://www.klimaateffectatlas.nl/en/retrieving-data

[70] Kadaster. Dataset: Key Register of Large-Scale Topography (BGT) [Online] Available: https://app.pdok.nl/lv/bgt/download-viewer/

[71] Department of Nature. *Nature Conservation in the Netherlands Contents*. (2005). Wageningen University & Research. Ministry of Agriculture, Nature and Food Quality. Accessed: January 17. [Online]. Available: https://edepot.wur.nl/118495

[72] Interprovinciaal Overleg. Dataset: Netherlands Nature Network (NNN) - Provinces (INSPIRE harmonised) [Online] Available: https://www.pdok.nl/introductie/-/article/natuurnetwerk-nederland-nnn-

[73] Government of the Netherlands. "National Ecological Network (NEN)." government.nl. https://www.government.nl/topics/nature-and-biodiversity/national-ecological-network-nen (accessed June 28, 2023).

[74] Government of the Netherlands. "Realising the new Dutch National Ecological Network - land acquisition and redevelopment, 1990 - 2012." clo.nl. https://www.clo.nl/en/indicators/en130710-new-ehs-acquisition-and-development (accessed June 28, 2023).

[75] the Directorate-General for Environment. "Natura 2000." European Commission. https://ec.europa.eu/environment/nature/natura2000/index_en.htm (accessed June 28, 2023).

[76] Ministerie van Economische Zaken en Klimaat. Dataset: National Parks [Online] Available: https://www.pdok.nl/introductie/-/article/nationale-parken

[77] Interprovinciaal Overleg. Dataset: Provincial Landscape Policy - Provinces (INSPIRE harmonised) [Online] Available: https://www.pdok.nl/introductie/-/article/provinciaal-landschapsbeleid

[78] Interprovinciaal Overleg. Dataset: Geological values [Online] Available: https://www.pdok.nl/introductie/-/article/aardkundige-waarden

[79] Ministerie van Economische Zaken en Klimaat. Data set: Natura 2000 [Online] Available: https://www.pdok.nl/introductie/-/article/natura-2000

[80] M. Stacy. "Lake vs. Pond: The 3 Main Differences Explained." AZ Animals. https://a-z-animals.com/blog/lake-vs-pond-the-3-main-differences-explained/ (accessed May 23, 2023).

[81] The World Bank Group. Solar resource maps of Netherlands [Online] Available: https://solargis.com/maps-and-gis-data/download/netherlands

[82] OpenStreetMap contributors. OpenStreetMap - Verkeer & Vervoer [Online] Available: https://services.arcgis.com/nSZVuSZjHpEZZbRo/arcgis/rest/services/OSM_Verkeer_en_Vervoer/FeatureServer

[83] Esri Nederland and Centraal Bureau voor de Statistiek. Buurten 2021 - CBS Wijk- en Buurtkaart [Online] Available: https://services.arcgisonline.nl/arcgis/rest/services/Demografie/CBS_WijkenBuurten_2021/FeatureServer/0

[84] Esri Nederland and Centraal Bureau voor de Statistiek. Wijken 2021 - CBS Wijk- en Buurtkaart [Online] Available: https://services.arcgisonline.nl/arcgis/rest/services/Demografie/CBS_WijkenBuurten_2021/FeatureServer/1

[85] Esri Nederland and Centraal Bureau voor de Statistiek. Gemeenten 2021 - CBS Wijk- en Buurtkaart [Online] Available: https://services.arcgisonline.nl/arcgis/rest/services/Demografie/CBS_WijkenBuurten_2021/FeatureServer/2

[86] T. L. Saaty, *The Analytic Hierarchy Process*. New York: McGraw-Hill, 1980.

[87] G. Zhang, Y. Shi, A. Maleki, and M. A. Rosen, "Optimal location and size of a grid-independent solar/hydrogen system for rural areas using an efficient heuristic approach," *Renewable Energy,* vol. 156, pp. 1203-1214, 2020/08/01/ 2020, doi: https://doi.org/10.1016/j.renene.2020.04.010.

[88] H. Ao Xuan, V. Vu Trinh, K. Techato, and K. Phoungthong, "Use of hybrid MCDM methods for site location of solar-powered hydrogen production plants in Uzbekistan," *Sustainable Energy Technologies and Assessments,* vol. 52, p. 101979, 2022/08/01/ 2022, doi: https://doi.org/10.1016/j.seta.2022.101979.

[89] Y. Wu, Z. Deng, Y. Tao, L. Wang, F. Liu, and J. Zhou, "Site selection decision framework for photovoltaic hydrogen production project using BWM-CRITIC-MABAC: A case study in Zhangjiakou," *Journal of Cleaner Production,* vol. 324, p. 129233, 2021/11/15/ 2021, doi: https://doi.org/10.1016/j.jclepro.2021.129233.

[90] R. W. Saaty, "The analytic hierarchy process—what it is and how it is used," *Mathematical Modelling,* vol. 9, no. 3, pp. 161-176, 1987/01/01/ 1987, doi: https://doi.org/10.1016/0270-0255(87)90473-8.
[91] K. D. Goepel. "AHP Priority Calculator." BPMSG. https://bpmsg.com/ahp/ahp-calc.php (accessed Jul 01, 2023).
[92] K. Goepel, *Implementing the Analytic Hierarchy Process as a Standard Method for Multi-Criteria Decision Making in Corporate Enterprises – a New AHP Excel Template with Multiple Inputs*. 2013.
[93] S. Pant, A. Kumar, M. Ram, Y. Klochkov, and H. K. Sharma, "Consistency Indices in Analytic Hierarchy Process: A Review," *Mathematics*, vol. 10, no. 8, doi: 10.3390/math10081206.
[94] ROM3D. *Zon op Kaart*, Mar 27, 2023.
[95] Environmental Systems Research Institute Inc. "Geometrical interval." ArcGIS Desktop Help. https://webhelp.esri.com/arcgisdesktop/9.2/index.cfm?topicname=geometrical_interval (accessed June 30, 2023).
[96] ArcGIS Pro. "Change the symbology of imagery." ESRI. https://pro.arcgis.com/en/pro-app/latest/help/data/imagery/symbology-pane.htm (accessed June 31, 2023).
[97] P.J.T.M. van Puijenbroek and J. Clement, "Basiskaart Aquatisch: de Watertypenkaart: Het oppervlaktewater in de TOP10NL geclassificeerd naar watertype," Den Haag/Bilthoven, 2010. [Online]. Available: https://www.pbl.nl/sites/default/files/downloads/500067004.pdf
[98] ArcGIS Pro. "Kernel Density (Spatial Analyst)." ESRI. https://pro.arcgis.com/en/pro-app/latest/tool-reference/spatial-analyst/kernel-density.htm (accessed July 06, 2023).
[99] ArcGIS Pro. "How Kernel Density works." ESRI. https://pro.arcgis.com/en/pro-app/latest/tool-reference/spatial-analyst/how-kernel-density-works.htm#:~:text=Kernel%20Density%20calculates%20the%20density,is%20fitted%20over%20each%20point. (accessed July 06, 2023).